Biosensor Platform Development for Studying Carbohydrate-Mediated Bacterial Adhesion

Jeffrey W. Chamberlain

A dissertation

submitted in partial fulfillment of the

requirements for the degree of

Doctor of Philosophy

University of Washington

2012

Reading Committee:

Daniel M. Ratner, Chair

Barry Lutz

David Danley

Program Authorized to Offer Degree:

Bioengineering

University of Washington

Abstract

Biosensor Platform Development for Studying
Carbohydrate-Mediated Bacterial Adhesion

Jeffrey W. Chamberlain

Chair of the Supervisory Committee:
Assistant Professor Daniel M. Ratner
Bioengineering

Infectious diseases are the second leading cause of mortality worldwide, accounting for 14.9 million deaths each year. Diarrheal diseases, usually a result of infection by enteric pathogens, cause 1.8 million of these deaths, a disproportionate number of which are infants and children. Pathogen adhesion to host tissue is a prerequisite for a majority of infectious diseases, so these adhesion mechanisms are of primary concern to understand the pathogenesis of infectious disease and to develop strategies to combat these ailments. Of the many adhesion mechanisms that pathogens have evolved, cell surface glycoconjugates are one of the most common targets. A biosensor capable of screening pathogens against many carbohydrate structures at one time would help address the challenges of identifying binding partners, understanding bacterial adhesion, and developing anti-adhesives. To better understand the challenges associated with studying whole cell binding with biosensors, as well as to maximize opportunities, two very different biosensing platforms were chosen as promising technologies for studying bacterial adhesion: (1) a complementary metal oxide semiconductor (CMOS)-based microelectrode array and (2) an instrument based on silicon photonic microring resonators. For each of these platforms, we developed and implemented functionalization techniques and experimental protocols to enable the study of carbohydrate-mediated bacterial interactions. In the case of the microelectrode array, a polypyrrole functionalization technique was used to evaluate bacterial adhesion to glyconconjugates immobilized on the microelectrodes, and the dose-dependent inhibition of *Salmonella enterica* binding demonstrated a real-world application of this platform. Achieving carbohydrate-mediated bacterial adhesion on the microring resonators proved elusive, but significant advancements were made on this emerging biosensor platform in the form of several different functionalization techniques and antibody-based capture of *Campylobacter jejuni*.

TABLE OF CONTENTS

LIST OF FIGURES

LIST OF TABLES

ACKNOWLEDGEMENTS

"In my walks, every man I meet is my superior in some way, and in that I learn from him."

- Ralph Waldo Emerson

This degree would not have been possible without significant contributions from a number of people. First and foremost, I would like to thank my outstanding advisor, Dan Ratner, for the support and guidance that he provided over the last five years. I cannot over-emphasize the positive influence that Dan has had on my development as a scientist and as a person. He has taught me how to think and work like a scientist, and he has shown me the importance of establishing positive working relationships with others. Part of his ability as a mentor comes from the infectious nature of his own intellectual curiosity and enjoyment in learning, but it is also clear that Dan is deliberate about being the best advisor that he can be. He is, without a doubt, the best mentor I have ever had, and I will carry the lessons that I learned from him for the rest of my life.

Also crucial to the completion of this degree were the other members of the Ratner lab and the people who make up the department of Bioengineering. In addition to the scientific expertise that my colleagues provided, their cheerful demeanor made the work environment consistently pleasant. The community of people in the department of Bioengineering is one that I am proud to be a part of, and I hope to keep close ties even as my career takes me elsewhere. I would also like to thank my Supervisory Committee, Shaoyi Jiang, Barry Lutz, David Danley, Peter Pauzauski, and Krishna Rao, for their thoughtful contributions and mentorship.

Finally, I am deeply grateful to my family and friends for their unwavering support and for their role in making me the person who I am today. My parents, Scott and Lou Anne Chamberlain, instilled in me a desire to succeed and provided me with all of the tools to enable success, no matter the personal sacrifices that they had to make. I am forever indebted to both of them. The friends who have shared in my journey are too numerous to list, but I would like to specifically acknowledge the critical role that my girlfriend, Sarah Nowakowski, has played in making the last few years so special – I look forward to many more to come.

1. CHAPTER 1: CARBOHYDRATE CHEMISTRY AND CARBOHYDRATES IN BIOLOGY

Carbohydrates are the most abundant organic substance produced by living organisms, serving functions as diverse as providing structural support, storing energy, and mediating endless examples of biological interactions. In order to appreciate how carbohydrates are involved in such a wide array of structural and functional roles, one must first understand some of the basic carbohydrate chemistry that enables such complexity. The work presented in this document is focused on carbohydrates that act as binding targets for both commensal and pathogenic bacteria. The large role that the human microbiota plays in health, as well as the burden of infectious disease, demands an improved understanding of these interactions. Studying carbohydrate-mediated bacterial adhesion is a significant challenge, however, and improved tools are needed that will identify and characterize glycan-microbe binding partners. Such knowledge will enable the development of pre- and probiotics for establishing a healthy gut microbiota and antiadhesive therapies for preventing and treating infectious disease.

1.1 Introduction and Significance

Carbohydrates are one of the four classes of macromolecules found in nature, along with proteins, nucleic acids, and lipids, with carbohydrates being the most abundant organic substances produced by living organisms. It has long been known that carbohydrates are ubiquitous in nature as structural components and sources of energy, but only relatively recently have they been recognized as serving critical functional roles in areas such as cell-cell communication,[6] cell signaling,[7] and host-microbe interactions.[8] The work presented herein focuses on the development of methods for studying the role that carbohydrates play in host-pathogen interactions.

Infectious diseases are the second leading cause of mortality worldwide, accounting for 14.9 million deaths each year;[9] in the poorest countries, they account for over half of all deaths. Diarrheal diseases, usually a result of infection by enteric pathogens, cause 1.8 million of these deaths, a disproportionate number of which are infants and children. Severe diarrhea alone accounts for 18% of worldwide deaths in children under the age of five.[9a] While it is a humanitarian burden upon the developed world to understand and combat infectious diseases in order to reduce the high mortality rate in developing nations, it is no less important to fight the infectious diseases that are clinically relevant in the developed world. Each year in the United States, foodborne illness affects 9.4 million people, leading to

56,000 hospitalizations and 1,400 deaths, costing more than $23 billion[10]—and these are just confirmed cases. When taking into account unspecified cases (i.e. those that cannot be confirmed as foodborne illness), the numbers jump to 47.8 million illnesses, 127,839 hospitalizations, and 1,686 deaths.[11] Since pathogen adhesion to host tissue is a prerequisite for a majority of infectious diseases, these adhesion mechanisms are of primary concern to understand the pathogenesis of infectious disease and to develop strategies to combat these ailments. Of the many adhesion mechanisms that pathogens have evolved, cell surface glycoconjugates are one of the most common targets, which demonstrates the importance of both carbohydrate expression and pathogen specificities for these carbohydrytes.[12]

In addition to disease-causing pathogens, the diverse bacteria that inhabit our bodies outnumber our cells by more than a ten to one ratio.[13] The important roles that these bacteria, often collectively referred to as the indigenous microflora or the human microbiota, play in human physiology are becoming increasingly apparent, and we have only begun to understand the extent and mechanisms of their influence. The highest concentration of bacteria is found in the human gastrointestinal (GI) tract, where, like enteric pathogens, their colonization is often dependent on the carbohydrates expressed on the luminal epithelium and within the mucosa.[14]

Before exploring the role of carbohydrates in host-microbe interactions further, it is important to understand basic carbohydrate chemistry as well as where carbohydrates are found in biological systems.

1.2 Carbohydrate Chemistry

1.2.1   <u>Defining Carbohydrates</u>

The term carbohydrate, literally meaning "hydrate of carbon," was first used in the 19th century to describe molecules with the empirical formula of $(CH_2O)_n$. This formula no longer holds true because of the many molecules with different formulas which are now classified as carbohydrates. An improved, more specific definition is that carbohydrates are polyhydroxyaldehydes or polyhyrdroxyketones with three or more carbon atoms.[15] This definition arises from the two broad classes into which carbohydrates fall, namely aldoses and ketoses, so named because of the location and type of the carbonyl group in the monosaccharide. Aldoses are the most common, the general open-chain structure of which contains an aldehyde group (CHO) on one end, a primary alcohol (CH_2OH) on the other end, and a varying number of carbon atoms in between which are secondary alcohols (CHOH). Ketoses have a

primary alcohol on both ends of the open chain, and secondary alcohols and a single ketone (C=O) within the chain. Monosaccharides are the basic building blocks of carbohydrates and they can be linked together via glycosidic bonds to form disaccharides, trisaccharides, tetrasaccharides, and so on. The term oligosaccharide collectively refers to chains of two to roughly 10-20 monosaccharides, and anything larger is generally considered a polysaccharide. The distinction between the terms oligosaccharide and a polysaccharide is not clearly defined, but a rule of thumb is that oligosaccharides usually have a defined name for each of the structures – such as those that decorate proteins and lipids – and polysaccharides are much larger and often contain many repeating units.

Other generic terms for carbohydrates include sugar, saccharide, and glycan, which can all refer to monosaccharides, oligosaccharides, and polysaccharides. Exactly what each of these terms refers to can vary depending on the context and individual bias – some are more specific than others – but an important distinction is generally made for the term "glycan" to describe the carbohydrate portion of glycoconjugates; this convention is applied in this document.

1.2.2   Monosaccharides

Monosaccharides are the basic units of all carbohydrates. They contain a chain of at least three carbons and up to nine or more, but they are all characterized by the fact that they cannot be further hydrolyzed. The carbons within the open chains of monosaccharides, with the exception of the ketone in ketoses, are chiral centers, meaning that the carbon atom has two possible configurations (i.e. the hydroxyl groups can exist on either side of the chain). This gives rise to monosaccharide epimers, each one being a different molecule with unique properties. While monosaccharides do temporarily exist in the open chain form as described above, the equilibrium conformation in aqueous environments heavily favors the cyclic form.[15b] Intramolecular bonds with the carbonyl groups lead to five-sided ring structures known as furanoses or six-sided ring structures known as pyranoses. In addition to the multiple chiral centers, monosaccharides in their ring form can be further differentiated based on the position of the oxygen that is attached to the anomeric carbon.If the oxygen is in the axial position, the monosaccharide is in the α form; if the oxygen is in the equatorial position, the monosaccharide is in the β form.

While the majority of carbohydrates are found as oligo- or polysaccharides, the monosaccharide building blocks are important on their own. D-ribose and 2-deoxy-D-ribose form the backbones of RNA and DNA, respectively, in all living organisms. D-glucose is the most abundant monosaccharide found in

nature, owing to its central position in sugar biosynthesis; it is the final product of photosynthesis and most other sugars are derived from it. It is also the primary source of energy in cellular aerobic respiration. D-galactose and D-mannose are epimers of glucose (at the C4 and C2 positions, respectively), and are the two most prevalent hexapyranoses found in biology behind glucose. Fructose is the most common ketose, present in many fruit juices. Neuraminic acid (also commonly referred to as sialic acid, though this is technically incorrect because neuraminic acid is the N-acetylated form of sialic acid) is the most abundant residue on the terminal portion of the carbohydrates that decorate human cells, and since it is negatively charged at neutral pH, it is the primary reason that most cells have a net negative charge. In addition to these conventional monosaccharides, the hydroxyl groups can be replaced with other groups to form monosaccharide derivatives. The resulting structures include deoxy-sugars, sugar acids, amino sugars, sugar phosphates, nucleotide sugars, and sugar alcohols. Monosaccharides can also be modified on the anomeric carbon – which is either a hemiacetal or a hemiketal – via a glycosidic linkage with an alcohol.

1.2.3   Linkages Between Saccharides

If the alcohol that reacts with the anomeric carbon is the hydroxyl group of another monosaccharide, then the resulting molecule is a disaccharide. All oligo- and polysaccharides are also formed in this manner, where monosaccharide units are joined together by glycosidic bonds. The formation of a glycosidic bond is catalyzed by enzymes known as glycosyltransferases, which are highly specific for the particular sugars involved in the linkage. The bond between monosaccharides can occur in either the α or the β form, depending on the relative positions of the monosaccharide subunits. These differences have important biological consequences, a common example of which is the difference between α-linked and β-linked polymers of glucose. The α-linked glucose polymer is known as amylose (starch), which is soluble in water and can be broken down by mammals to be used as a food source. The β-linked glucose polymer, on the other hand, forms cellulose, which has a densely-packed tertiary structure that gives plants their rigidity, and mammals do not have glycosidases to digest it.

Multiple glycosidic linkages can be made to a single core monosaccharide through the multiple hydroxyl groups it contains. This leads to the possibility of highly-branched oligo- and polysaccharides, which is in contrast to nucleotides and amino acids, which can only form linear polymers. Together, the ability to form branched molecules, the many different monosaccharide building blocks, and the possibility of both α- and β-linkages allow a virtually limitless number of unique carbohydrate structures. It is illustrative to consider that three different nucleotides or amino acids can combine to create a total of

six possible trimers, whereas three different hexoses can produce up to 27,648 unique trisaccharides. This complexity increases exponentially, such that over one trillion combinations can result from just six different hexoses.[16] The large potential diversity is often cited as one of the primary reasons that glycobiology has lagged behind molecular biology. Other commonly cited reasons for this relative lag in scientific understanding of glycobiology are the difficulties involved with laboratory synthesis of carbohydrates and the lack of a direct template for biological synthesis (i.e. as compared to the DNA template for proteins). Thankfully for glycomics research, patterns are repeated throughout biological systems, so this complexity is not quite at the scale of trillions of carbohydrate structures, but it is still staggering.

1.2.4   Oligosaccharides

The term oligosaccharide is not clearly defined, but it generally refers to carbohydrate molecules containing between two and 20 monosaccharides that are not linked in a repeating pattern. Many commonly-occurring oligosaccharides have accepted but trivial names. These names are "trivial" because they do not specifically define the monosaccharides or the linkages that make up the molecule, but they are useful because of their reappearance in many biological systems. Biologically important disaccharides are a good example of this, a list which includes maltose (Glc(α1$\rightarrow$4)Glc), lactose (Gal(β1$\rightarrow$4)Glc), sucrose (Fru(α1$\rightarrow$2)Glc), and cellobiose (Glc(β1$\rightarrow$4)Glc). Trisaccharides are relatively common in nature, but larger oligosaccharides rarely exist in the free form. Instead, oligosaccharides with more than three monosaccharide units are commonly found on glycoconjugates and play critical roles in cell biology. For example, the oligosaccharides found on the exterior of red blood cells determine a person's blood type[8c] and human milk contains various oligosaccharide glycoconjugates that function not only as a food source for the infant, but they are also known to have an immunostimulating effect and they have been shown to act as pathogen antiadhesives.[17]

1.2.5   Polysaccharides

Polysaccharides are linear or branched polymers of monosaccharides that are generally characterized and distinguished from oligosaccharides by repeating patterns and large size. Polysaccharides can contain as few as 10-20 monosaccharide units but most are much larger and can have molecular weights as high as 10^9 daltons (Da).[16] The most common polysaccharides include starch, glycogen, cellulose, and chitin. Starch is synthesized by plants and acts as their principal food reserve; glycogen acts as the primary energy storage molecule for animals; cellulose is the major structural component in the cell walls of plants and represents the most abundant naturally occurring organic substance; and chitin

makes up the exoskeleton of invertebrates and can also be found in the cell walls of most fungi and many algae. Other biologically important classes of polysaccharides include glycosaminoglycans and heparin. Various glycosaminoglycans form ground substance, the gel-like matrix that helps give cartilage, tendon, skin, and blood vessels their elasticity. Heparin acts as an anticoagulant and it has become one of the most commonly used drugs in hospitals, but it is also naturally present in the body in the mast cells that line the walls of arteries.

1.2.6   Summary of Carbohydrate Chemistry Section

The basic carbohydrate chemistry described above sets the stage for a discussion of the functional roles that carbohydrates play in biology. Saccharides on their own are incredibly important and make up the majority of the Earth's biomass, but they are largely limited to passive roles such as structural support, protection, and energy storage. The true breadth of their functional roles becomes clear when the discussion involves glyconjugates – glycolipids and glycoproteins – where carbohydrates not only play structural roles but are also intimately involved in cell communication and signaling events. The large diversity of carbohydrate structures stems from the various epimers of monosaccharides and the many linkages that they can form.This diversity is harnessed in nature to add a new level of functional space via the modification of proteins and lipids, giving way to the many roles that carbohydrates play in mediating cell-cell, cell-matrix, and cell-molecule interactions.

1.3 Carbohydrates in Biology

1.3.1   Glycobiology

The field of glycobiology is concerned with the many functions of carbohydrates when they are attached to proteins and lipids. While the structural and energy storage roles that pure carbohydrates play are clearly important, they are generally considered to be outside this field of study. The term glycoconjugate refers to a protein or lipid modified with carbohydrates; the resulting molecule can contain just one monosaccharide or it can be predominantly composed of carbohydrates. It is important to note that the field of glycobiology is distinct from the classical central dogma of molecular biology, where proteins are built from an RNA code which itself is encoded in DNA. No such template exists for controlling glycosylation.

The ability to perform whole genome sequencing and the resulting publication of the human genome led to a few surprises, notably that all of the diversity in nature and the complexity of human biology is

contained within a relatively small number of genes. The human genome is thought to contain around 20,000 protein-encoding genes, which is a substantial number but still does not seem sufficient to account for the biological complexity of human physiology. Part of this complexity can be attributed to epigenetic factors, but it is now clear that carbohydrate modification of proteins and lipids adds an entirely separate level of functional space for these molecules.[18] Indeed, nearly all secreted and membrane-associated proteins are glycosylated.[19] The exact processes by which glycoconjugates are formed and the genetic and environmental determinants which control these processes are still not completely understood, largely because there is no clear genetic template like there is for the synthesis of proteins. Elucidating these pathways and understanding the many functions of glyconjugates is the thrust of glycobiology, and much progress has been made in the last few decades.

1.3.2   Forming Glycoconjugates

Glycosylation of proteins and lipids involves multiple enzyme-catalyzed reactions that sequentially add and sometimes remove glycans as the protein or lipid travels through the endoplasmic reticulum (ER) and the Golgi apparatus. As previously mentioned, this process is not directly controlled by the genetic code, but rather indirectly through the production of specific glycotransferases and glycosidases. These enzymes are highly specific for the two sugars that they attach or the bond that they cleave, such that one glycotransferase, for example, will only catalyze the formation of a glycosidic bond between two specific monosaccharides.[20] There are three different classes of glycoconjugates, differentiated by the type of glycosylation reaction that occurs. The first two classes are protein glycoconjugates, with the glycans being either N-linked or O-linked. The third class is glycolipids, for which there is only one known conjugation reaction. Once glycosylated, the molecules can remain within the cell (although this is less common), get embedded in the lipid bilayer of the cell membrane, or get secreted from the cell.

1.3.2.1   N-linked Glycosylation

Most glycoproteins are formed through N-linked glycosylation. The name comes from the fact that the glycans are attached exclusively to the amino acid asparagine (abbreviated with an "N") within the polypeptide backbone of the glyconjugate. The linkage is similar to the glycosidic bond formed between carbohydrates, but instead of attaching to a hydroxyl, the anomeric carbon is attached to the amide nitrogen of the asparagine side chain. N-linked glycosylation is further specific to asparagines that are found in a sequence of Asn-Xaa-Ser or Asn-Xaa-Thr, where Xaa is any amino acid except proline. These sequences must also be present on the outside of the protein and, as a result, N-linked glycans are never found buried within the protein core. N-linked glycosylation is initiated in the lumen of the ER and

proceeds through several steps where additional glycans are added and subtracted, after which the glycoprotein is advanced through the Golgi where more processing takes place. The step-wise addition and subtraction of glycans acts both as a way to build the glycan as well as a signaling mechanism to guide the glycoprotein to subsequent compartments where it undergoes additional modifications in preparation to be secreted from the cell or embedded in the cell membrane. While many of these steps are unique to the particular glycoprotein, there are some modifications that take place with all glycans. For instance, N-linked glycosylation is always initiated with the same precursor structure which has N-acetylglucosamine (GlcNAc) as the reducing sugar which gets attached to the asparagine in the β orientation. Much of this precursor is cleaved as part of glycan processing, but a pentasaccharide core structure remains attached to the protein, and all N-linked glycans have it.

1.3.2.2 O-Linked Glycosylation

O-linked glycosylation is less defined than N-linked glycosylation in the sense that the mechanisms of glycosylation are more diverse. The common trait that defines O-linked glycoproteins, however, is that it is initiated by the attachment of N-acetylgalactosamine (GalNAc) to the side chains of serine or threonine residues on a polypeptide backbone. Additional monosaccharides are added one at a time by glycosyltransferases, most commonly in the Golgi apparatus, but some O-linked glycans are also known to be added to proteins in both the cytoplasm and the nucleus of cells. The most abundant O-linked glycoproteins are mucins and proteoglycans, both of which rely on abundant glycosylation to give them the physical properties needed for the important biological functions that they serve, which will be discussed later.

1.3.2.3 Glycosylation of Lipids

Lipids are most often glycosylated in much the same was as N-linked glycoproteins. A nucleotide sugar donor attaches either a glucose or a galactose to the ceramide in the lumen of the ER, at which point the Glc-ceramide or Gal-ceramide is transported to the Golgi for further modification by glycosyltransferases and glycosidases. Almost all glycolipids (also called glycosphinoglipids) end up embedded in the plasma membrane, where the glycans serve similar cell-cell signaling and recognition roles as the glycans on membrane-bound glycoproteins. Glycolipids can also act as the anchors to which membrane proteins are attached, and these glycolipids have a unique synthesis pathway. The glycolipid, in this case a glycosylphosphatidylinositol (GPI), is created in the ER and the C-terminus of the newly-synthesized protein is attached to the free amine of ethanolamine that is attached to the terminal mannose residue on the GPI.

1.3.3 Functional Roles of Glycoconjugates

Carbohydrates attached to proteins and lipids play both intrinsic and extrinsic roles. The intrinsic functions are similar to the roles that pure carbohydrates play, which include acting as structural components (e.g. in cell walls and the extracellular matrix) and modifying the properties of proteins (e.g. directing protein folding, contributing to their stability and solubility, and sometimes altering their function). The extrinsic functions include directing the intracellular and extracellular trafficking of glycoconjugates, controlling cell-cell and cell-matrix interactions, and mediating and modulating intracellular and extracellular signaling.[8c] A common method for studying the role of a particular biomolecule or pathway is by using genetic knockout organisms, where the genes controlling the synthesis of the biomolecule or pathway of interest are removed so that its function can be better understood by observing the resulting changes. Interestingly, cell lines and single-celled organisms that have had important glycotransferases or glycosidases knocked out can still proliferate, seeming to suggest that glycosylation is not immediately important to the single cell. When these same pathways are knocked out in multicellular organisms, however, the development of the embryo is halted almost immediately, showing their importance in development.[8a, b] When glycosylation pathways are blocked in more mature organisms, widespreadmalfunctions, such as tumor growth, arise. In fact, many tumors are characterized by cells with faulty glycosylation pathways, which leads to tumor growth and metastasis.[21] In addition to their involvement in cell-cell and cell-matrix interactions, carbohydrates mediate interactions with the outside world. For instance, many microorganisms, both commensal and pathogenic, have evolved to recognize and bind carbohydrates expressed on the luminal surface of host tissues.[8b, 22]

The long list of carbohydrate-mediated interactions is entirely unsurprising, given that nearly all secreted and membrane-associated proteins are glycosylated, and a survey of the makeup of the cellular surface and the cell matrix reveals that they are abundant in carbohydrate-modified species (i.e. glycolipids, glycoproteins, and glycosaminoglycans) (Figure 1).[8c, 19, 23] Of particular interest to this work are the roles that carbohydrates play in mediating host-microbe interactions in the gastrointestinal (GI) tract.
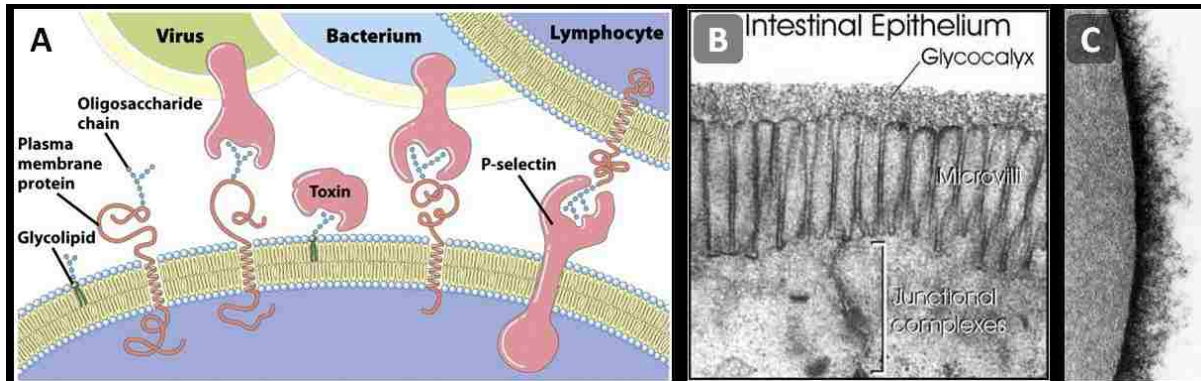
Figure 1. Cellular surfaces are covered in carbohydrates which perform a variety of functions. (A) Oligosaccharides (small chains of blue dots) are anchored to molecules in the plasma membrane as glycolipids or glycoproteins, where they mediate interactions with viruses, bacteria, and other cells.(Credit)[3] (B) The glycocalyx is the layer on top of the intestinal epithelium, that is largely composed of sugars.(Credit)[24] (C) The glycocalyx of a erythrocyte can be as thick as 140 nm.(Credit)[25] Both B and C demonstrate the abundance of carbohydrates on the cellular surface.

1.3.4   Glycan Expression in the Gastrointestinal Tract

Carbohydrates are abundant on the luminal surface of the GI tract, including glycosylated structures anchored to cells in the form of glycoproteins and glycolipids (the glycocalyx) as well as in the secreted mucus layer. The mucus layer, composed primarily of O-linked glycoproteins, acts as both a passive barrier to chemical insults and pathogens and as an active physiochemical sensor.[26] Despite the protective roles that glycans play in the GI tract, their abundance also serves as an opportune target for pathogenic bacteria to anchor themselves in an effort to colonize and infect the host.

The glycans in the gut are in a constant state of flux, with their expression changing both spatially and temporally as a function of genetic and environmental factors.[27] For instance, the expression of glycans in the infant gut changes as it develops and its diet is altered, which leads to changes in its GI microbiome.[27-28] On the other hand, changes in the secreted and cell surface-expressed glycans can also occur in response to bacterial colonization.[29] This interplay between genetic and environmental determinants of glycosylation, where each influences the other through a variety of mechanisms, introduces a complex dynamic to consider when studying host carbohydrate-microbe interactions.

1.3.5   Carbohydrates and the Indigenous Microflora

Various non-pathogenic bacteria, which make up the human microbiota, are known to bind carbohydrates,[30] and it is becoming increasingly clear that the gut microbiota is an important factor in human health.[31] The highest concentration of bacteria that form the indigenous microflora is found in the human GI tract where they aid in the digestion process and provide a source of key nutrients. More

recently, however, research has shown that GI bacteria can have other widespread effects on our bodies and our overall health, including acting as a defensive barrier against pathogenic bacteria[32], influencing drug metabolism and toxicity,[33] and modulating our immune system.[14, 34] In addition, each person's microbiota is different, the composition of which depends on a variety of environmental, genetic, and additional unknown factors.[35] The full extent of the consequences of these differences is far from being understood, but the gut microbiota has been directly linked to pathological conditions such as obesity,[36] circulatory disease,[37] and inflammatory bowel diseases.[38] Thus, an improved understanding the role of the microbiota in human health and disease presents many opportunities to develop new prophylactic and interventional strategies for improving health and combating pathologies. It is especially relevant to the ever-growing field of personalized medicine.

The symbiotic GI microbiota has an interdependent relationship with the carbohydrates expressed on the luminal surfaces of cells and within the mucosa, wherein carbohydrate expression can be both a prerequisite to microbe colonization and a determinant of colonization.[14, 22a, 39] For example, during child development, the species makeup of the GI microflora shifts in response to changes in both the expression profiles of epithelial glycans and the glycans that are found in breast milk.[28] Conversely, it has been shown that the intestinal microbiota are important in developing and maintaining the gut mucus layer and normal glycosylation states.[29a, 40] This cross-talk between gut microbes and the host glycosylation pathways reveals the mutualistic dependencies that mammals and microbes have evolved, further increasing the awareness of the importance of the microflora in human health and supporting the development of new tools to study carbohydrate-mediated host-microbe interactions.

1.3.6 Carbohydrate-Mediated Host-Pathogen Interactions

In the case of infectious disease causing bacteria, binding to carbohydrates is often the first step of pathogenesis, particularly in areas of the body such as the GI tract where mucosal surfaces are constantly shed and washed by fluids.[41] In order to colonize and infect the host, pathogens must resist this constant efflux of the gut contents, so the high density of glycan epitopes makes them ideal targets for adhesion. This behavior is not limited to the GI tract, as it can be found in other areas of the body where fluids and mucosal surfaces are constantly washed away. *Kelbsiella pneumonia*, a common cause of pneumonia in humans, is known to have mannose binding specificities in respiratory tissue, and uropathogenic *E. coli* bind mannosylated glycans in the urinary tract.[12b] Interestingly, binding of uropathogenic *E. coli* to mannose receptors is actually enhanced by the shear forces of the fluids passing

through the urinary tract through the shear-activated "catch bond" of the mannose binding lectin FimH.[42]

Table 1 shows an abridged list of pathogenic bacteria and bacterial toxins that have known carbohydrate binding specificities, demonstrating the widespread nature of these interactions. Among the bacteria in this table, *Campylobacter jejuni* and *Salmonella enterica* are the two most common bacteria that cause foodborne illness worldwide.[10a] *Helicobacter pylori*, a human enteric pathogen that binds to the Lewis[b] blood group antigen expressed on cells in the stomach epithelium (Figure 2), is carried by 50% of the population in the developed world and 80% of the population in the developing world.[43] In nearly 20% of infected individuals, *H. pylori* leads to conditions such as chronic active gastritis,[44] gastric and duodenal ulcers,[45] and gastric adenocarcinoma.[46] An important observation from Table 1 is that many of these bacteria have multiple known carbohydrate specificities – *H. pylori* alone has 10 distinct specificities,[12a] thought to be important in the multiple stages of binding, colonization, and cell entry that this pathogen is known to have.[26] The multiple and dynamic carbohydrate specificities of pathogens makes the task of developing anti-adhesives to prevent infection all the more difficult, but it emphasizes the importance of developing tools that can identify and study these interactions in a high-throughput manner.
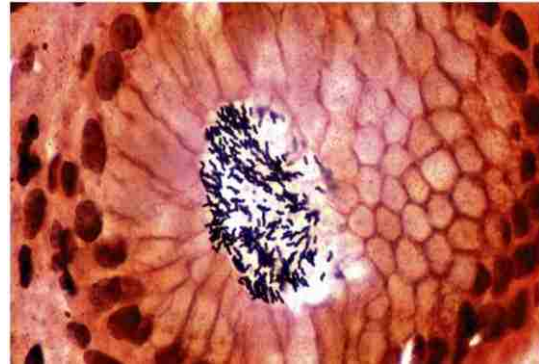
Figure 2. H. pylori binds to the the surface of the stomach through interactions between lectins on the bacteria and Le[b] oligosaccharides. (Credit)[3]

Table 1. Specific examples of host-pathogen interactions mediated by carbohydrate host receptor targeting of bacterial adhesins/antigens. The following bacterial pathogens and toxins are among the most prevalent causes of foodborne illness and have been listed as Category B biothreat agents due to their role in food safety.

Bacteria/Toxin	Carbohydrate-Containing Receptor(s)	Lit
Burkholderia pseudomallei (melioidosis)	GM1 and GM2 gangliosides	47
Campylobacter jejuni	Fucosylated oligosaccharides	2
Clostridium botulinum toxin (Botulism)	Gangliosides	48
Clostridium difficile	Mucus, Glc, Gal, Lac	49
Coxiella burnetii (Q fever)	CR3 integrin	50
Escherichia coli (EHEC, O157:H7)	Man	51
Escherichia coli (EPEC)	Oligosaccharides, gangliosides (GM3)	52
Escherichia coli spp. (S fimbriated)	Sialyllactose, Mucins	53
Helicobacter pylori	NANA, Lewis antigens, sialyllactose, gangliosides	54
Salmonella enterica	Man, Fuc, Gal	55
Shigella	NANA, Man, Fuc, NAc-mannosamine	56
Shiga toxin	Globotriaosylceramide (Gb3)	57
Stable Toxin (from *E. coli*)	Fucosyloligosaccharides	58
Staphylococcus enterotoxin B	Galabiosyceramide	59
Vibrio cholerae	Man, Fuc, Mucus, Nac-D-glucosamine, glucosamine, Man-Glu	60
Vibrio cholerae toxin	Fucosylated oligosaccharides, gangliosides, sialyllactose	52b, 61
Yersinia enterocolitica	Mucin carbohydrates, Gal, GalNAc	62
Yersinia pestis (plague)	GM1A, GM2A (gangliosides), lactosylceramide	63

1.3.7   Carbohydrate-Based Bacteria Anti-adhesives

The use of carbohydrates as prebiotics and as pathogen anti-adhesives is not a novel approach for establishing and maintaining a healthy gut microbiota – such a system has evolved naturally in the form of human breast milk. Milk glycans form the third largest solid component of breast milk behind fat and lactose. The monosaccharide L-fucose (6-deoxy-L-galactose), one of the building blocks of the ABO(H) and Lewis antigens, is also an essential component in human milk.[41] The benefits of breast-feeding for infant health have long been known[64] – a 1934 study of 20,000 mother-infant dyads found that morbidity or mortality due to enteric disease was significantly higher for infants who were not breast fed.[65] While the infant's immune system develops,
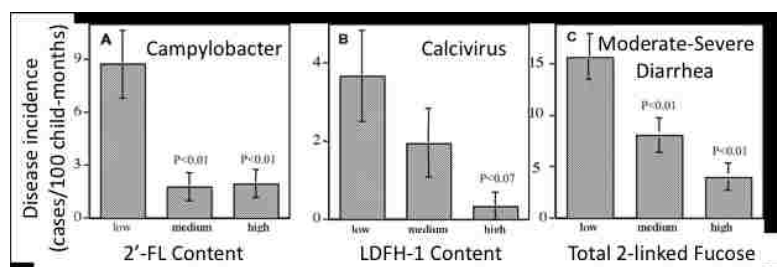
Figure 3. The incidence of diarrheal disease in breastfed infants is inversely proportional to the concentration of fucosylated oligosaccharides in human milk. (Credit)[1]

components in breast milk such as sIgA, lactoferrin, lysozyme, haptocorrin, and triglycerides provide protection against invading pathogens either through direct mechanisms or due to downstream products from the digestion of these molecules in the infant gut.[17b] In addition to these components, soluble milk glycans that mimic the glycans expressed on cell surfaces within the infant GI tract have been shown to inhibit infection from enteropathogens and are associated with protection against infant diarrhea.[66] Breast milk has also been shown to stimulate gut colonization by bacteria that have a positive effect, thus also acting as a prebiotic.[67] Among these milk glycans, L-fucose, in the form of 2'-fucosyllactose (2'FL), has been identified as having a particularly important role in preventing diarrhea in breast-fed infants (Figure 3).[1, 68] It is hypothesized that the protection is due to fucosyoligosaccharides in the breast milk competitively inhibiting pathogens from binding to the glycans expressed in the mucins and glycocalyx in the infant gut. A variety of enteric pathogens recognize fucosylated epitopes, including *H. pylori*, *C. jejuni*, and enterpathogenic *E. coli* (EPEC) (Figure 4). Further, the presence of 2'FL and other oligosaccharides in breast milk and glycan expression on the cells in the infant GI tract is genetically determined and related to blood type.[69] In epidemiological studies, our collaborators have shown that infants that do not express 2'FL on their cells (non-secretors) and that are breast-fed from mothers who have L-fucose in their breast milk (secretors) have the lowest incidence of diarrhea. When the opposite is true (i.e. secretor infant, non-secretor mother), the highest incidence of diarrhea is observed.

Discoveries such as these have prompted increased efforts to investigate carbohydrate-based anti-adhesives for a variety of pathogens.[17d, 54f, 70] Given the problem of ever-increasing antibiotic resistance, carbohydrate anti-adhesives are particularly attractive because they do not kill or arrest the growth of pathogens or normal gut bacteria, and, therefore, do not exert the same level of selective pressure that antibiotics do. Glycan-based inhibitors are also likely to make the FDA's list of GRAS (Generally Regarded as Safe) substances, so regulatory hurdles are less daunting. Two other benefits of glycan-based therapeutics are that they are soluble and they are stable in ambient conditions. One of the current challenges facing anti-
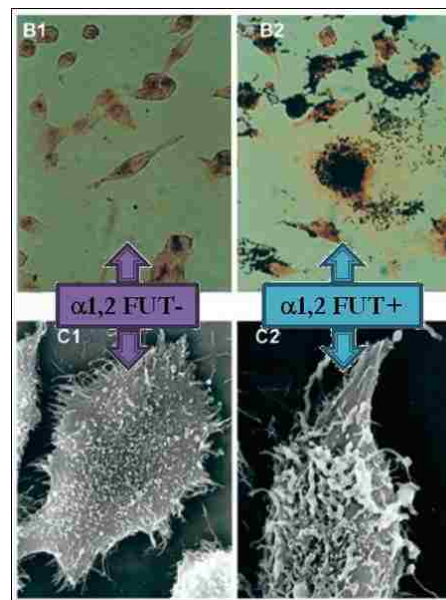
Figure 4. *C. jejuni* bind to CHO cells that express fucosylate epitopes, as indicated by the black dots (top right) and the spiral shaped rods (bottom right) on the bacterial surface. (Credit)[2]

adhesive therapies is the difficulty of producing these molecules on a large scale. However, Glycosyn, Inc. (Medford, MA), has developed methods to synthesize α1,2-fucosylated oligosaccharides and glycoproteins using bacteria and yeast on a large and economically-feasible scale in order to combat infant and childhood diarrhea. Developing a biosensing platform to test the inhibitory strength of their materials will be of benefit in studying the effect that multivalency has on the anti-adhesive's inhibitory potential.

1.4 Methods for Studying Bacterial Adhesion to Carbohydrates

The critical role that adhesion plays in bacterial colonization and pathogenesis has led to a variety of methods for studying such adhesion events, ranging from routine laboratory assays such as agglutination and ELISAs to more complex technologies such as microarrays. Haemagglutination and ELISAs have been used for determining the 50% inhibitory concentration (IC_{50}) of multivalent mannose derivatives for preventing *E. coli* HB 101 binding to erythrocytes and yeast mannan,[71] demonstrating the utility of these assays for testing binding inhibitors. In this case, the investigators were working with the well known interaction of FimH, a fimbrial lectin expressed by this strain of *E. coli*, and mannose. A seminal paper that identified intestinal H(O) antigen (a fucosyloligosaccharide) as a binding epitope for *Campylobacter jejuni* demonstrates the difficulty of using these traditional assays for elucidating bacterial carbohydrate specificities.[2] The authors' investigation began with the knowledge that complex carbohydrates in breast milk protect infants from diarrhea caused by campylobacter infection. Fucose-containing carbohydrates were thought to be excellent candidates for the binding epitopes for *C. jejuni* because of their high concentration in breast milk and their presence on gut epithelial cells. The authors tested their hypothesis by developing a cell-binding assay, which used Chinese hamster ovary (CHO) cells transfected with human glycotransferases such that the CHO cells would express different fucosylated glycans on their surface. While this assay helped identify a specific fucosylated epitope that mediates the attachment of *C. jejuni* (Figure 4), the labor involved to conduct these studies was daunting. Each of the CHO cell lines had to be created and validated for glycan expression prior to the bacterial binding assays, and the authors had the advantage of previous research that limited the candidate library to just a few structures.

The amount of time that is required to prepare the components of the assay – whether it is a cell line or an animal model genetically modified to express the glycans of interest – is not compatible with studies

that are aimed at screening for binding partners between an array of carbohydrates and multiple strains of bacteria. For example, in order to screen for carbohydrate binding targets for a single bacterial species using *in vitro* cell binding assays, a unique cell expression system must be developed for each carbohydrate. While the assay itself is relatively straightforward to perform, the complex regulation of glycosylation makes creating cells expressing particular glycans a challenge unto itself. ELISAs represent an important step in the direction of high-throughput, but they are still laborious and require large amounts of precious carbohydrate reagent. An additional challenge of studying carbohydrate-mediated bacterial interactions is the fact that the affinity of glycan binding proteins for their glycan ligands is weak, with dissociation constants (K_d) ranging from 1-1000 µM.[72] In biological systems these relatively low binding affinities are counteracted by multivalent interactions,[73] but these interactions are more difficult to measure so experimental platforms must take this into account.[74]

The consumption of the carbohydrate reagents is closely related to the throughput of an assay, and it is an important consideration when conducting these studies. Glycan binding targets must be either isolated from natural sources or created synthetically, both of which are far more challenging than obtaining reagents such as nucleic acids or proteins. As has been mentioned, glycosylation is not template driven, and there is no viable amplification method as there is for nucleic acids (i.e. PCR). Assays that consume the smallest amount of carbohydrate-based reagents are therefore of foremost importance if experimental throughput is to reach necessary levels for screening many bacterial species for their glycan binding targets.

Carbohydrate microarrays provide the glycomics community with an answer to the issues of assay throughput and reagent consumption. Immobilized nucleic acid,[75] protein,[76] and carbohydrate microarrays [77] have become instrumental research tools for conducting high-throughput studies of binding interactions. In addition to the ability to conduct multiplexed analysis, microarrays can be fabricated using small volumes of reagent (pl to nl volumes per spot; 1 µg of a glycan is sufficient for printing up to 100 glycan arrays [72]), and the 2-dimensional presentation of binding ligands mimics the cell surface.[22b] While DNA and protein microarrays have been and will continue to be valuable research tools, glycobiology may stand to benefit the most from microarray technology: the structural complexity of carbohydrates and the difficulties involved with their synthesis necessitate high-throughput and low-volume reagent consumption, respectively.[78] Many glycomics researchers have pursued the opportunities that carbohydrate microarrays offer, and two large consortiums have been formed to facilitate the large scale multidisciplinary efforts that are needed to make advances in this field. The

Consortium for Functional Glycomics (CFG, www.functionalglycomics.org) and the UK Glycochip

Consortium (www.glycochips.org.uk) provide a variety of resources, including open access to glycan

libraries that researchers can use in their microarrays, pre-functionalized microarrays, array analysis

services, and a repository for data collected from these experiments. Among the growing applications of

carbohydrate microarrays are studies on microbe interactions with glycans.[72, 74, 78a, 79]

The majority of microarray technology, however, relies on a secondary reporter, usually a fluorophore,

to detect binding events. The shortcomings of requiring a secondary label are discussed in more detail in

Chapter 2, but labels generally increase the cost and time to conduct assays and they can prevent

quantitative measurements. An ideal platform is one that combines high throughput, low reagent

consumption and a label-free method for detecting binding. Carbohydrate microarrays are also limited

in the amount of information that they provide. They are ideally suited for high throughput screening for

binding specificities, but they do not provide the same depth of information that can be garnered from

bacterial-cell adhesion assays or *in vivo* experiments. In order to fully characterize the role of

carbohydrates in host-microbe interactions, it is clear that a multiplicity of methods needs to be

employed. For example, carbohydrate microarrays would be used to screen glycan libraries for bacterial

binding specificities, which could then be confirmed using bacterial adhesion to cells genetically

modified to express the glycan(s) of interest, at which point clinical samples or animal models could be

used to understand the bacteria-glycan interaction in a physiologically-relevant environment.

1.5   Conclusions

The many roles that carbohydrates play in biological systems stem from the inherent diversity in

carbohydrate structures – modifications of proteins and lipids with this diverse class of biomolecules

adds additional levels of functional control. The abundance of carbohydrates on cell surfaces and on the

luminal surface of the respiratory, urinary, and gastrointestinal tracts makes them common targets for

bacterial adhesion. Despite knowledge of the importance of carbohydrate-mediated bacterial adhesion,

there is a paucity of research tools for identifying and studying these interactions. With the exception of

carbohydrate microarrays, most of the tools suffer from high resource consumption (reagents, time, and

labor), precluding their use as high-throughput assays. Given the diversity of microorganisms and the

complexity of carbohydrate expression profiles in humans, the first challenge lies in identifying the

carbohydrate specificities of pathogens. Once pathogen-receptor binding partners are known, improved

methods will be needed to further characterize these interactions and to quantitatively screen binding inhibitors for their abilities to prevent this first step of pathogenesis. A biosensor capable of screening pathogens against many carbohydrate structures at one time would help address the challenges of identifying binding partners, understanding bacterial adhesion, and developing anti-adhesives. A high-throughput biosensor could also find applications as a diagnostic tool, particularly if it could be adapted for a point-of-care (POC) setting.

2. CHAPTER 2: OVERVIEW OF BIOSENSING TECHNOLOGIES

Biosensing technology is as diverse as the applications to which biosensors are applied. It is therefore difficult to clearly define a biosensor, but a broad definition describes a biosensor as a device that converts a biological event to a digital output signal. Converting biological events to an output signal relies on a transducer, which is normally functionalized with some bioactive component which facilitates binding between complementary biomolecules. The transduction mechanism can be electrochemical, mechanical, optical, piezoelectric, or magnetic, and the many manifestations of transducers that have been reported are the primary driver behind the diversity of biosensor technology. The following chapter addresses the requirements and desired features of biosensors for biomedical applications, emphasizing the goal of realizing fully-integrated and distributable lab-on-a-chip (LOC) devices. Silicon photonics is highlighted as an advantageous technology for such LOC applications, particularly for label-free optical biosensing. In addition, other label-free biosensors, including electrochemical, mechanical, and optical biosensors, are described through a brief survey of current research in the field. Finally, some considerations for performing biosensing experiments are discussed, ranging from sensor functionalization to data analysis. The intention is to provide a perspective on the field of biosensing such that one gains an understanding of the general capabilities and performance constraints of biosensing platforms, including those described in Chapters 3 and 4 of this document.

2.1 Introduction

Sensors, in their most general form, measure signals from the environment for interpretation and analysis, with the objective of providing actionable information to the user. A biosensor is any device that converts a biological event – typically, but not limited to, binding between complementary biomolecules – to an output signal that can be analyzed to describe the sensed event. Converting biological events to an output signal requires some form of a transducer – which can be electrochemical, mechanical, optical, thermometric, piezoelectric, or magnetic – that is modified with a biological material, a biologically derived material, or a biomimic to act as the capture reagent for the analyte of interest. Biosensors have found widespread applications in medical research, healthcare, environmental monitoring, chem-bio defense, and food safety. In biomedicine, biosensors are used for discovering new drugs, elucidating biological pathways, and studying biomolecular interactions. Within the healthcare setting, biosensors can be implemented as biometric assays and can serve as diagnostic tools,

potentially predicting disease or suggesting disease susceptibility when combined with genetic screening. Biosensors are also used for environmental monitoring, such as detecting the presence of specific allergens or environmental contaminants and for biological threat agents such as anthrax, ricin, or other toxins. While this chapter focuses on considerations for biosensor design in medicine (research, diagnostics, etc.), nearly all of the devices discussed have far-reaching applications beyond the exclusive domain of biomedical research. For instance, a biosensor for detecting malaria could also be modified to detect pathogenic organisms in food, as an environmental sensor, or as a research tool to screen for bacterial binding inhibitors to prevent infectious disease.

2.2 Characteristics of an Ideal Biosensor

The ideal biosensor, within the realm of biomedicine, should: rapidly detect any analyte of choice from a low-volume, unprocessed sample; be disposable or contain reusable low-cost components; require minimal training; integrate the source, transducer, and detector into a single portable device; allow long-term storage in ambient conditions; and produce a readout that allows the user to make an appropriate decision (e.g., quantitative readout of the amount of target analyte in the sample). While such an ideal biosensor has not been realized, it is useful to keep the desired characteristics in mind when discussing biosensors. It is also important to note that all of these qualities are not required for a technology to have value, and that what determines whether a biosensor is "ideal" or not will depend heavily on the specific application of the biosensor. Given the current state of biosensing technology, there are many trade-offs that must be considered for any given application since certain desired features conflict with each other. For example, if high detection sensitivity is the main requirement, the ability to use unprocessed samples decreases and the cost and operator expertise required are both likely to increase. Despite these conflicting design constraints and requirements, incremental steps toward an integrated biosensing platform could still have important applications. Simplifying the operator requirements and allowing use with unprocessed samples, for instance, would significantly improve the utility of diagnostic biosensors in a clinical setting.

The biosensors described in Chapters 3 and 4 are good examples of how incremental improvements on existing technologies and experimental protocols can facilitate research. Importantly, we consider a biosensing platform to be more than just a sum of its components, but also the methods that are used for operating the biosensor for a particular assay. Advances in a biosensing technology can thus

encompass improved functionalization techniques and operational protocols that influence the desired features of a biosensor.

2.2.1   Sensitivity and Selectivity

A biosensor must, first and foremost, be selective for the target it is designed to detect and sensitive enough to detect it. While seemingly obvious, understanding the limitations of different types of biosensors is necessary in order to choose the right platform to achieve the desired outcomes. A biosensor's selectivity, also commonly referred to as the specificity, describes its ability to accurately detect the target for which it is designed. The sensitivity of a biosensor, simply defined, is the degree to which the signal changes in response to a change in the sensor's environment. This is also commonly referred to as the responsivity of the sensor. The selectivity is primarily determined by the deposition of a bioactive surface onto the transducer, which is also called the functionalization method. On the other hand, the sensitivity of a biosensor is determined both by the functionalization method and it is also an intrinsic feature of the transducer itself; no matter the sensing mechanism (e.g. mechanical, optical, etc.), all transducers have a lower sensing threshold below which no meaningful signal will be obtained. This illuminates an important distinction between the different ways that the sensitivity of a biosensor can be defined. The first describes the sensitivity of the sensor to detect changes in the environment irrespective of a binding interaction – this is the inherent sensitivity of the transducer. For instance, the sensitivity of an optical transducer is described by the signal generated by a change in the refractive index within the sensing region. For a mechanical biosensor, the transducer's sensitivity is described the by the change in signal due to a given change in mass on the sensor surface. The second way to define the sensitivity is the change in signal generated by specific binding of the analyte of interest to a functionalized sensor. In this case, the sensitivity takes into account the specific interaction that the biosensor is designed to detect. A simple way to distinguish between these two definitions of sensitivity is to refer to the former as the "transducer sensitivity" and the latter as the "assay sensitivity."

A common method of improving assay sensitivity is the incorporation of amplification steps into the assay, but the amplification still must be large enough to exceed the transducer's limit of detection (LOD), and it is generally more desirable to eliminate any amplification steps. It is clear from this that the sensitivity is intimately tied to the LOD. Important to both the selectivity and sensitivity of the biosensor is its ability to differentiate between background noise and non-specific binding events of non-target molecules. Most biosensors, therefore, incorporate blocking methods to prevent such interactions from occurring.

A final subtlety regarding the definitions of sensitivity and specificity relates to how these terms are used in statistics for classification. In this context, the sensitivity of a classification system refers to the ability of the test to identify "positive" results, and it is calculated by dividing the number of "true positives" by the sum of the "true positives" and the "false negatives." Conversely, the specificity describes the ability of the test to identify "negative" results, and it is calculated by dividing the number of "true negatives" by the sum of the "true negatives" by the "false positives." In the case of statistical classification systems, the specificity is a clearly defined term, and selectivity cannot be used interchangeably as it is when describing a biosensor. While these definitions of sensitivity and specificity are relevant for biosensors that are used in classifying groups of samples or patients (e.g. disease state vs. healthy), the use of these terms in this document is limited to the definitions of sensitivity and specificity/selectivity as they refer to the biosensor itself, and not the biosensor's application to classifying samples.

With the hope of using unprocessed samples such as saliva, blood, urine, or other bodily fluids, the analyte to be detected will usually be at low relative concentrations within the complex biological milieu of cells, proteins, lipids, and salts found within a typical biological sample. A comprehensive study of potential cancer biomarkers reported that 88% of cancer biomarkers found in plasma (out of 211 surveyed) are below 10 μg/ml, and 49% are below 10 ng/ml.[80] As a comparison, common plasma proteins such as albumin and fibrinogen exist at mg/ml levels, and the salinity is roughly 150 mM. Even when sample processing is an option in a properly-equipped laboratory, it can be laborious and time consuming, and the motivation for using unprocessed or minimally-processed samples reemerges. Rapid testing and analysis is of the utmost importance in a clinical setting, where diagnostics can be used to guide medical intervention, significantly influence patient outcome, and dramatically reduce the time and cost associated with patient care.

In many research contexts, including the biosensor platform development described in Chapters 3 and 4, analytes are spiked into buffers at known concentrations and well-characterized binding interactions are used – a much different scenario than the one given above where analytes must be detected from unprocessed physiological samples. This is done to limit the experimental variables in order to isolate the interaction of interest or to validate the experimental methods. Even in such cases, selectivity and sensitivity is of the utmost importance to obtain meaningful information from the biosensor platforms.

2.2.2 Label-Free

It is desirable to detect target analyte without the need for a label for detection. In biosensors and diagnostic assays, the label is usually a chromophore, fluorophore, or enzyme that is either directly attached to one of the interacting molecules or attached to a secondary reporter molecule in order to amplify the signal generated by binding (Figure 5A). While assays that employ labels continue to find widespread use in research and medicine – take, for instance, the ubiquitous enzyme-linked immunosorbant assay (ELISA) – there are many reasons why it is desirable to eliminate the indicator (Figure 5B). Labeling increases the time and cost of an assay, it may alter binding interactions[81] and it may obscure quantification.[82] Labels can be unstable molecules that require careful storage, and this makes assay standardization difficult and limits their use in a POC setting. Finally, when the target analyte is unknown, such as high-throughput screening of molecular libraries, labeling may not be an option. Label-free biosensors can decrease cost and assay time; provide quantitative information of unaltered binding interactions in real time; and potentially enable portable biosensing of unprocessed samples. The lack of a label, however, may reduce assay sensitivity and require on-chip controls to ensure that signals being analyzed are due to the analyte and not non-specific interactions with the sensor.
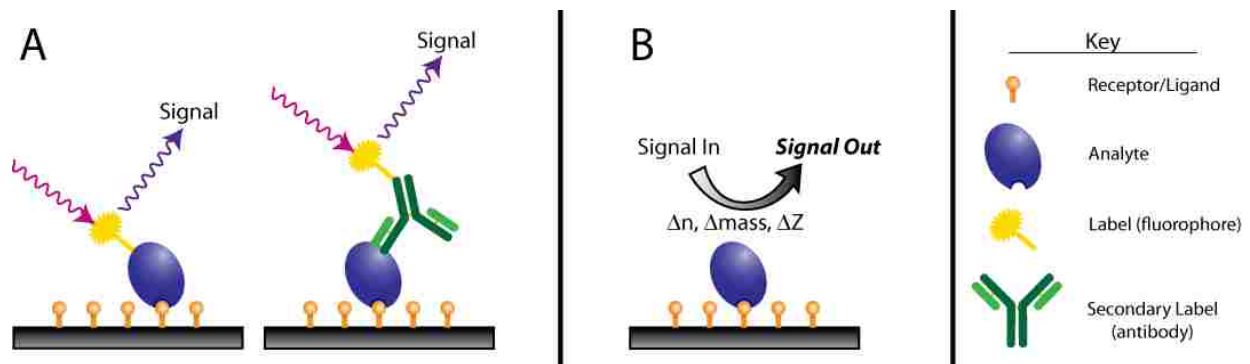
Figure 5. Label-based and label-free biosensing differ by the means with which the analyte is detected. (A) Example of label-based sensing via a fluoscently-labeled analyte or secondary probe (antibody). (B) Illustrates label-free biosensing, where an inherent property of the analyte, such as refractive index (n), mass, or impedance (Z), alters the input signal such that detection can occur.

2.2.3   Multiplexing

Multiplexing describes a biosensor's ability to run multiple assays simultaneously (Figure 6), which requires that the sensor "chip" contains multiple sensors or sensing regions, each of which can be interrogated independently. Even in basic experiments, where a single analyte of interest is present in buffer and a single complementary ligand is used to capture the analyte, it is highly preferential to have on-chip controls consisting of non-complementary ligands in order to demonstrate that any detected binding between the analyte and the ligand is specific. For screening applications and disease diagnostics, the ability to test for multiple binding interactions is very useful. Disease states are often described by multiple biomarkers, and the ability to provide a conclusive diagnosis is reliant on taking a systems approach of measuring the concentrations of more than one biomolecule.[83] A good example of the dangers of relying on a single biomarker for disease can be found in prostate specific antigen (PSA), an FDA-approved cancer biomarker, which was once widely thought to be a direct indicator for prostate cancer. As a result, researchers developed a number of diagnostic assays and recommendations for diagnosing cancer based on the detected concentration of PSA. However, it became apparent that PSA levels varied widely between individuals and it served as a poor indicator for the presence or prognosis of cancer.[83a, 84] Investigators have found similar poor diagnostic values for the remaining eight FDA-approved cancer biomarkers, highlighting a shortcoming of single biomarker-based diagnostics.[80] In contrast, a systems approach operates on the hypothesis that disease introduces perturbations that alter biological networks; the resulting changes are widespread, being reflected in the levels of multiple proteins and other biomarkers present in the body. Considering the complexity of a physiologic system, it is clear why multiple biomarkers may be needed to diagnose disease.
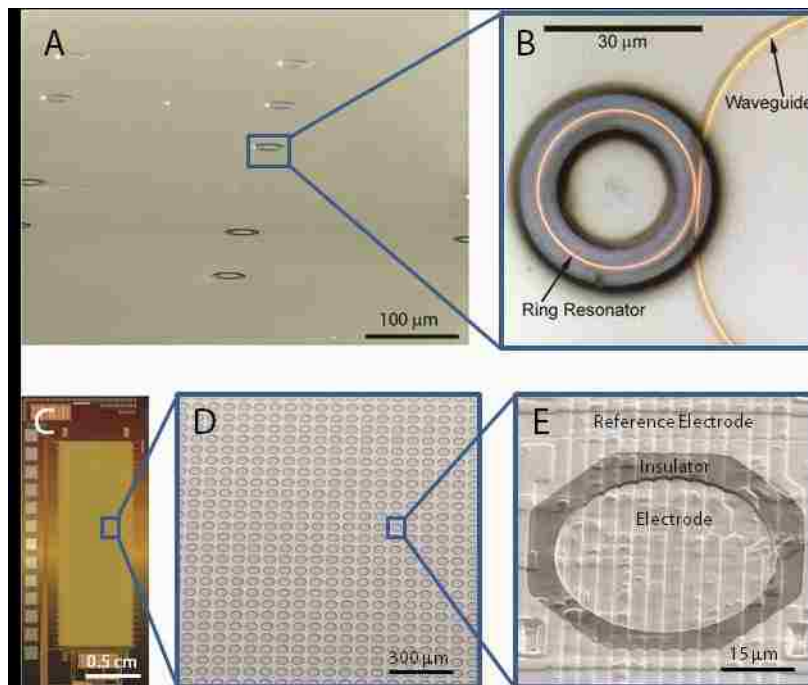
Figure 6. Two examples of multiplexbile biosensor platforms, both of which are used in this research. (A) Each donut-shaped depression seen in the scanning electron micrograph represents an individual microring resonator (B) exposed through lithographic etching of a polymer coating. Microrings are interrogated with a bus waveguide that comes within 100nm of the resonator. C-E illustrate a commercial microelectrode array manufactured by CustomArray, Inc. (Mukilteo, WA). The array contains 12,544 individually-addressable microelectrodes. Each electrode is 44 µm across and is separated from the reference electrode by an insulating layer (E). Photo Credits: (A) Nanophotonics Laboratory, University of Washington; (B) Tate Owen; (C) CustomArray, Inc.; (D,E) Authors

In addition to accurately diagnosing single diseases, multiplexible biosensors could be used to screen for multiple diseases or pathogens at once, which would be especially useful for POC applications where resources are limited and visits to the clinic are rare. In the case of pathogen detection, multiple tests may be needed to positively identify a pathogenic organism. Currently, diagnosticians employ various culture and biochemical tests, requiring days to reach a positive conclusion. The most accurate tests rely on polymerase chain reaction (PCR), but this process is prohibitively expensive and unavailable in areas of the world where such tests are most needed. As an alternative to pathogen detection based on nucleic acid assays, many pathogens can be uniquely characterized by their ligand binding affinities and antigenic profiles; [8a, 79, 85] a quantitative biosensor containing a panel of known pathogen-binding ligands and antibodies could detect the presence of these pathogens from patient samples.

In biosensor design, multiplexing requires multiple sensors or multiple sensing regions that can be differentially functionalized and interrogated. Microarrays using DNA,[86] proteins,[87] and carbohydrates[77b,]

[c, 78b, 88] provide an excellent example for the potential of high-throughput screening, yet they almost always rely on using a fluorescent label that can be detected on commercial microarray readers.

2.3 Label-Free Biosensors

As previously discussed, biosensors that do not require labeling of the target molecules significantly increase the potential applications and the amount of information that can be obtained from their use. Label-free biosensing facilitates quantitative real-time binding analysis of unaltered analyte and makes it possible to use unprocessed samples, thus enabling high information content POC and distributed devices. Instead of using a label, these biosensors rely on inherent properties of the target such as impedance, mass, or refractive index to measure binding. Silicon-based optical biosensors are the focus of the following discussion because of their novelty and their prominent role in this research, but electrochemical and mechanical label-free biosensors are discussed as well in order to paint a broader picture of the field. Many of the technologies have potential for realizing fully-integrated platforms and stand to benefit from some of the same fabrication and integration capabilities provided by silicon-based biosensors.

2.3.1 Electrochemical Biosensors

Generally speaking, electrochemical biosensors operate by detecting the change in the resistance or capacitance on an electrical sensing component in response to the formation of binding complexes or to environmental perturbations. The most prevalent and well-known example of electrochemical biosensors are those used in the majority of glucose monitors.[90] However, all of these devices, along with most electrochemical biosensors for other applications, possess limited sensitivity and require the use of an electroactive indicator to generate a detectable signal.[90-91] Nonetheless, electrochemical biosensors remain attractive because they can be mass produced at low costs, they have low power requirements, and they can be scaled down to allow miniaturization and multiplexing.[92] Given these benefits, there are significant ongoing efforts to improve label-free electrochemical biosensors, through the construction of more sensitive nanoscale devices based on nanowires, nanotubes, and nanofibers.[93]

2.3.1.1 Electrical Impedance Spectroscopy with Microelectrodes

Electrical impedance spectroscopy (EIS), in the case of affinity biosensors, measures the change in the impedance of an electrical circuit due to the binding of analyte to a functionalized electrode. EIS is favored over voltammetry and amperometry because the measurement technique is less damaging to

the biofunctional capture layer.[92] The electrodes used for EIS can also be miniaturized and multiplexed.[94] A significant advantage of microelectrodes is that by applying a current or voltage at the electrodes, one can create localized reaction environments – this opens up the possibility of on-chip synthesis and functionalization in a highly multiplexed fashion. Despite these examples, performance with EIS sensing regimes is tied to the properties of the electrodes, and it remains unclear how binding can be quantified and how miniaturization may alter the equivalent circuits used to describe binding.[92] Further, due to the lower sensitivity of label-free EIS, there exists a limit to how small the electrodes can be before the surface area available for biomolecule functionalization is too small to generate a detectable signal upon target binding.

2.3.1.2   Nano Field Effect Transistors

Nanoelectrochemical sensors primarily act as field effect transistors (FETs), a sensing technique that is free from the size limitations discussed for the electrodes used for EIS. In a standard transistor, a semiconducting material supports source and drain electrodes; a third electrode, known as a gate electrode, separated from the semiconductor by a thin dielectric, controls the conductance of the semiconductor by applying positive and negative voltages. In this manner, the gate electrode acts as a switch for the current flowing from the source to the drain. In a FET-based biosensor, biomolecules take the place of the gate electrode, and the conductance of the semiconductor is altered by the binding of biomolecules (Figure 7).Changes in current between the source and the drain are correlated with binding events.
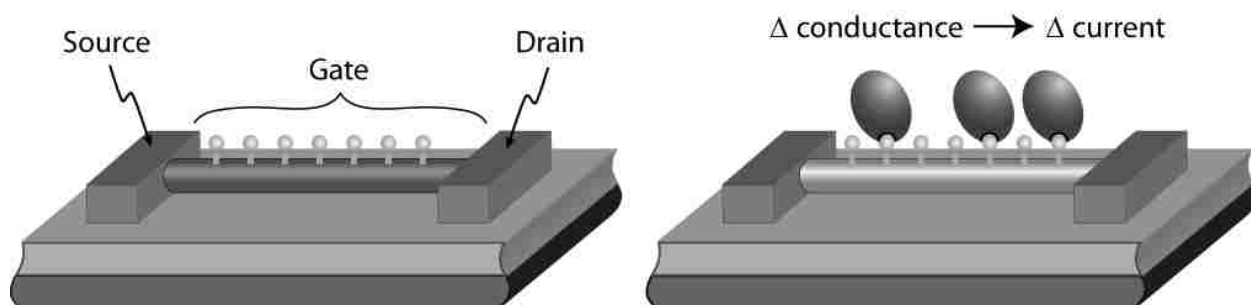
Figure 7. A nano field effect transistor biosensor is shown schematically. The intrinsic electrical properties of biomolecules that bind to the functionalized semiconducting material (e.g. nanowire, carbon nanotube) changes its conductance and therefore influences the amount of current that flows from the source to the drain.

Researchers have investigated nanowires,[97] nanofibers,[98] and carbon nanotubes[97b, 99] as semiconducting materials to use in nanoelectrochemical biosensors. A primary motivation is the potential sensitivity of these materials to biomolecular binding events – these one-dimensional materials have similar sizes to biomolecules, such that extremely small amounts of bound analyte will significantly affect the electrical properties of the transistor. Investigators have demonstrated detection of proteins,[97b, c, 99a], single viruses,[97a] and DNA with concentrations reported down into the picomolar range[99b] and even down to 10 fM.[97d, e] The limited size of these sensors, coupled with the pre-established microelectronics infrastructure, also make them good candidates for multiplexing, and devices containing up to two hundred sensors have been reported.[97a, 100]

Some hurdles remain before FET-based nanoelectrochemical biosensors can be used as reliable research instruments, let alone as biosensors in healthcare. Despite the apparent potential to achieve highly multiplexed devices, there are no good solutions for high-throughput fabrication. Carbon nanotubes must be synthesized off-chip and then placed in position, while nanowires can be patterned lithographically[97e, 101] or grown on-chip,[97c, d] they still suffer from fabrication inconsistencies. Given their size and high sensitivities, heterogeneity between sensors can result in altered performance and poor reproducibility. FET sensors are also ion-sensitive, and ions in solution will act as a gating mechanism and dramatically reduce sensitivity. This, along with the structural fragility of the FETs, limits the potential samples and experimental applications that can be used. Lastly, the mechanisms by which biomolecules influence electrical properties are not well understood, and different biomolecules alter the sensor response in ways that do not correlate predictably with the size of the biomolecule or its concentration in solution.

2.3.2   Mechanical Biosensors

Mechanical biosensors directly detect the change in mass on the sensor surface due to the binding of biomolecules, viruses, or cells. Mechanical sensors represent the most sensitive of the biosensing techniques, with noise floors and mass resolutions reported as low as 20 and 7 zg, respectively.[102] Given their potential sensitivity, mechanical biosensor research has largely been directed toward reaching very low detection limits for applications such as rare analyte sensing and weighing individual viruses and cells. Surface acoustic wave sensors, including the quartz crystal microbalance (QCM),[103] utilize the sensitivity of piezoelectric crystal resonance to perturbations in the surrounding environment. In QCM, the quartz surface is usually coated with an anchoring layer to which biological receptors are immobilized. Electrodes attached to the quartz apply an alternating voltage which elicits a resonant

mechanical oscillation. Tracking changes in the oscillatory frequency in response to binding at the sensor surface produces the signal, with reported limits of detection (LOD) down to 10 pg/mm^2.[104] QCM biosensors have been used to detect binding interactions of proteins,[105] oligonucleotides,[106] carbohydrates,[107] lipids,[108] viruses,[109] and cells.[110] A distinct advantage of QCM over both electrical and optical biosensors is the wide range of materials that can be deposited on top of the quartz. Since the sensing mechanism does not rely on the transmission of an optical signal or the propagation of light, QCM supports the study of interfacial interactions using a wide variety of materials.[103a, 111] However, QCM is not without its limitations. While QCM is amenable to performing binding experiments in a liquid environment, this reduces sensitivity and it can be difficult to separate the effects of mass, density, and viscosity in the QCM signal.[112] It is also difficult to fabricate dense arrays of acoustic wave devices, although it has been demonstrated.[113]

2.3.2.1 Micro- and Nanoelectromechanical Systems

Researchers have investigated micro- and nanobiosensors using mechanical transduction mechanisms in an effort to increase sensitivity and allow multiplexing. These devices employ standard photolithography techniques and are usually made out of silicon or silicon nitride, allowing high densities of devices and the possibility of integration with electronic components and flow cells. The majority of these devices are based on analyte binding to functionalized cantilevers; binding of analyte either changes the deflection of the cantilever (static devices) or its resonant frequency of oscillation (dynamic devices). Static devices (Figure 8A) have the advantage of being able to operate in both gas and liquid environments, but they have decreased sensitivity because the cantilever is only deflected when a near-monolayer of analyte is bound.[93c] Nevertheless, static cantilever devices have been shown to detect single base-pair mismatches of 12-mer DNA strands and picomolar limits of detection of oligonucleotides[114] and nanomolar concentrations for proteins.[114-115] An impressive study also showed detection limits of PSA down to 0.2 ng/ml (6 nM) in a background of both 1 mg/ml BSA and HSA, which matches detection limits of ELISA for PSA and is physiologically relevant.[116]

Dynamic cantilever devices (Figure 8B) have significantly higher potential sensitivities and researchers have shown the ability to detect viruses down to the single virus;[117] single cells;[118] a single 1587-mer strand of DNA;[119] and PSA down to 10 pg/ml.[120] The Bashir group has also used their devices for weighing single viruses[117b] and cells.[118b] As with QCM, an important drawback of most dynamic mechanical biosensors is that their sensitivity is limited by the dampening effects of liquid, so detection must be done in vacuum or air. However, several recent papers have implemented nanofluidic channels

fully confined within the cantilevers (Figure 8C).[121] In this configuration the cantilevers are maintained in a vacuum and the channel within the cantilevers allows biological interactions to occur in solution – not only are the interactions measured in a physiologic (aqueous) environment, but they are detected in real time. Studies using these devices have measured the changing masses of individual cells during growth,[122] detected cancer biomarkers in serum down to 10 ng/ml,[123] and IgG antibodies below nM concentrations.[121a]
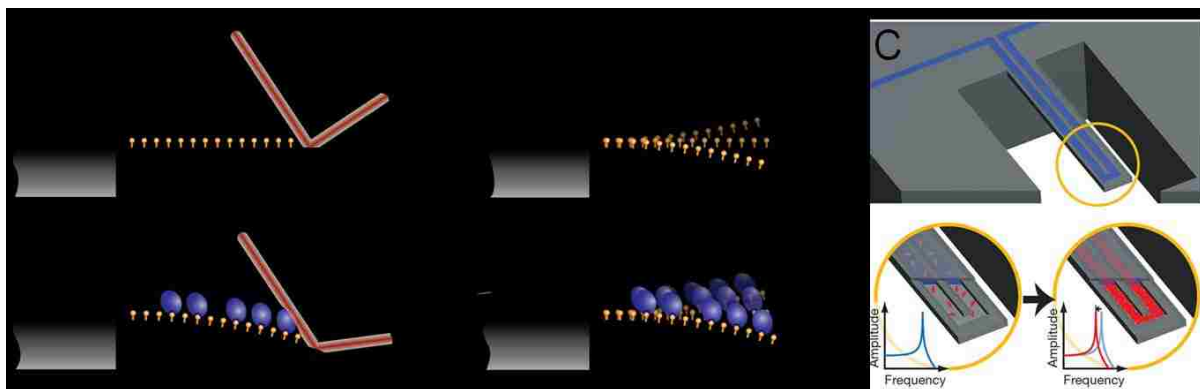
Figure 8. The two different modes of operation for microcantilever-based mechanical biosensors are demonstrated schematically. In both cases, the cantilevers are functionalized with the appropriate receptor or capture molecule. (A) Static microcantilever biosensors correlate the deflection of the cantilever arm upon the binding of biomolecules. (B) Dynamic microcantilever biosensors sense binding of biomolecules through changes in the oscillatory frequency. The mass of bound material can be calculated because the deflection or the change in the frequency (f) of oscillation can be related to the spring constant (K) and the effective mass (m^*) of the cantilever. (C) Since viscous damping of liquids leads to a dramatic decrease in sensitivity for dynamic microcantilever biosensors, Burg et al. have fabricated devices which contain a nanofluidic channel inside of the cantilever arm. (Credit for C)[121a]

2.3.3   Optical Biosensors

Optical biosensors are the most widely used label-free biosensing platforms to study biomolecular interactions because of their relative ease of use, high sensitivity, and the high information content of the data they generate. In 2008 alone, there were over 1400 articles published on optical biosensors.[124] Compared to many electrochemical and mechanical platforms, optical biosensors are more flexible and easy to use from an operational standpoint. Additionally, the sensitivity of optical biosensors is not drastically reduced by physiological salinity or viscosity in the analyte buffer, making them amenable to a wide range of samples. Label-free detection methods using optical biosensors include refractive index (RI) detection, optical absorbance detection, and Raman spectroscopic detection,[125] with the most common form being RI detection. RI detection is based on the sensitivity of light to changes in RI. Biomolecules have a higher RI than buffer solutions (e.g., 1.45 for proteins vs. 1.33 for water), which

allows their detection by monitoring the properties of the interacting light. A number of RI-based optical biosensors exist, including surface plasmon resonance (SPR), optical fibers, planar waveguides, interferometers, photonic crystals, and resonant cavities.

2.3.3.1 SPR and SPRi

First reported in 1983,[126] biosensors based on surface plasmon resonance (SPR) are among the most widely used optical biosensor. As of 2008, a total of 24 manufacturers offered commercial platforms, including instruments made by GE, Bio-Rad, Biosensing Instruments, and Reichert.[124] SPR detection relies on the sensitivity of evanescent fields to changes in the local RI of the dielectric. In most SPR instruments, the evanescent field is associated with surface plasmon modes that are created from the coupling of light with a metallic film, usually gold, via total internal reflection (TIR) within a prism (Figure 9). The conditions of TIR (the wavelength of light and the incident angle of light that couples with the metallic film) vary with the RI of the dielectric above the metal film. A flow cell delivers biomolecules to the surface of the metallic film, where binding of analyte to immobilized receptors causes changes in the local RI. The instrument tracks these changes in real time and reports them as a shift in resonant wavelength (angular SPR) or as changes in the intensity of reflected light (SPRi). Traditional angular SPR has superior limits of detection than SPRi – the RI detection limit for SPR typically ranges from 10^{-6}-10^{-8} refractive index units (RIU), whereas SPRi is usually in the range of 10^{-5}-10^{-6} RIU [125, 127] – but SPR is only able to monitor binding in a single region at once for each light source. SPRi, on the other hand, uses a CCD array to detect the intensity of reflected light from the entire chip surface, allowing arrayed and simultaneous sensing of multiple binding interactions. The number of interactions that can be monitored simultaneously is limited only by the spatial resolution of the instrument (e.g. ~4μm)[89b] and the arraying density of functionalization, the latter of which has been widely addressed by the microarray community. Creating 100 interaction regions on a single SPRi chip is common, with reports of systems that allow up to 10,000 spots.[128] Given its high-throughput capabilities, SPRi appears to have significant potential as a multiplexed POC device. Most studies using SPRi have employed it for multiplexed interaction screening and characterization,[129] whereas angular SPR is favored for the higher sensitivity measurements required for analyte detection.
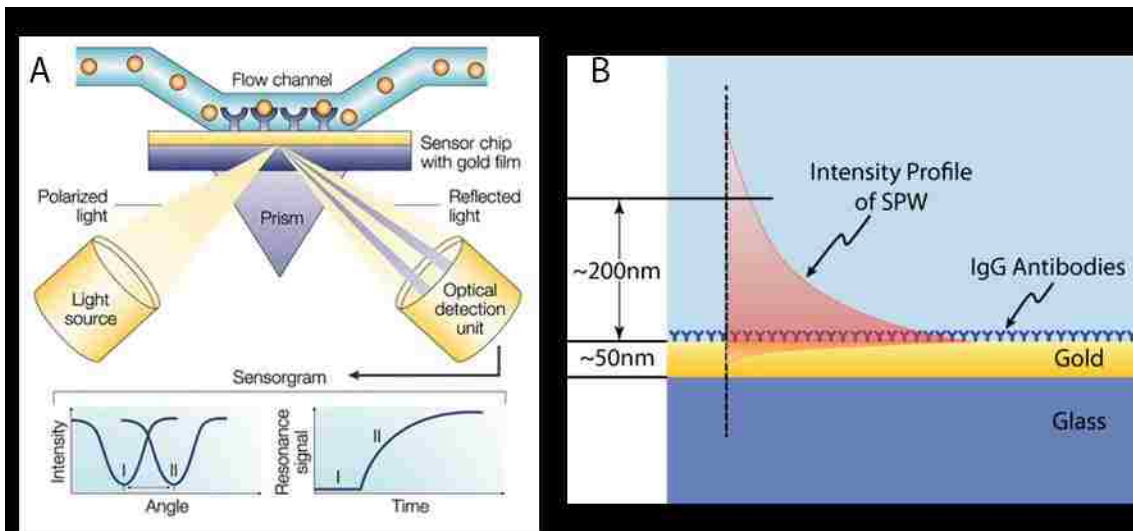
Figure 9. (A) In an SPR biosensor, the binding of biomolecules to immobilized receptors changes the coupling properties (in this case, the coupling angle) of light reflected off of a metallic film (Credit)[130]. These coupling angle changes, documented over a given time period, generate a sensorgram that describes the binding events. (B) The coupling properties of light are sensitive to changes in refractive index within the surface plasmon wave (SPW) which extends ~200 nm (Intensity = 1/e) from the metal-dielectric interface. The schematic includes IgG antibodies drawn to scale for perspective.

Several commercial SPRi instruments exist, including the FlexChip from BIA-CORE,[131] GWC's SPRimager®II,[132] and Texas Instruments' Spreeta system.[133] Other groups have developed prototypes of portable SPRi systems that make important advancements to realizing POC applications.[134] Unlike the aforementioned non-optical multiplexed devices, SPRi benefits from the fact that different sensing areas can be defined by the user based on the locations of the functionalized regions, and the gold surface of SPRi sensor chips is relatively robust. This greatly reduces the alignment difficulties that are encountered when attempting to functionalize specific devices on multiplexed electrochemical and mechanical devices. As a biosensing platform, SPR benefits from the extensive literature on the biofunctionalization of gold surfaces – one of the best understood surfaces for functionalization and the standard for biological surface analysis.[135] Among the important properties of gold are its biocompatibility and its ability to bind strongly to thiol groups (at near covalent strength), which allows for facile tethering of biomolecules and the inclusion of non-fouling self assembled monolayers (SAMs).[136] Despite these advantages, SPRi has yet to realize widespread use in the clinic or in POC settings.

2.3.3.2 Grating-based sensors

Optical fibers and planar waveguides can both be incorporated into surface plasmon wave (SPW) biosensors, and they operate similarly to SPR. In these cases, an optical fiber or a waveguide acts in

place of the prism to couple light with a metallic layer, which generates the SPW and the corresponding evanescent wave that is used for sensing RI changes in the dielectric. Alternatively, in non-SPW biosensing conformations, optical fibers and planar waveguides often rely on coupling light with a grating structure. A grating consists of a periodic physical perturbation on the surface of the sensor; light couples into the grating at a specific angle and wavelength that are determined by the effective refractive index (n_{eff}) of the fiber or waveguide and the grating period. Binding of biomolecules changes n_{eff}, enabling real-time detection. In the case of fibers, the gratings are etched into the optical core or into the cladding immediately surrounding the core, such that a biofunctionalized grating provides the sensing region (Figure 10A). While these devices are more widely used for sensing load, strain, temperature, and vibration,[137] examples of their application for biosensing include: the detection of DNA 20 base pairs in length down to 0.7 μg/ml using a device with a RI LOD of 7x10^{-6} RIU;[138] real-time monitoring of antibody binding with a dynamic range from 2-100 μg/ml and antigen detection from crude *E. coli* lysate;[139] and the detection of hemoglobin in sugar solutions with an inferred sensitivity to a change in hemoglobin concentration of 0.005%.[140] While fiber gratings are inexpensive and straightforward to manufacture, they suffer from relatively poor sensitivities.[125]
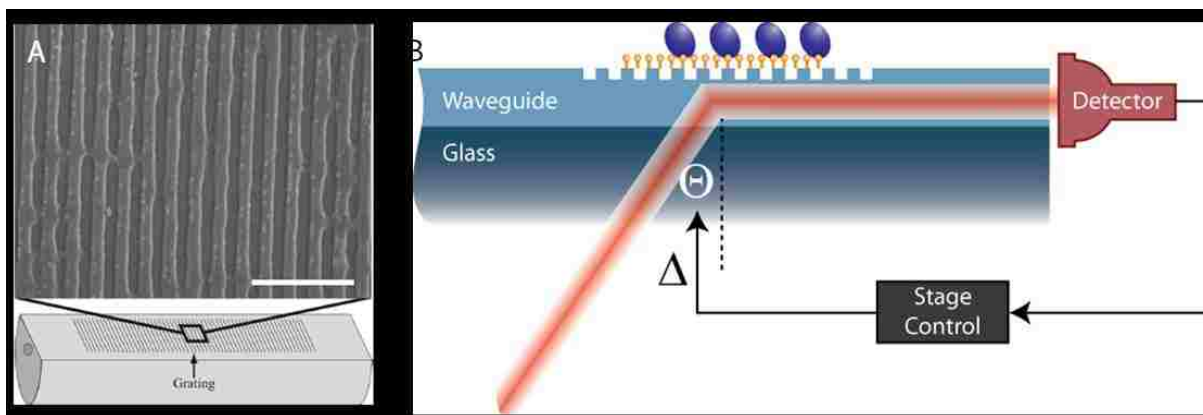
Figure 10. Grating-based biosensors have been shown in a variety of conformations, two of which are depicted below. (A) A Bragg grating is etched into the cladding of a D-shaped fiber. (Credit for A)[141] (B) An OWLS biosensor changes the angle of the stage in response to biomolecule binding to maintain coupling These changes are recorded over time to generate the sensorgram.

Grating-coupled planar waveguides are also easy and cheap to fabricate, as they consist of a thin-film waveguide deposited on a glass support into which a grating can be etched using photolithography or imprinting.[142] Optical waveguide light-mode spectroscopy (OWLS) is one well-known implementation of this sensing modality; these devices measure the change in the coupling angle due to changes in the RI

on the grating (Figure 10B). They have been used for biosensing applications including antibody capture of the herbicide trifluralin down to 100 ng/ml[143] and the detection of mycotoxins down to 0.5 ng/ml.[144] OWLS has been more widely applied to studying biomolecular adsorption kinetics and conformation on a variety of material surfaces.[145] OWLS does not permit multiplexing capabilities, but a very similar technique employing planar waveguide gratings known as wavelength-interrogated optical sensors (WIOS) addresses this issue. A device with 24 different sensing regions has been used to simultaneously monitor four different classes of veterinary antibiotics in milk with a LOD ranging from 0.5 ng/ml to 34 ng/ml, depending on the class of antibiotic.[146]

2.3.3.3 Mach-Zehnder Interferometers

In a Mach-Zehnder interferometer (MZI), a single frequency, coherent polarized light source is split into two paths. The sample is placed in one of these paths where light interactions with the sample cause a shift in the phase of the light, and the other path acts as the reference. The light is then recombined and the phase shift caused by sample binding in the sensing arm leads to interference which can be detected by a change in the light's output intensity. Although traditionally done in free space, MZIs can be fabricated in a planar structure using waveguides to split and recombine the light – these are called integrated MZIs. In such a setup, the sensing arm is functionalized and binding of the sample changes the RI within the evanescent field of the waveguide, thus modulating the phase of the propagating light and leading to interference upon recombining with light from the reference arm (Figure 11). The first biosensing demonstration of integrated MZIs detected human chorionic gonadotropin (hCG) down to 50 pM using immobilized capture antibodies.[147] This device had an RI LOD of 5×10^{-6} RIU, but improvements in MZI fabrication and analysis have led to demonstrations of LODs down to 10^{-7} RIU,[148] which is on par with most SPR instruments. Other demonstrations of MZI biosensing include detection of IgG down to 1 ng/ml,[149] and the ability to distinguish wild-type DNA (58-mer) from a mutated sequence down to 10 pM concentrations.[150] Very few reports of biosensing with MZIs have emerged following the initial interest in the 1990s. This could be due to the two main drawbacks of these devices, namely the difficulties in multiplexing and the requirement of a relatively long sensing region to generate a detectable signal. Long sensing regions not only require a larger footprint on the device, but they also work against sensitivity because of increased loss. A more recent publication addressed both of these issues by demonstrating a multiplexed device that used coiled waveguides as sensors.[151] The device had six sensors, four of which were functionalized with two different antibodies (two sensors for each antibody) and the remaining two were used as reference sensors. The sensor response corresponded to a surface

coverage of just 0.3 pg/mm^2. However, it remains to be seen if integrated MZIs for biosensing applications will have a significant impact in biomedical research.
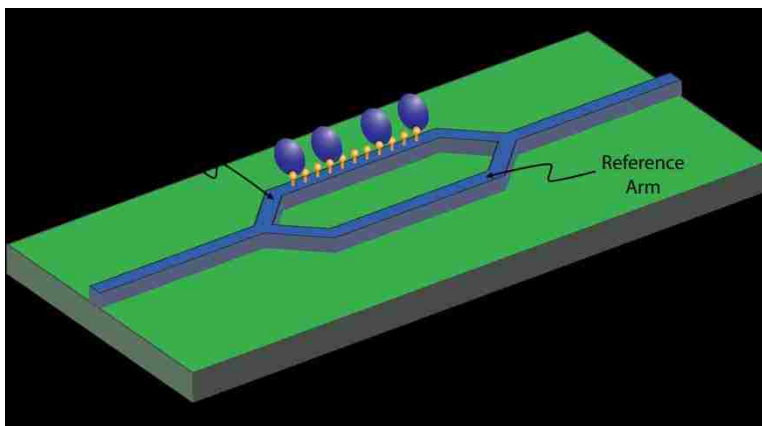
Figure 11. Schematic representation of a chip-based MZI biosensor. Changes in the RI surrounding the sensing arm induce a phase change, resulting in interference upon recombination with the reference arm.

2.3.3.4 Young's Interferometers

The Young's interferometer (YI) can be integrated onto a chip surface in much the same way as MZIs to be used for biosensing. Similar to MZIs, YIs split light from a single waveguide into multiple arms, including at least one reference arm. Instead of recombining the light back into a single waveguide, however, a CCD is used to record the interference fringes that result from the optical output of the waveguide arms (Figure 12), permitting multiplexed sensing with just one reference. An integrated YI for sensing was first demonstrated in 1994,[152] and the technique has an established RI LOD of 10^{-7} RIU.[153] YIs have been used in a number of proof of concept applications since this first application. For instance, a multiplexed device containing three sample arms and one reference arm enabled biosensing of herpes simplex virus type 1 (HSV-1).[154] The authors were able to detect as few as 10^5 HSV-1 particles in serum and 10^3 particles in buffer, highlighting the potential for the device to be miniaturized and integrated for POC applications.[155] Hoffman and colleagues developed a planar waveguide YI that they used to determine the binding kinetics for protein G capture of IgG and demonstrated its compatibility with biotin-streptavidin functionalization techniques.[156] The authors reported an RI LOD of 10^{-9} RIU which corresponds to a surface coverage of just 13 fg/mm^2, one of the lowest reported RI LODs of any optical biosensor. It should be noted that while there have been a number of reports demonstrating MZI and YI multiplexed sensing, interferometric biosensing has not proven to be readily amenable to high-

throughput multiplexing due to the large sensing regions required and because the complexity of analysis increases significantly with each additional sensing arm.
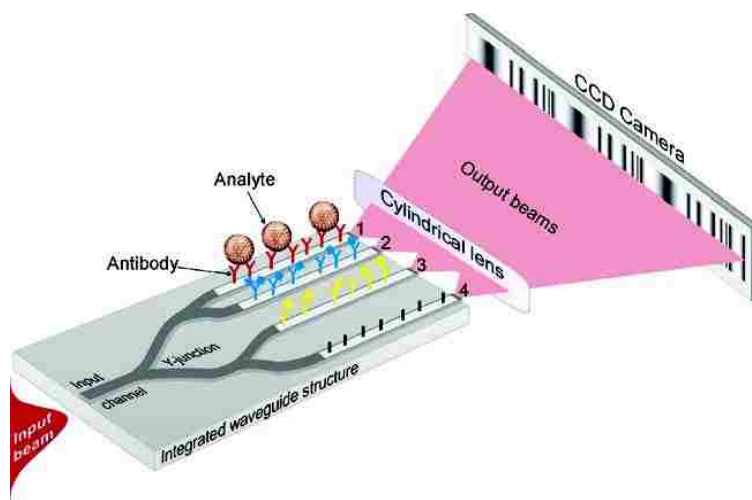
Figure 12. Schematic representation of a multiplexed integrated YI. Antibodies with different specificities are functionalized on the waveguide arms such that specific recognition and binding of analyte alters the local RI, leading to changes in the interference pattern detected by the CCD camera. (Credit)[155]

2.3.3.5   Resonant Cavity Sensors

Resonant cavities represent one of the most rapidly expanding and promising label-free optical biosensing techniques, due largely to their high sensitivity and their potential to be integrated into multiplexed chip-based devices. In resonant cavity sensors, which include microspheres (Figure 13A), microtoroids (Figure 13B) microrings (Figure 6A&B), and microcapillaries, light is coupled into an optical cavity where certain wavelengths are confined; this confinement generates a narrow dip in the transmission spectrum. The wavelengths of light that travel around the outside of the cavity and return in phase are the resonant wavelengths and can be described by the equation $\lambda = 2\pi r n_{eff}/m$, where λ is the wavelength of light, r is the radius of the cavity, n_{eff} is the effective RI of the waveguide mode, and m is an integer. A fiber or integrated bus waveguide in close proximity to the resonant cavity delivers light to the cavity for coupling and away from the cavity so that the transmission spectrum can be tracked. Resonant wavelengths appear as dips in the transmission spectrum because the resonant condition extracts power from the light in the fiber/waveguide that reaches the detector.[157] The dependence of the resonant wavelength on n_{eff} is due to the evanescent field that extends and decays exponentially away from the surface of the cavity, and, like the other optical biosensors discussed in this chapter, it is this relationship that creates the sensing mechanism. By changing n_{eff}, biomolecules binding to the

resonant cavity shift the resonant wavelengths supported by the structure. In contrast to the other evanescent sensing techniques already described (SPR, grating-coupled devices, and interferometers), where each photon only interacts with the biomolecules one time, a photon coupled into a resonant cavity interacts with biomolecules each time it travels around the cavity, which can reach into the thousands for some resonant cavities.[157b] This feature bestows high sensitivities to small devices, which is not possible with other optical biosensors (e.g. interferometric sensors). The number of revolutions a photon makes around a resonant cavity before dissipating is related to the quality factor (Q) of the resonator and determines the sensitivity of the device.[157b] Q is determined by the full-width half maximum ($\delta\lambda_r$) of the resonant dip at the resonant wavelength (λ_r), according to the equation $Q = \lambda_r/\delta\lambda_r$. Thus, a higher Q corresponds to a more narrow dip in the transmission spectrum which facilitates sensitive tracking of the resonant wavelength.

2.3.3.6 Microspheres and Micro-toroids

Microspheres exhibit Q-factors over 10^6 and they have had RI LODs reported as low as 10^{-7} RIU.[158] Resonant cavity microspheres are generally constructed by melting the tip of an optical fiber or a glass rod,[125] which must then be brought into close proximity to and aligned with a tapered fiber. Demonstrations of resonant microsphere biosensors include the detection of protease activity with a LOD of trypsin at 10^{-4} units/ml;[159] detection and mass determination of single influenza A virus particles;[157b] and the detection of single nucleotide mismatch of DNA with a LOD of 6 pg/mm^2.[4] The device used for DNA detection used two microspheres of different sizes brought into proximity of a single tapered fiber. Because of their different size, each microsphere has a unique resonant wavelength and they could be interrogated simultaneously. Despite this proof-of-concept multiplexed device, microsphere-
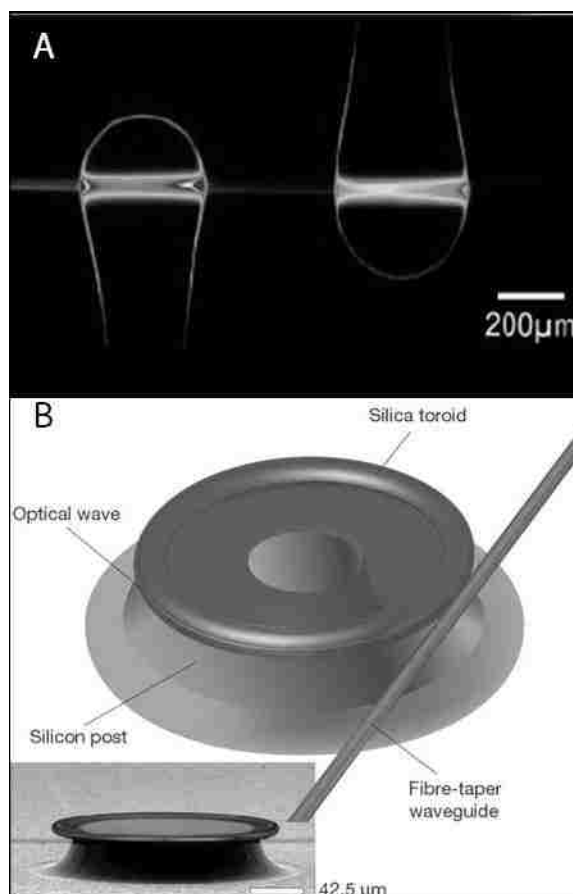
Figure 13. Resonant cavity biosensors confine the wavelengths of light which, after circumnavigating the cavity, constructively interfere with itself. Biosensing is possible because the resonant frequency is sensitive to perturbations in the surrounding RI. Examples include (A) silica microspheres (Credit)[4] and (B) silica microtoroids fabricated on a silicon support. (Credit)[5]

based resonant cavity biosensors are resistant to large-scale multiplexing because of the sensitive alignment required between the microspheres and the tapered fiber and because they are incompatible with planar fabrication techniques.[160]

Armani et al. developed micro-toroid resonant cavities with extremely high Q (>10^8) which were fabricated using planar lithography. The authors report remarkable single-molecule label-free detection of interleukin-2 (IL-2) via capture by immobilized IL-2 antibody in 10-fold diluted fetal bovine serum.[161] This, while impressive, also raises a number of questions related to the reported sensing mechanism[162] and the observed mass transport,[163] suggesting that we still have much to learn about ultra-sensitive optical biosensing. Armani's results have set a high standard for optical sensing, but they do not address the need for high-throughput multiplexed sensing. While the micro-toroids were fabricated on-chip using photolithography, the technique still requires alignment of a tapered optical fiber for coupling. Further, the inherent fragility of both microsphere and micro-toroid systems make them sensitive to flow, particularly with viscous fluids such as blood plasma.

2.3.3.7 Microrings

Planar microrings have arguably become the most popular form of resonant cavity biosensors, owing to their small size, high sensitivity, ease of manufacture, and multiplexing potential. Ring size can vary, but nearly all are on the order of tens of microns in diameter, which is favorable as compared to interferometric devices which require sensing lengths on the order of a centimeter.[104] Microring resonators do not have decreased sensitivity based on their small size because of the increased light interaction imparted by the resonance condition, as previously discussed. They do have lower Q (10^4-4x10^4) and slightly higher (worse) reported RI LODs (10^5-10^7 RIU)[164] than microspheres and microtoroids; but their simple and scalable fabrication, multiplexing capability, and potential for integration with other components make them attractive for biosensing applications.

Microring resonators can be fabricated using standard silicon wafer processes, enabling passive alignment of multiple microrings with on-chip bus waveguides, which is a significant advantage over the microsphere and micro-toroid devices. While they are almost universally fabricated on a silicon substrate, the waveguides and rings can be made out of polymers,[164c, 165] silicon oxide,[166] silicon nitride,[164b, 167] and SOI.[168] Sensitive multiplexed detection and binding assays using microring resonators are demonstrative of the advantages of this biosensing platform. Using a device containing five independent microrings, Ramachadran et al. showed specific binding of *E. coli* O157:H7 to microrings functionalized with antibodies, detection of complementary DNA probes, and quantitative detection of

IgG.[166b] Three shortcomings of their technology, which are common with many of these platforms, were apparent: (1) relatively low acquisition rates, (2) the lack of integrated fluidics, and (3) a paucity of high-throughput functionalization techniques. In the device reported by Ramachandran et al., the scan rate was 15 seconds per microring, limiting measurement frequency to 75 seconds per device, if all rings were interrogated.[166b] Faster scan rates are required to extract binding kinetics and for truly high-throughput multiplexed measurements. An instrument containing integrated fluidics and peripheral instrumentation for using disposable chips was reported by Carlborg et al.[164b] Device characterization showed a RI LOD of 5×10^{-6} RIU and a mass density detection limit of 0.9 pg/mm^2. The authors have since published on characterization of the temperature sensitivity of this device,[169] but they have yet to report on its implementation in a biosensing experiment.

Another instrument (the Genalyte Microring Resonator Biosensor) used extensively by ourselves and the Bailey group at the University of Illinois Urbana Champagne directly addresses the issues of scanning speed and fluidic integration, and both of our groups have devised improved techniques for differential functionalization of the microrings.[170] The platform has a detachable microfluidic chamber and uses high-speed scanning instrumentation which interrogates all of the rings on the device in fewer than 10 seconds.[164a] For multiplexed functionalization, Bailey has employed a six-channel microfluidic device to functionalize multiple capture ligands on groups of microrings.[171] Using the same microring-based biosensor, our group has implemented a piezoelectric spotter to differentially functionalize microrings on multiple chips in a single run, thus demonstrating a rapid and scalable approach.[170b]

An alternative method for addressing the issue of scan speed mentioned above was demonstrated by Xu et al.[168a] Instead of increasing the scan speed, the investigators used a single waveguide to interrogate five rings of different sizes. Since rings of varying diameter will support resonances of different wavelengths, Xu was able distinguish shifts in the resonant frequency due to binding of species-specific IgG on each microring simultaneously. In addition to demonstrating specific and simultaneous detection of two different IgG antibodies, the researchers deduced an impressive mass density sensitivity of 0.3 pg/mm^2. The combination of high sensitivities, ease of manufacture, multiplexibility, and potential for integration has positioned the microring resonator-based device as one of the most promising optical sensing technologies to emerge from the biosensing community.

2.4   Considerations for Biosensor Operation

While biosensing literature often focuses on the transduction mechanism used to detect biomolecular binding, a biosensing platform is also composed of the supporting instrumentation, the functionalization method, the experimental design, and the data analysis. These other factors are as important and as diverse as the sensors themselves, and optimization of all of the components of a biosensing platform is necessary to perform meaningful research or to produce a useful medical instrument.

2.4.1   Supporting Instrumentation

In addition to the transducer element of a biosensor, its operation relies on a variety of support instrumentation and additional components. This additional equipment is obviously dependent on the particular biosensor being used, but almost all biosensors share a few broad classifications of components beyond the sensor itself. First, a biosensor requires some way to deliver the sample to the sensing region. With the exception of gas-based sensors, this usually requires a fluidic handling system (pumps, tubing, channels, etc.) that can effectively deliver aqueous samples while simultaneously minimizing reagent consumption. The signal generated by biomolecular binding at the sensor must be analyzed and correlated with the sample, whether quantifying analyte concentration, binding kinetics, or simply the presence of the target. These additional aspects of the biosensor require instrumentation that: actuates (e.g. signal generator, light source), detects (e.g. oscilloscope, photodetector), and processes (e.g. microprocessor) the signal. Nearly all of these components require power, which is readily available in most research laboratories, but it is unreliable or unavailable in the developing world and in many POC settings. It is just as important to understand the capabilities of the support instrumentation as it is to understand the capabilities of the sensor itself, since these additional components may be the limiting factor of the system. For example, the CCD array that detects the changes in reflected light intensity of a SPRi biosensor is usually the limiting factor for the sensitivity and the imaging resolution of the instrument.

2.4.2   Biosensor Functionalization

When no label is used, detecting the binding event relies on a transducer, the mechanism of which can be electrochemical, mechanical, or optical. The transducer must be functionalized with a bioactive surface which captures the target biomolecules or changes in response to the target, such that these changes on the surface of the transducer elicit a detectable signal (Figure 5B). The bioactive surface is generally composed of one or multiple biorecognition molecules such as oligonucleotides, peptides, antibodies, aptamers, phages, and carbohydrates. These molecules can be attached to the transducers

using non-covalent interactions or by specific covalent attachment. Regardless of the method used, surface functionalization must retain the bioactivity of the immobilized ligand. In the case of non-specific protein adsorption as a functionalization method, the adsorption of the protein to the surface may alter the protein structure in a way that reduces or eliminates its bioactivity. For functionalization with carbohydrates or other small ligands, the binding epitope must be sufficiently spaced from the surface so that binding is not sterically hindered; this problem is generally addressed by adding a spacer moiety between the binding epitope and its point of attachment to the surface.[74]

Regardless of the mechanism of attachment, the bioactive surface must be resilient to degradation and prevent non-specific binding by other biomolecules or contaminants. The degree to which a functionalized surface should withstand degradation – due to anything from the reagents used during the experiment to the storage conditions – depends on the desired application of the biosensor. For instance, it is often desirable to regenerate and reuse a functionalized biosensor, so the bioactive surface must withstand the regeneration buffer that removes the bound analyte. For any POC device, the surface must retain bioactivity through deployment and on-site storage until the device is used. Even if the functionalized surface will be tested a single time immediately after functionalization, bioactivity must remain throughout the course of the experiment.

Closely related to the stability of the functionalized surface is its ability to resist non-specific binding of non-target molecules – if the background signal is too high, then the binding event that the biosensor is designed to detect may be hidden in the noise. Even if a signal can be detected from the target interaction, any non-specific interactions will increase the LOD. The most common method for blocking a biosensor surface to non-specific binding is through adsorption of non-reactive proteins, such as BSA or milk proteins. These proteins coat the biosensor surface, thus preventing additional adsorption during the binding assay. Including surfactants in the reagent buffer is also useful, though this can significantly alter the binding interaction of interest. Self assembled monolayers (SAMs) of poly(ethylene glycol) (PEG) are another common way to prevent non-specific binding, whereby the tightly-packed PEG SAM prevents undesired fouling molecules from reaching the sensor surface.[172] A more recent approach uses zwitterionic polymer surface coatings, which render the surfaces they coat non-fouling by nature of the strong hydration layer that they create.[173] In both of these examples, the functional molecules are deliberately introduced within the SAM or directly attached to the distal (i.e. solution-facing) end of the polymer.

2.4.2.1 Non-Covalent Functionalization

Non-covalent functionalization methods are generally more straightforward to perform, though they can be more difficult to control and they require specific considerations such as the surface to which the ligand is attached and the conformation of the ligand once immobilized on the surface. For example, proteins are known to adsorb strongly to hydrophobic surfaces, whereas adsorption to hydrophilic surfaces is less reliable. Regardless of the nature of the surface, adsorption can lead to conformational changes that render the protein inactive. The biosensor surface can also be modified in order to facilitate adsorption. Successful approaches for this include surface modification with nitrocellulose,[77b, 78a, b] fluorine,[174] and polypyrrole.[96b, 175] Nitrocellulose enables passive adsorption of polysaccharides and glycoproteins,[77b] and mono- and oligosaccharides can be modified to contain a lipid tail which attaches the ligands to nitrocellulose or other hydrophobic surfaces. These lipid-modified carbohydrates are known as neoglycolipids (NGLs), and they are used by the Feizi group and the UK Glycochip Consortium.[176] Similar to the lipid tails on NGLs, fluorous-tagged ligands can be adhered to fluorine-coated surfaces.[174] Polypyrrole (Ppy) belongs to a family of electro-conducting polymers that includes polythiophene and polyaniline that have been used to fix proteins and other biomolecules on biosensor surfaces. In addition to acting as a stable surface to which molecules can be adsorbed (largely through electrostatic interactions), the electrically-active nature of these polymers makes them attractive for biosensors based on electrochemical detection because the polymer can be deposited to maximize transmittance of the electrical signal to the sensing electrodes.[175b, 177]

Functionalization through physioadsorption works well with many proteins, but capture ligands such as carbohydrates resist such immobilization, and other proteins lose their bioactivity when directly adsorbed on surfaces. In order to combat this, researchers have modified "carrier" proteins by covalently attaching carbohydrates, DNA, and antibodies so that they can be adsorbed to a biosensing surface and retain their bioactivity.[96, 178] Using bovine serum albumin (BSA) as a carrier for carbohydrate binding ligands was identified as the preferred method for functionalization in many of the biosensor experiments described in Chapters 3 and 4; this method displays the ligands in such a way that promotes multivalent interactions and the BSA carrier adheres strongly to a variety of surfaces, including gold, polystyrene, nitrocellulose, and SiO_2.

In addition to physioadsorption and the incorporation of affinity tags on ligands (e.g. NGLs), non-covalent immobilization can also be achieved through receptor-ligand or nucleic acid hybridization interactions. Examples of receptor-ligand interactions include streptavidin-biotin and protein A/G-

antibody coupling. In most applications that use these receptor-ligand interactions, the anchoring protein is immobilized on the biosensor surface (either non-covalently or covalently) and it is used to capture the ligand of interest. Importantly, the ligand itself must be modified with the complementary immobilization molecule (e.g. biotin), adding additional steps to the functionalization process.

A unique non-covalent conjugation method that is widely employed in biosensors, particularly SPR, is the gold-thiol interaction. There is extensive literature on the biofunctionalization of gold surfaces, making it one of the best understood surfaces for functionalization and the standard for biological surface analysis.[135] Among its important properties are gold's biocompatibility and its ability to bind strongly to thiol groups (at near covalent strength), which allows for facile tethering of biomolecules and non-fouling self assembled monolayers (SAMs).[136]

2.4.2.2 Covalent Functionalization

Covalent immobilization of capture ligands generally requires more steps and specific considerations need to be made for the sensor material, but it is useful because the resulting functionalized surfaces are more resilient to degradation and the final conformation of the ligands is more predictable. Specific covalent attachment is achieved via functional groups that are either native to the biomolecules or introduced through molecular biology or synthetic techniques. Most covalent attachment methods take advantage of the amine and thiol side chains of lysine and cysteine, respectively, which are inherent to the protein to be immobilized. In the case of some proteins and most carbohydrates, however, the functional group must be introduced to the molecule. Similarly, complementary functional groups are either native to the surface to which the ligands are to be attached (e.g. hydroxyl groups on cleaned SiO_2 surfaces) or they can be added to the surface. Covalent methods of functionalization are as diverse as bioconjugate chemistry itself, so they will not be discussed in detail, but some of the most common interactions that are employed are thiols and maleimides;[77c, 179] amines and N-hydroxysuccinimide (NHS)[88, 180] or epoxides;[181] and azides and alkynes.[182] Various photoreactive chemistries are also used,[183] with the benefit of an additional level of control on the functionalization process.

2.4.3   Experimental Design: Reagent Preparation and Operational Considerations

The quality of data obtained from a biosensing experiment is dependent on far more than the instrument itself – in order to generate high quality data, the reagents must be pure and the experimental design must be sound. The specifics of the experimental design will vary greatly depending on the biosensor being used the interaction of interest, and the desired information one wishes to extract from the experiment, but there are a few considerations that can be applied to biosensor

experiments in general. Possibly most important is the inclusion of non-specific binding controls, ideally in a multiplexed format such that the controls are tested simultaneously with the interaction of interest. If multiplexing is not an option, then running additional experiments with control surfaces is sufficient. Sensors should be functionalized with a non-complementary ligand or the blocking reagent (ideally both) so that binding to the complementary ligand can be deemed specific. This seems obvious for any scientific investigation, but biosensing literature is replete with examples of poorly controlled experiments.[124]

It is also critical to be able to distinguish between noise or signal artifacts from actual binding. Appropriate controls can help to serve this purpose, but there are other considerations regarding the experimental solutions that also factor in to this. For example, in the case of optical biosensors, the refractive indices of the samples being passed over the sensing surface must be matched so that any shift in signal can be attributed to analyte binding rather than a bulk refractive index shift. (Note: in instances when the RI cannot be matched between the running buffer and the analyte solution, one must run control experiments so that the signal due to bulk shift can be subtracted). The equivalent consideration for mechanical biosensors is that the viscosity of the solutions must be matched, since changes in viscosity will also cause a bulk shift.

Closely related to being able to extract the signal due to specific binding is establishing a baseline for the instrument. For biosensing platforms such as the microelectrode arrays that are described in Chapter 3, which uses end-point measurements, control surfaces essentially act as the baseline. For instruments that acquire data in real-time, such as SPR and the microring resonators described in Chapter 4, establishing a stable baseline prior to introducing the sample is required.

Lastly, the biosensing instrumentation needs to be completely cleaned to prevent contamination from previous experiments. This is especially important for fluidic delivery systems, which can harbor a variety of contaminants and hidden complications. For example, residual protein that adhered to the inlet tubing during a previous experiment can break free and be exposed to the sensing surface. Tubing and flow cells can also accumulate salt, which could alter the flow rate or stop flow altogether.

In summary, it is easy to forget that biosensors are simply passive sensors that will detect any changes to which they are sensitive, regardless of the specific interaction that is of interest to the experimenter. This emphasizes the importance of understanding the fundamentals of how the biosensor operates as well as the methods involved with running well-controlled experiments.

2.4.4   Analyzing Biosensor Data

Properly executed experiments can yield both qualitative and quantitative information, such as the selectivity, the strength, the kinetic binding parameters, and the thermodynamic parameters of a binding interaction, as well as identify the concentration of the target molecule. Emphasis must be placed, however, on the careful design, execution, and analysis of biosensing experiments if meaningful information is to be extracted. An unfortunate reality of the widespread use of SPR, for example, is that many investigators make incorrect conclusions from their data as a result of poorly run experiments or faulty analyses. Rich and Myszka reviewed the optical biosensor literature every year from 1998-2008 and found that a large majority contain major flaws in some aspect.[124, 184] These reviews are excellent sources for understanding the proper utilization of optical biosensing technologies and they also communicate the wide range of applications of these instruments.

2.5 Towards Fully-Integrated Biosensors

While not an area of focus of the research presented in this thesis, fully-integrated biosensors are an area of great interest in the biosensing community. Further, the biosensors that we chose to develop, particularly the microring resonator platform, both show promise for integration in the future. It is thus relevant to describe some of the efforts that are underway to achieve biosensor integration and highlight the promise of silicon photonics for this purpose.

Significant effort has been dedicated to miniaturization and integration of biosensing components to construct LOC devices. Fully-integrated chip-based biosensors will allow biosensor applications to expand beyond research laboratories into clinics, households, and the point-of-care. In addition to the aforementioned desired characteristics of a biosensor, the devices need to be cheap, robust, reliable, easy to use, and consume low amounts of power. While many technologies and disciplines are converging to achieve this goal, two stand out as especially enabling for the future of biosensors. The first is miniaturized and integrated electronic devices, which has been spearheaded by the microelectronics industry, whose techniques have had far-reaching applications in micro- and nanotechnologies. The other is microfluidics (also a beneficiary of microelectronic fabrication processes), which enables the handling and manipulation of small volumes of fluidic samples and is particularly amenable to device integration. In order to realize an integrated LOC biosensor, researchers will, without a doubt, need to leverage both of these technologies. It follows that these devices would

greatly benefit from having planar, chip-based components in order to integrate microfluidics while capitalizing on semiconductor fabrication technologies.[160]

Silicon photonics has become a focal point of many parallel efforts to achieve fully-integrated biosensors complete with on-chip light sources, detectors, and data processors;[185] the high-throughput, cost-effective, and scalable manufacturing techniques developed by the microelectronics industry and the sensitivity, efficiency, and pervasiveness of optical biosensing are united by their ability to be implemented on silicon. Jokerst et al. point out the components necessary for a fully integrated planar photonic biosensor.[160] Importantly, all of the components – a light source (e.g. thin film III-V edge emitting laser)[186], a sensor (e.g. microring resonators)[164a], and a photodetector (e.g. InGaAs metal-semiconductor-metal photodetector)[187] – have been fabricated in planar formats and tested independently by different groups, so all that remains is piecing everything together. This is no trivial task, especially considering the other hurdles such as microfluidic integration, sensor functionalization, and device characterization, yet the technologies exist and efforts are underway to make fully-integrated and distributable biosensors.

Steps towards this goal have been made. Microresonators have been integrated with chip-based photodetectors that were able to monitor the resonant condition of the microresonators.[188] Chip-based light sources (e.g. thin-film edge emitting lasers[189] and dye lasers[185d]) have also been integrated with an interferometric coupler,[189] as well as a waveguide and a photodetector in series.[186] A variety of traditional optical components such as microlenses,[190] mirrors,[191] filters,[192] laser diodes, and photodiodes,[192a] as well as sensing components like interferometers and microresonators, have been integrated into microfluidic devices.[160, 185a, b, 193] Microfluidic devices have also incorporated valves,[194] pumps,[195] and sample processing capabilities such as mixers,[196] target concentrators,[197] and target separators.[198]

2.5.1   Silicon Photonics for Device Integration – Why Silicon?

Traditional optical components are bulky and expensive; they require exotic materials, such as indium phosphide (InP), gallium arsenide (GaAs), and lithium niobate (LiNbO$_{3.}$). In addition, compound optical devices are usually assembled by hand, such that the difficulty of assembly increases exponentially with the number of components. [199] This makes the large-scale production of complex free space optical systems onerous. Silicon, on the other hand, has a history of automated processing, and the microelectronics industry has developed extensive manufacturing infrastructure. This industry has invested hundreds of billions of dollars to the processing and implementation of silicon in

microelectronic devices, driven by silicon's advantageous electronic properties and its low cost. More recently, much attention has been directed to determining ways to implement silicon as an optical material to address the cost and manufacturing limitations of current optical devices and to advance the microelectronics industry.[200] Importantly, silicon has properties that also make it attractive for photonics, most notably its transparency to wavelengths of light greater than 1100nm and its high refractive index (RI = 3.5). These properties, coupled with CMOS-processing techniques, allow optical devices to be defined in silicon substrates such that fabricating thousands of silicon photonic components has become a trivial task. Device alignment, typically the most critical and time-consuming step of assembling traditional compound optical systems, becomes a fully passive process because the photolithographic masks define the device layout.

An important feature of silicon-based devices is the facile modification by oxidation, doping, and metallization. The incorporation of oxygen into silicon (forming SiO_2) is the most common modification, and it is ubiquitously used as the insulator in silicon-on-insulator (SOI) microelectronic devices. As applied to silicon photonic structures, the lower RI of SiO_2 (RI = 1.46) compared to silicon allows it to serve as a cladding material and confine the light modes within features, known as waveguides, defined in the silicon. Doping is necessary to impart electrical functionality, such as diodes, into silicon. A simple example which demonstrates this feature is a p-i-n diode, where group III and group V ions are implanted in discrete regions on the silicon to introduce p-type and n-type behavior, respectively.[199] Finally, the metallization of silicon (i.e. deposition of metallic structures on silicon) allows for the inclusion of device interconnects and contact pads for external manipulation and interrogation. These common processes utilized by the microelectronics industry can also be incorporated into the fabrication of silicon photonic devices to act as, for example, optical switches and modulators.[201]

Waveguides can shuttle and manipulate light on the devices in a way that is analogous to how metallic wiring guides electrical signals, and since using photons instead of electrons significantly increases potential data transfer rates and decreases loss, silicon photonics is of particular interest to the communications industry and assures continued investment in this area. Fiber optic cables are already used to rapidly transmit data over long distances with little loss, and the transition to replace on-chip electronics with optical components has begun.[202] Further, because of silicon's excellent electrical properties, the extensive tools available for modifying silicon (e.g. silicon doping and metallization),[199] and the demonstrations of on-chip optical components discussed above, it is clear that fully integrated optoelectronic chips are achievable in the near future.

2.6   Conclusions

Frustratingly, biosensor technology remains largely confined to the research setting, and very few technologies have made it to the clinic, to the general public, or to the POC setting—where the need is great. In a survey of the biosensing literature, and even within this chapter, it becomes apparent that this is not for want of new sensing techniques or increased sensitivity. Instead, the biosensing community continues to produce new devices with new or improved approaches for accomplishing similar goals. All too often, promising new technologies are falling short of the goal of making an impact in healthcare, drug discovery, environmental monitoring, defense, etc. Clearly, increased attention needs to be directed toward realizing impactful applications of the technology.

Fully integrated devices open up many possibilities for real-world applications, but in order to gain traction and establish biosensors as an effective tool, researchers must identify and focus on a few strategic areas where biosensors can make the most immediate and meaningful impact. More focused, application-driven, and collaborative research and development efforts would increase the likelihood of overcoming the hurdles that are currently preventing biosensors from being implemented in POC settings. For instance, targeting specific applications that demonstrate the most need will attract the funding that will be needed to fully develop the biosensor and get it through clinical trials. Simply put, technology is no longer the limiting factor to more fully incorporating biosensors into healthcare—increasingly it has become a problem of systems integration and design of application centric biosensors.

Over the past several decades, significant effort has been invested with the aim of developing sensing technologies that will impact the practice of biomedical research and healthcare. This investment has yielded a plethora of sensing technologies built upon a variety of sensing modalities (i.e. electrochemical, mechanical, optical, etc.). Ultimately, there is no one-size-fits-all solution for biosensing, and in this chapter, we have argued for a few important design considerations for developing application-based sensors. (1) A biosensor should be sensitive and selective for the intended analyte(s) within complex samples, such as saliva, blood, or urine. (2) Label-free detection can decrease assay time, costs, and complexity, and is generally more flexible than its label-based counterpart. (3) Multiplexing confers enhanced reliability by allowing in-line controls and increased assay information density, thereby reducing costs associated with multiple tests. Finally, (4) a fully integrated platform, including peripheral instrumentation (e.g. a light source, a detector, and a microprocessor) and sample

handling capabilities (e.g. pumps, microfluidic channels) in addition to the sensor, is essential for these devices to expand beyond the lab and to the point of care.

Silicon photonic optical biosensors are a very promising candidate technology with the potential to integrate all of these design features. As an optical biosensing technique, these devices are label-free because they rely on the inherent refractive indices of the analytes to generate the signal. Their limited size and high sensitivity will enable massively parallelized multiplexed sensing using wafer-scale processing, dramatically reducing the cost and complexity of fabricating thousands of devices onto a single chip. In addition, by leveraging microelectronic fabrication techniques, silicon photonic biosensors can be integrated with planar on-chip light sources, detectors, and microprocessors. Microfluidics, including pumps, sample preparation strategies, and optical components, can be readily incorporated onto these planar features. Ultimately, the barriers to achieving a fully integrated biosensor using silicon photonics appear to be lower than they are for other sensing modalities.

For the purposes of studying carbohydrate-mediated bacterial adhesion, we chose two different biosensing platforms that are united by a few important features. The microelectrode array is based on a more mature technology and the previous research done on microelectrodes has established a large body of work that supports its development. Binding assays are done under static conditions, which are ideal for many bacteria, but flow systems could easily be incorporated. The microring resonators, on the other hand, are based on the emerging technology of silicon photonics, which has attracted much interest and investment from the telecommunications and microelectronics industries. This assures continued investment in this technology and thus the biosensors utilizing silicon photonics stand to benefit from the advancements that are made, particularly from the standpoint of device integration. Experiments are performed under flow, so they are particularly useful for studying bacteria that are shear-enhanced binders. Despite being a relatively new technology, the experimental design and execution is essentially identical to SPR, which has an extensive history of biosensing experiments. What the microelectrode array and the microring resonator platforms share is the future potential to be translated into POC biosensors. Both are fabricated using technologies developed by the microelectronics industry, and thus can benefit from the economies of scale and increasing the numbers of sensors on the chips is a trivial task. Further, the supporting instrumentation for both platforms can be incorporated in planar formats, such that all of the instrumentation can be contained on a single device. While device integration is not immediately relevant to the research reported in this thesis,

establishing ourselves as early users of these platforms for conducting bacterial adhesion studies is important.

3. CHAPTER 3: MICROELECTRODE ARRAY BIOSENSOR FOR STUDYING CARBOHYDRATE-MEDIATED INTERACTIONS

Carbohydrate-mediated host-pathogen interactions are essential to bacterial and viral pathogenesis, and represent an attractive target for the development of anti-adhesives to prevent infection. We present a versatile microelectrode array-based platform to investigate carbohydrate-mediated protein and bacterial binding, with the objective of developing a generalizable method for screening inhibitors of host-microbe interactions. Microelectrode arrays are well suited for interrogating biological binding events, including proteins and whole-cells, and are amenable to electrochemical derivitization, facilitating rapid deposition of biomolecules. In this study, we achieve microelectrode functionalization with carbohydrates via controlled polymerization of pyrrole to individual microelectrodes, followed by physisorption of neoglycoconjugates to the polypyrrole-coated electrodes. Covalent functionalization of thiolated carbohydrates to amine-terminated oligiomers that were built off of the microelectrode surface was also investigated, but this method was found to be unreliable and time consuming. Bioactivity of the immobilized carbohydrates was confirmed with carbohydrate-binding proteins (lectins) detected by both fluorescent and electrochemical means. The platform's ability to analyze whole-cell binding was demonstrated using strains of *Escherichia coli* and *Salmonella enterica*, and the dose-dependent inhibition of *S. enterica* by a soluble carbohydrate antiadhesive.

3.1 Introduction

Increasing demand for biosensors in fields such as medical diagnostics, basic research, drug design, environmental monitoring, and food safety has led to a rapid expansion in biosensing technologies. Out of the various biosensor architectures, those based on microelectrode arrays stand out as one of the most versatile and promising for studying binding interactions [203]. Part of this versatility stems from the fact that microelectrode array biosensors can be fabricated using well-established techniques such as simply depositing gold on glass substrates or more complex complementary metal oxide semiconductor (CMOS) processing, which enables the production of sensitive, compact, and affordable biosensors with varying multiplex capabilities. Electrode-based arrays are compatible with a diverse range of detection modalities including fluorescence, electrochemical, and label-free, adding further to their versatility. Fluorescent detection is expedient for platform development and research purposes because of the simple readout and amenability to existing fluorescent microarray infrastructure. Additionally, the

electrically-active nature of the platform facilitates the development of compact and portable instrumentation based on electrochemical detection (ECD) and label-free detection. When coupled with microfluidics and portable computers, microelectrode biosensors are readily adapted for distributed point of care (POC) applications [203a, 204].

Immobilized nucleic acid [75], protein [76], and carbohydrate microarrays [77] have become instrumental research tools for conducting high-throughput studies of binding interactions. In addition to the ability to conduct multiplexed analysis, microarrays can be fabricated using small volumes of reagent (pl to nl volumes per spot), and the 2-dimensional presentation of binding ligands mimics the cellular surface [22b]. While DNA and protein microarrays have been and will continue to be valuable research tools, glycobiology may stand to benefit the most from microarray technology: the structural complexity of carbohydrates and the difficulties involved with their synthesis necessitate high-throughput and low-volume reagent consumption, respectively [78].

Improved methods are needed to identify and further characterize carbohydrate-mediated pathogen binding to host tissues, such as those in the gastrointestinal tract. A platform capable of screening these interactions would facilitate the development of binding inhibitors to disrupt adhesion and thereby prevent pathogenesis. Specifically, soluble carbohydrates have been suggested for bacterial anti-adhesive prophylaxis and therapy [17d, 54f, 70c], where they act as competitive inhibitors to the tissue-expressed glycan receptors. The inhibitors decrease bacterial binding or prevent it altogether while minimizing the selective pressure exerted on the pathogen, thus addressing the growing problem of microbial resistance to antibiotics. The effectiveness of this approach has been demonstrated *in vitro* [205], in animal models [51, 206], and in the protection of infants from diarrheal disease by the naturally-occurring glycans present in human breast milk [17a, 17c, d].

In this study we bring together the microelectrode biosensor and the carbohydrate microarray using a highly multiplexed, CMOS microelectrode array to study carbohydrate-mediated ligand-receptor interactions using lectins (carbohydrate-binding proteins) and bacteria. Glycans are covalently linked to bovine serum albumin (BSA) and adsorbed on polypyrrole (PPy) coated electrodes. We have previously demonstrated this approach for immobilizing antibodies and DNA onto the CustomArray (Bothell, WA) microelectrode array [96]. Herein we describe an extension of this methodology for the functionalization of microelectrodes with glycoconjugates for applications in glycomics research. PPy is deposited via electropolymerization on designated electrodes and BSA glycoconjugates are adsorbed on the PPy immediately thereafter. We validate carbohydrate functionalization by showing specific binding of

lectins to BSA-sugar conjugates using both fluorescence and electrochemical detection methods. We subsequently confirm specific bacterial binding with the mannose-binding K12 strain of *Escherichia coli* via fluorescent detection and scanning electron microscopy (SEM). We also demonstrate the utility of this platform for studying carbohydrate bacterial binding inhibitors through the inhibition of mannose-binding *Salmonella enterica* with methyl-α-D-mannopyranoside (αMM). Finally, we investigate the use of a novel instrument which was designed to perform high-throughput experiments using the Ppy functionalization technique (the MX3120). Together, this technology could play a critical role in the development of anti-adhesive prophylactics by indentifying bacteria-carbohydrate binding specificities and characterizing binding inhibitors.

3.1.1   Description of the Microelectrode Microarray

The microelectrode array (Figure 14) and supporting instrumentation were developed by CustomArray (formerly CombiMatrix), as described in detail previously [96b, 207]. The array used in these studies contains 12,544 platinum microelectrodes,

Figure 14. (A) The single chamber flow cell is clamped against the chip using plastic clips on either side. (B) The four-chamber flow cell requires a clamping structure to secure it in place.

each 44 µm across, that are fabricated using standard CMOS processing (Figure 15). Each microelectrode is separated from the counter electrode with an insulating layer of silicon nitride. The array is embedded in a ceramic support the size of a standard 1x3" microscope slide to facilitate experimental handling. Custom-built flow cells (Figure 14) allow fluidic isolation of the microelectrodes from the electrical contact pads, which enables solution-based experimental protocols, such as hybridization, to be carried out on the microelectrodes. Both single chamber and four-chamber hybridization flow cells are available; the single chamber flow cell allows simultaneous processing of all microelectrodes, while the four-chamber flow cell divides the microelectrodes into four regions of ~2000 electrodes each for different assay protocols. The flow cells are used throughout the process of experimentation and can be taken off to switch from one flow cell to the other (e.g. single-chamber to four-chamber) or replaced with a cover slip before fluorescent detection with the microarray scanner. Through on-chip integrated microelectronic circuitry and supporting instrumentation and software, each electrode or specified patterns of electrodes can be specifically controlled and interrogated. This allows high-throughput and

specific modification of microelectrodes because the electrical actuation of electrodes can elicit changes in the localized environment. Using this platform, it has been shown that electrochemically generated acidic environments are contained within the region surrounding each electrode in the presence of a suitable buffer. This method is used to control chemical reactions, such as the sequential removal of dimethoxytrityl (DMT) 5' protecting groups from electrode-anchored oligonucleotides being fabricated *in situ*, a process which CustomArray (formerly CombiMatrix, Mukilteo, WA) uses to construct custom DNA microarrays using standard phophoramidite chemistries.[208] Upon removal of the protecting groups from oligonucleotides on specified electrodes, the array is exposed to a solution containing the desired nucleotide base to be added. Each base contains the protecting group on the 5' hydroxyl group, such that this process can be repeated for each sequential base addition. In this way, using automated instrumentation, CustomArray is capable of producing custom DNA microarrays containing as many unique sequences as there are electrodes on the array. The primary commercial focus of the company is the production of custom DNA microarrays and the sales of supporting instrumentation. . However, additional capabilities have been explored, including a similar *in situ* synthesis approach for peptides and high-throughput generation of molecular libraries using various chemistries adapted for this platform.[209]

The microelectrode array supports both fluorescent detection and enzyme-enhanced electrochemical detection (ECD).[207, 210] Fluorescent labeling of the analyte or of a secondary indicator allows detection on a standard microarray scanner, such as the GenePix 4000B (Molecular Devices, Sunnyvale, CA)(Figure 16A). ECD utilizes a palm-sized instrument (the ElectraSense™, Figure 16B) to measure redox reactions
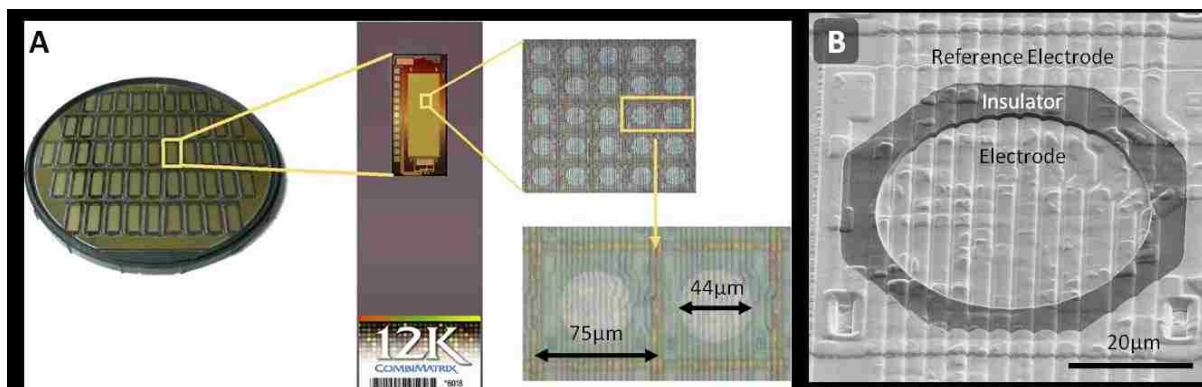
Figure 15. (A) Multiple arrays are made on a single wafer using standard CMOS fabrication. Each array is embedded in a ceramic chip. In the light micrographs, some of the underlying circuitry can be seen. (B) An SEM of a single electrode reveals the exposed rings of insulator that separate the electrodes from the reference electrode.

associated with bound HRP-labeled analyte when exposed to a TMB solution. The ElectraSense™ connects to a personal computer through a USB cable that also provides power to the unit (Figure 16C). One of the traditional challenges to ECD with electrode arrays is the technical difficulty of extracting an output signal from each electrode because of the wiring complexity and the need for a multi-channel

Figure 16. (A) The GenePix4000B. (B) The Electrasense, developed by CustomArray. This version of the Electrasense is completely portable, and it allows both Ppy deposition and ECD measurements to be taken. (C) It is powered through the USB cable and it can rapidly transmit data to the user.

detector. The integrated microelectronics of CustomArray's chips allows high-throughput electrical readings of the entire array in 15 seconds using the ElectraSense™. These signals can then be readily analyzed on the computer to which the reader is attached. It has been shown that ECD has equivalent sensitivities as fluorescent detection for genotyping and gene expression assays,[207a] and ECD is more attractive for POC applications because the measurement equipment is smaller, less expensive, and more robust and because it produces a digital data output which facilitates rapid analysis. Nevertheless, both detection formats are useful for assay development and research purposes.

3.1.2   Previous Applications of the Microelectrode Microarray

CustomArray chips functionalized through complementary oligonucleotides have been used for various applications, including the detection of serum micro-RNAs (miRNAs) associated with cancer;[211] the genotypic subtyping of influenza virus;[209d, 212] the detection of pathogens such as *Bacillus anthracis*, *Yersinia pestis*, *Bacillus subtilis*, and *E. coli* based on genotyping;[207a] and the detection of ricin, M13 phage, *Bacillus globigii* spores, and human α1 acid glycoprotein.[210] Approaches for immobilizing non-DNA (e.g. antibody) receptors on the chips utilized complementary strands of DNA attached directly to the receptor[210] or biotinylated complementary DNA and receptors held together with streptavidin.[213] While both of these methods proved effective, they require multiple assay preparation steps including the *in situ* synthesis of oligonucleotides on the electrodes and conjugation of complementary

oligonucleotides or biotin to the receptors. As an alternative approach, CustomArray developed a polypyrrole (Ppy)-based functionalization method that requires fewer preparation steps, thereby decreasing costs and time required to complete the assay.[96b] Activation of desired microelectrodes polymerizes pyrrole from solution onto the electrode surfaces, and unlabeled biomolecules are immobilized to the Ppy-coated electrodes through electrostatic adsorption. Using this approach, an immunoassay for staphylococcal enterotoxin B was developed that could reliably detect 0.01 pg/ml SEB, which is an order of magnitude lower than what could be detected using a conventional enzyme-linked immunosorbant assay (ELISA).[96b] CustomArray also showed that the Ppy functionalization approach applied to DNA could produce higher hybridization signals as compared to their traditional on-chip DNA synthesis functionalization.[96a]

3.1.3 Description of the MX3120

The MX3120 (Figure 17A) is an investigational platform designed to improve the multiplexing potential of Ppy functionalization on the microelectrode array. This work represents a collaborative effort to bring together two high-throughput platforms – a microelectrode array biosensor (CustomArray Inc.) and a microfluidic continuous flow microspotter (CFM, Wasatch Microfluidics, Salt Lake City, UT) – to produce an integrated high-throughput biosensing instrument. The MX3120 combines the MX300 instrument described by Cooper et al.,[178] which automates Ppy deposition on the microelectode arrays, with Wasatch Microfluidics' CFM, a silicone-based microfluidic device used to print biomolecules in an arrayed fashion.[214] The flow cell incorporated with this instrument
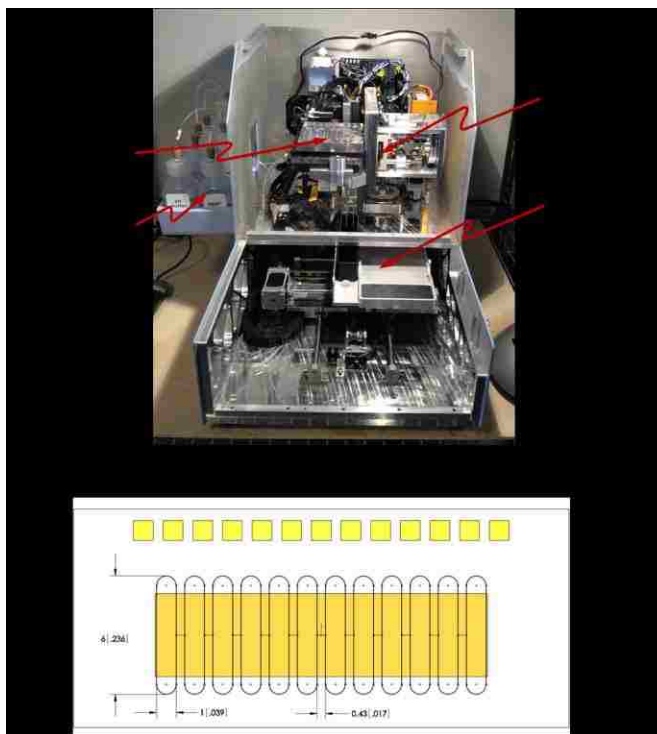
Figure 17. (A) Picture of the MX3120 with the cover removed to expose the internal components. Some of the primary components are highlighted. The PDMS flow cell (i.e. the CFM) is enclosed in a plexiglass casing. The "High-Volume Solutions" include buffers and cleaning reagents that are used in high volumes. The microelectrode array is inserted horizontally in a slot such that the CFM can be pressed onto the array surface. A 96-well plate is placed on the "Microplate Platform," from which reagents are pulled by a fluidic pump (not shown). (B) Schematic representation of the flow cells as they are overlaid on the microelectrode array.

divides the microelectrode arrays into 12 distinct sections (Figure 17B); this separation not only allows for multiplexed functionalization, but it was also intended to permit 12 simultaneous binding experiments to be performed at once. For simultaneous binding experiments, the instrument would rely on the ECD capabilities of this platform.

3.2 Materials and Methods

3.2.1 <u>Materials</u>

Sulfosuccinimidyl-4-(N-maleimidomethyl)cyclohexane-1-carboxylate (Sulfo-SMCC), Tris(2-carboxyethyl)phosphine hydrochloride (TCEP-HCl), Zeba spin desalting columns with 7,000 MWCO, Slide-A-Lyzer dialysis cassettes with 10,000 MWCO, and DyLight 649 amine-reactive dye were purchased from Pierce (Rockford, IL). SYTO 62 red fluorescent nucleic acid stain was acquired from Invitrogen (Carlsbad, CA). Fraction V BSA was purchased from EMD Chemicals (Darmstadt, Germany). Methyl-α-D-mannopyranoside (αMM) was acquired from TCI America (Portland, OR). Tween-20 was purchased from BioRad (Hercules, CA). Concanavalin A (ConA) was obtained from MP Biomedicals (Sodon, OH) and diluted into HEPES buffer containing divalent cations (1 mM $CaCl_2$ and 1 mM $MnCl_2$) to maintain the tetrameric structure of the lectin. Pure ricin agglutinin (RCA_{120}) and HRP-conjugated RCA_{120} were purchased from EY Labs (San Mateo, CA) and were diluted into PBS. Pyrrole (Sigma-Aldrich, St. Louis, MO) was distilled and stored under argon at 4°C and protected from light. Working solutions of 0.1 M pyrrole in 0.1 M dibasic sodium sulfate were prepared fresh for each experiment. Casein was purchased from Sigma-Aldrich (St. Louis, MO) and the casein blocking solution was prepared by mixing 3 g/L of casein into PBS and stirring for 1-2 h, followed by gravity flow filtration through a 0.22 μm filter (Steritop-GP, Millipore, Billerica, MA) for 24 h at 4°C. Thiolated biotin (HS-$(CH_2)_{10}$-CONH-$(CH_2)_3$-$(OCH_2CH_2)_3$-CH_2-NH-Biotin) was purchased from nanoScience Instruments (Phoenix, AZ).

All buffers were made with ultrapure DI water (Barnstead Nanopure; ThermoFisher Scientific) and brought to the correct pH using 1 M HCl or 1 M NaOH. Phosphate buffered saline (PBS, pH 7.4) contained 10 mM phosphate (1.9 mM KH_2PO_4 and 8.1 mM Na_2HPO_4) with 150 mM NaCl. HEPES buffer (pH 7.3) with divalent cations was composed of 20 mM HEPES, 150 mM NaCl, 1 mM $CaCl_2$, and 1 mM $MnCl_2$. PBS with 0.1% Tween-20 (w/v) (PBST) was mixed for washing the chips. Thiolated sugars with oligoethylene glycol spacers (HS-OEG_3-sugar) and thiolated OEG (HS-OEG_3) were synthesized in the Ratner laboratory as previously described [77c].

3.2.2   BSA Conjugate Synthesis

BSA conjugates were fabricated to provide a facile method to immobilize and display small ligands (biotin and sugars) on PPy-coated microelectrodes. Thiolated biotin, thiolated sugars, and thiolated OEG were attached to the free amines of the BSA via the heterobifunctional cross-linker sulfo-SMCC. First, 10 mg/ml BSA in PBS was activated for thiol conjugation by incubating for 30 min at room temperature with 0.5 mg/ml sulfo-SMCC. After the reaction, free sulfo-SMCC was removed using Zeba desalting columns, following the manufacturer's instructions for a buffer exchange into PBS. Biotin-, sugar- and OEG-thiols (4 mM in water) were reduced for 10 min at room temperature with 2mM TCEP-HCl. Equal volumes of each of the reduced biotin-, sugar-, and OEG-thiols (final concentration of 2 mM) were mixed with the 10 mg/ml maleimide-activated BSA (final concentration of 5 mg/ml) and incubated for 30 - 60 min at room temperature. After conjugation, free thiols were removed using Zeba desalting columns. A BCA assay was performed on the BSA conjugates to determine the protein concentration, at which point they were aliquoted and stored at -20°C at 4 mg/ml in PBS. Prior to functionalization of the microelectrodes, BSA conjugates were diluted in PBS to a working concentration of 0.5 mg/ml.

3.2.3   Fluorescent Labeling

Probe proteins (lectins and antibodies) were labeled following the published protocols for DyLight amine-reactive dyes. DyLight 649 conjugation was performed in PBS for 1 h at room temperature, at which point unconjugated fluorophore was removed by dialysis (twice overnight at 4°C in 2L of buffer – HEPES with divalent cations for ConA, PBS for all others) using Slide-A-Lyzer Dialysis cassettes with a 10,000 MWCO. Conjugation of the dye was confirmed and the final concentration of protein was determined using UV-vis spectroscopy (data not shown). Ligand-binding functionality of the fluorescently-labeled probes was verified prior to use on the microarray using SPR (data not shown). Probes were stored at 4°C for up to six months.

3.2.4   Bacterial growth and preparation

All strains of *Escherichia coli* and *Salmonella* spp. were graciously donated by the Sokurenko lab at the University of Washington (Seattle, WA). All bacteria were genetically modified to either (a) express fimbria containing a terminal FimH mannose-binding adhesin or (b) lack FimH binding adhesin and act as control strains. For brevity, the mannose-binding *E. coli* will be referred to as "*E. coli* FimH+" and the non-binding strain will be referred to as "*E. coli* FimH-." The mannose-binding *Salmonella* will be referred to as "*S. enterica* FimH+" and the non-binding *Salmonella* will be "*S. enterica* FimH-."

E. coli were *fim* null strains of K12 (AAEC191A) [215]. KB18 *E. coli*, the non-binding control strain, was AAEC191A complemented with pPKL114 plasmid carrying all of the *fim* operon genes from K12 *E. coli* with the exception of *fimH* [216]. The mannose-binding strain was AAEC191A with the pPKL114 plasmid and the pGB plasmid which carries the *fimH* gene from wild-type K12 *E. coli*. For brevity, the mannose-binding *E. coli* will be referred to as "*E. coli* FimH+" and the non-binding strain will be referred to as "*E. coli* FimH-." Culture tubes with 3 ml Lysogeny broth (LB) containing the appropriate antibiotics were inoculated from freezer stocks (15% glycerol in LB) and allowed to culture in static conditions for 16-18 h at 37°C. The single plasmid in *E. coli* FimH- (pPKL114) gives it a resistance to ampicillin, which was added to the LB at 100 µg/ml. *E. coli* FimH+, a double plasmid bacteria (pPKL114 and pGB), is resistant to ampicillin and chloramphenicol, which were added to the LB at concentrations of 100 µg/ml and 25 µg/ml, respectively.

Both *Salmonella* strains were *fimH* knockouts of *Salmonella enterica* serovar Typhimurium [217]. The mannose-binding *Salmonella* strain was complemented with pISF255b plasmid carrying *fimH* from *Salmonella* Choleraesuis strain 1656/04 which leads to expression of type I fimbria with a high-binding variant of fimH. The non-binding control strain contained the same plasmid with no *fimH* gene. For brevity, the mannose-binding *Salmonella* will be referred to as "*S. enterica* FimH+" and the non-binding *Salmonella* will be "*S. enterica* FimH-." Bacteria were inoculated from freezer stocks (15% glycerol in LB) in 3 ml LB containing 30 µg/ml chloramphenicol and then cultured in static conditions at 37°C. After 24 hr, 50 µl of the bacteria suspension was transferred to new culture tubes with 3 ml LB containing 30 µg/ml chloramphenicol for a second 24 h incubation. This extended growth is done to enrich the expression of fimbria.

Following growth, the bacterial suspensions were transferred to 15 ml conical tubes and centrifuged for 5 min at 4000 rcf. The broth supernatant was discarded, and the pellet was washed with 10 ml PBS. The bacteria were then resuspended in PBS and diluted to an OD_{600} of 0.8 (+/- 0.05).

Binding of *E. coli* was detected using labeled antibodies, so no further modification was necessary prior to biding studies. *Salmonella* strains were labeled with Syto 62, a cell-permeable fluorescent nucleic acid stain. *Salmonella* in PBS (OD_{600} = 0.8) were pelleted by centrifugation at 4000 rcf for 5 minutes, the PBS was removed, and the bacteria were resuspended in PBS containing 5 µM SYTO 62. After a 15 min incubation, the *Salmonella* were pelleted again at 4000 rcf for 5 min, washed twice with PBS, and then resuspended in PBS containing 0.2% (w/v) BSA at an OD_{600} = 0.8.

3.2.5   Microelectrode functionalization via Silanization

We first explored covalent immobilization of carbohydrates to the microelectrodes using fluorescently-labeled ConA to probe for successful functionalization of mannose. ConA was labeled with DyLight 649 amine-reactive fluorescent dye (Pierce, Rockford, IL), a wavelength supported by the GenePix 4000B microarray scanner. For covalent immobilization, we modified CustomArray's conventional DNA array production to include a primary amine on the termini of poly-thymine (poly-T) oligonucleotides. Initial attempts of using acrylic acid NHS ester to act as a cross-linker between the primary amines and the thiolated glycans proved unsuccessful. In an effort to trouble-shoot this problem, we compared acrylic acid NHS ester to sulfo-SMCC (Pierce, Rockford, IL) for attaching thiolated mannose to the free amines of BSA. Using SDS PAGE and a Western blot, we found that the sulfo-SMCC was a far more efficient way to cross-link thiolated glycans with terminal amines. Thus, we used sulfo-SMCC for the *in situ* modification of the microelectrodes, demonstrating that we could covalently immobilize thiolated glycans to the maleimide-modified oligonucleotide array (Figure 18). Despite some success, there were still several issues including high background binding (especially on the silicon oxynitride rings surrounding the electrodes), unexplainable chip-to-chip inconsistencies, and low conjugation efficiency (as indicated by low binding signal). It is important to note here that the CustomArray chips underwent various processing steps to prepare them for

Figure 18. Covalent immobilization strategy using amino-terminated oligonucleotides (Poly T). Thiolated glycans are attached to the electrodes via SMCC chemistry. Results illustrate the difference in fluorescent ConA-binding between mono-mannose and tri-mannose.

oligonucleotide synthesis, including cleaning by oxygen plasma and coating with a proprietary sugar solution to generate high concentrations of hydroxyls to which the DNA oligonucleotides were anchored. We hypothesized that one or both of these steps introduced some functionality on the silicon nitride rings surrounding the microelectrodes, and undertook a systematic study using chips removed from the production line at different points. One possibility was that the plasma treatment introduced amines on the silicon nitride as had been reported in the literature.[218] In order to test this, we attempted sulfo-SMCC linking of thiolated mannose on chips that came straight from the plasma cleaning process. While some rings could be seen after exposure to fluorescent ConA, control electrodes

which were exposed only to thiolated mannose and not sulfo-SMCC showed the same level of ConA binding to the rings. Interestingly, another region of control electrodes to which a thiol-terminated oligoethyleneglycol (OEG) was added after sulfo-SMCC, and before the thiolated mannose, significantly reduced binding to the rings. Since OEG is commonly used to passivate surfaces from protein binding,

Figure 19. A zoomed in view of a small area of the electrodes. It appears that NEM blocks binding, possibly by preventing thiol interactions. Alternating rows of electrodes contained aminated oligos, hence the bright and dark rows.

this led us to believe that mannose could be binding to the rings through a thiol-mediated interaction. We proceeded with additional experiments to test this hypothesis, using N-ethylmaleimide (NEM) to react with the thiolated mannose in solution prior to functionalization. Results from this investigation suggested that thiolated mannose could be attaching to the silicon nitride rings through a thiol-mediated interaction, as the NEM-blocked group of electrodes showed no binding (Figure 19)**.** At this point we were confident that the production process was not introducing amine functionality and we had a possible explanation for binding to the rings. However, after additional attempts continued to generate inconsistent results, even in identical experiments done concurrently, we decided to explore other functionalization methods.

3.2.6   Microelectrode functionalization with BSA-conjugates via polypyrrole

3.2.6.1 PPy Deposition

A functionalization map for the ElectraSense instrument was created using CustomArray software for PPy deposition. The map designates which electrodes to activate, as well as the current to maintain and the amount of time to keep the electrodes activated. PPy was deposited from a solution of 0.1 M pyrrole in 0.1 M sodium sulfate buffer using a current of 90 nA for 1 to 4 seconds. The optimal deposition time was found to be 2 seconds, and all quantitative measurements were, therefore, performed on electrodes functionalized using these optimized conditions. The microelectrode array was divided into four regions, each corresponding to a single chamber of the four-chamber flow cell, to control for intrachip heterogeneity and allow screening of up to four analytes per chip. Each one of these regions was further divided into four rows of five 5x5 blocks of electrodes, with each of these four rows

containing a different biomolecule (Figure 20). Each row was individually functionalized via a stepwise addition of PPy, biomolecule, BSA block, and rinse (see Array Biofunctionalization section, below).
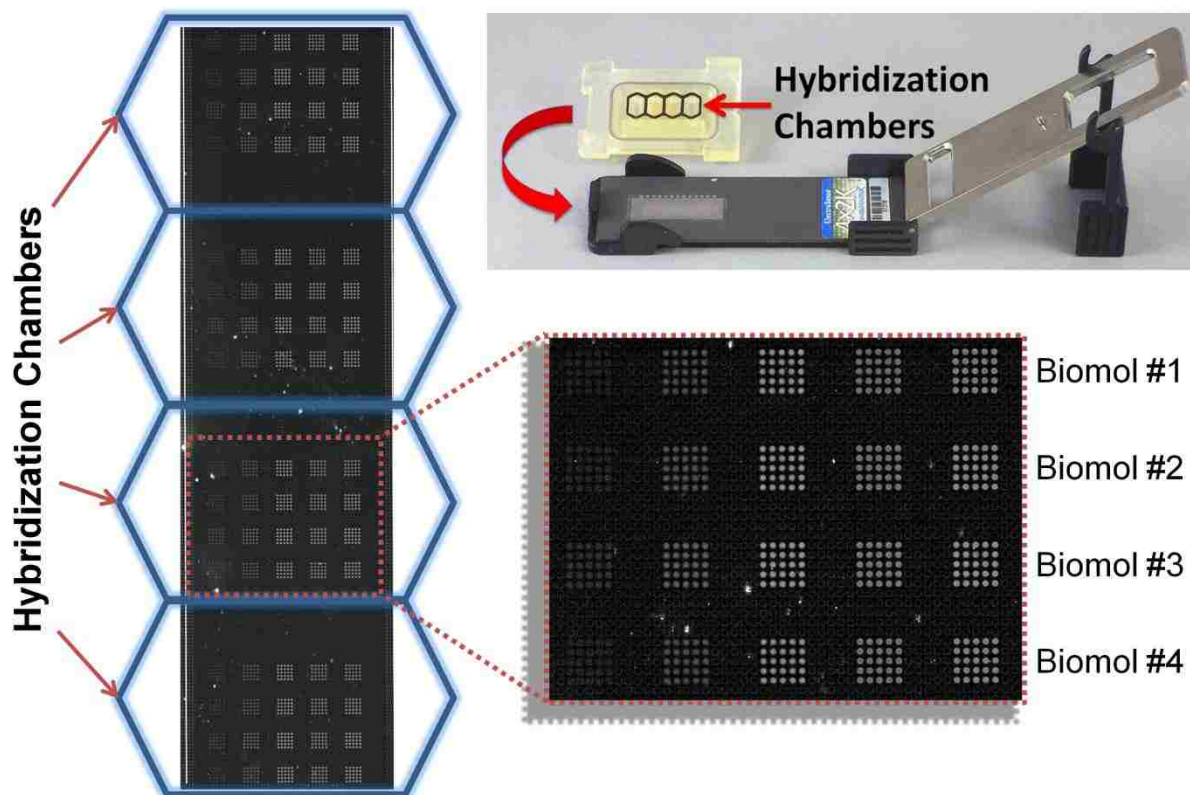
Figure 20. During the binding assays, the array can be divided into four fluidically-isolated hybridization chambers using the 4x2k hyb cap that is secured on the microelectrode array using a custom clamp. The fluorescent image on the left and the magnified inset on the right show the PPy deposition layout that was used for all experiments reported herein. Each sector corresponding to the 4x2k hyb cap contains four different biomolecules (Biomol). Image was created using a GenePix 4000B observing PPy autofluorescence at 532 nm. The PPy deposition time was varied for the array in this figure, which can be observed in the difference in fluorescent intensity between columns of 5x5 regions of electrodes.

3.2.6.2   Array Biofunctionalization

Blocking solutions used during the functionalization process were either a saturated casein solution or 2% (w/v) BSA in PBS. Bare CustomArray microelectrode microarrays were placed in a single-chamber hyb cap and blocked for 5 min with blocking solution to prevent non-specific binding. The chip was rinsed with PBST (3 times), PBS (3 times), and 0.1 M sodium sulfate (3 times) – the standard wash sequence – prior to the addition of pyrrole solution (0.1 M pyrrole in sodium sulfate) and PPy electrodeposition. Immediately following deposition of the first row of PPy, the array was washed twice with PBS and then blocked again with 2% BSA for 5 min. This row served as a negative control for binding. Depending on the experiment, BSA conjugates were deposited on the next three rows by iterative application of the aforementioned wash sequence, PPy deposition, and bioconjugate

functionalization. Each bioconjugate, at a concentration of 0.5 mg/ml, was incubated on the chip for 15 min at room temperature to facilitate adsorption to the most recently deposited row of PPy. To prevent cross-functionalization, the chip was immediately blocked for 3 min with 2% BSA. This process was repeated for each remaining row using the desired biomolecules. A final incubation in 2% BSA for 1 h at room temperature was employed to prevent non-specific binding during subsequent assays. Prior to binding with fluorescently-labeled proteins, HRP-conjugated probe molecules, or bacteria, chips were washed twice with PBS. In most cases, binding assays were performed immediately after functionalization. However, to verify the stability of functionalized arrays, several chips were rinsed with water, dried, and stored over desiccant at room temperature for up to four months. Unless otherwise indicated, all chips contained a control for the protein carrier (BSA), a negative control sugar-BSA conjugate for which the target analyte has no known specificity, and a sugar-BSA conjugate to which the analyte is known to bind.

3.2.6.3 High Throughput Microelectrode Functionalization with the MX3120

Prior to the design and construction of the MX3120 platform, the ability of Wasatch Microfluidics' CFM was tested for its ability to form a seal when pressed against the non-planar surface of the microelectrode array. In order to do this, fluorescently-labeled BSA was flowed over the array surface and the chip was imaged using a microarray scanner. Preliminary binding experiments were also performed by functionalizing the chips with RNaseB and single-stranded DNA using the CFM on a Ppy-coated chip. Bioactivity of the deposited reagents was probed with fluorescently-labeled ConA and complementary ssDNA. After the successful pilot studies, the MX3120 was designed and built by CustomArray. The instrument has been used for preliminary biosensing experiments to detect the binding of ConA to mannose-BSA as well as ricin$_{60}$ to anti-ricin antibodies, as imaged by a GenePix 4000B microarray scanner. In addition to depositing the two target reagents, multiple control reagents including lactose-BSA and BSA were used.

3.2.7 Protein and bacterial binding and inhibition

3.2.7.1 Proteins

For imaging studies, fluorescently-labeled proteins were diluted in buffer (PBS pH 7.4 for all proteins except for ConA, which was diluted in 20 mM HEPES with 150 mM NaCl, 1mM CaCl$_2$, and 1 mM MnCl$_2$, pH 7.3) to the following working concentrations: streptavidin, 37 nM; ConA, 400 nM; and RCA$_{120}$, 4 μM. The functionalized chips were incubated with the probe for 30 min and then washed with PBST (twice) and PBS (twice) before the hybridization chamber was removed. The microarray was immediately

covered with PBS and a cover slip to prevent drying, and imaged on a GenePix 4000B. Arrays were scanned using instrument settings appropriate for DyLight 649 dye (ex: 635 nm, em: 670 nm) with a photomultiplier gain of 400.

For ECD, RCA_{120}-HRP, diluted to a final concentration of 50 μg/ml in 0.1% BSA (w/v) in PBS, was incubated on the chip for 30 min at room temperature. Unbound RCA_{120}-HRP was removed by washing the chip with 2% BSA (twice), PBS (twice), and with pH 4 Conductivity Buffer Substrate (BioFX, Owings Mills, MD) (twice). TMB Conductivity 1 Component HRP Microwell Substrate (BioFX) was added to the array, and it was scanned immediately with the ElectraSense® microarray reader.

The CustomArray software creates a pseudo image of the array where the intensity of individual electrodes, depicted as square pixels, is proportional to the current produced from the HRP-mediated reaction with TMB. The average intensities of each row were plotted for quantitative comparisons.

3.2.7.2 Bacterial Adhesion

In all bacterial adhesion assays, bacterial suspensions were incubated on the chip for 1 h at room temperature and unbound bacteria were washed with PBST (4 times) and PBS (4 times). Bacteria bound to the microelectrodes were detected through either fluorescently-labeled antibodies (for *E. coli*) or a fluorescent nucleic acid label (*Salmonella enterica*). Antibodies against fimbrial protein A (fimA), expressed on *E. coli*, were labeled with DyLight 649 using the same methods as reported above for the lectins.

For *E. coli*, the DyLight-labeled antibody probe was incubated on the chip for 30 min at room temperature, and washed twice with PBST and PBS. Since the *S. enterica* were pre-labeled with the nucleic acid stain, these arrays could be imaged immediately after the one hour binding step. After removing the flow cells, the arrays were covered with PBS and a cover slip to prevent drying, and then imaged at 635 nm with a photomultiplier gain of 400.

3.2.7.3 Inhibition of Bacterial Adhesion

Methyl-α-D-mannopyranoside (αMM) inhibition of *S. enterica* binding to mannose was investigated at concentrations of 0.01 mM, 0.05 mM, 0.1 mM, and 1 mM αMM in PBS. Each region of the chip had BSA-mannose and two different control biomolecules (BSA-lactose and BSA only). For inhibition studies, bacteria were labeled with Syto 62 and resuspended in PBS with 0.2% BSA (w/v) and the correct concentration of αMM. Bacterial suspensions were pre-incubated for 30 min at room temperature with the binding inhibitor. After the incubation, bacterial suspensions containing the inhibitor were added to

the functionalized microelectrode array using the four-chamber hyb cap to test multiple inhibitor concentrations on the same chip. On each array, one chamber contained *S. enterica* without inhibitor and the three remaining chambers contained *S. enterica* with different concentrations of inhibitor. We also included two controls: (1) a *S. enterica*fimbrial knockout strain (*S. enterica* FimH-) to verify that the bacteria were not binding through other interactions, and (2) *S. enterica* FimH+ incubated with 5 mM galactose in place of αMM to ensure that the inhibition was specific. Attachment was allowed to occur for 1 h before the suspensions were removed and the chip was washed. For washing, each chamber of the four-chamber flow cell was rinsed with 200 μl PBST (3 times), at which point the four-chamber hyb cap was replaced with the single hyb cap and the chip was washed again with PBST (4 times) and PBS (4 times). For imaging, the hyb cap was removed, the array was covered with PBS, a cover slip was added to prevent drying, and imaged at 635 nm with a photomultiplier gain of 400.

3.2.8   Analysis of fluorescent signal intensity for binding inhibition studies

A chip map corresponding to the microelectrode array was drawn using GenePix Pro software. Briefly, four blocks corresponding to the four regions of the array were drawn, each containing 1739 elements (37 x 47), with 40 μm diameter spots and a 75 μm pitch. This produced an array that directly overlapped with all of the electrodes in each region of the chip. Data files containing the coordinates of each of the spots and the corresponding mean intensities were extracted and analyzed using custom spreadsheets in Microsoft Excel. Data are reported as the median value of the mean intensities from each of the 75 electrodes analyzed for binding to the biomolecules of interest. The median fluorescent intensity for each row of biomolecules is normalized to the median fluorescent intensity of the positive control row (BSA-mannose with no αMM inhibitor). Error bars represent one standard deviation from the mean of the median intensities extracted from four separate experiments with each concentration of inhibitor.

3.2.9   Bacteria fixation and SEM imaging

Following the 1 h incubation of the *E. coli* on the array, unbound bacteria were removed by washing with PBST (4 times) and PBS (4 times). The hybridization chamber was removed and the chip was submerged in ½ Karnovsky's fixative in 0.1 M sodium cacodylate buffer for 15 min. The chip was washed twice in 0.1 M sodium cacodylate buffer, submerged in 1% (v/v) osmium tetroxide in 0.1 M sodium cacodylate for 5 min, washed twice more in 0.1 M sodium cacodylate buffer, and washed copiously with water. This was followed by ethanol dehydration, advancing through 50%, 60%, 70%, 80%, and 95% EtOH solutions for 2 min each. Finally, the chip was submerged in two successive 100% EtOH solutions

for 10 min each. Immediately following the final 100% EtOH solution, the sample underwent critical point drying. The samples were then stored in a desiccant chamber until SEM imaging (1-2 days).

Samples were coated with approximately 5 nm of a 60-40 mixture of gold-paladium alloy using an SPI Module™ sputter coater. Scanning Electron Microscopy was performed using a FEI Sirion SEM with a spot size of 3 and a beam accelerating voltage of 10 kV. Chip coating and SEM imaging were performed at the Nanotech User Facility at the University of Washington.

3.3 Results and Discussion

3.3.1 Verification of functionalization approach

Carbohydrate-mediated bacterial binding represents a diverse class of biomolecular interactions that play a significant role in pathogenesis and are of great interest to both basic and applied biomedical research. Our objective is to develop a fundamental research platform that is simultaneously capable of interrogating these host-microbe interactions and screening potential inhibitors against microbial adhesion. To achieve this goal, we required a functionalization strategy that could satisfy the following criteria: (1) the ability to screen analyte binding to multiple immobilized ligands including controls, (2) a proper display of ligands to allow binding of interrogating proteins and bacteria, (3) reproducible binding between assays, and (4) stable ligand immobilization chemistries. The PPy method meets all of these criteria and is a versatile strategy for microelectrode functionalization.[175b, 219] Further, this approach has previously been characterized and optimized for stable and reproducible functionalization using the CustomArray microelectrode array.[96b]

We confirmed the bioactivity of immobilized small molecule ligand BSA-conjugates using three different binding pairs: biotin-streptavidin, mannose-ConA, and lactose/galactose-RCA_{120}. Thiolated ligands were conjugated to the free amines of BSA using sulfo-SMCC and deposited on specified microelectrodes. Utilizing BSA as a scaffold to display ligands is advantageous because: (1) it reduced non-specific interactions and is frequently used as a carrier and blocking agent; (2) it adhered strongly to PPy; and (3) the BSA neoglycoprotein conjugate mimiced the presentation of carbohydrates found at the cell surface. In addition to the specific ligand-BSA conjugate, each array included negative control electrodes with unmodified BSA and orthogonal sugar-BSA conjugates to which the labeled protein should not bind.

Biotin-streptavidin, a model binding pair with strong binding affinity, was employed to validate our microelectrode array platform. Biotin is a useful model for carbohydrates, as it is similar in size to the mono- and disaccharides used for subsequent carbohydrate functionalization. As illustrated in Figure 3A, fluorescently-labeled streptavidin bound strongly to electrodes functionalized with BSA-biotin and not to either of the controls (BSA-Man and BSA-D1Man). After confirming the functionalization approach with biotin-streptavidin, we tested carbohydrate-lectin binding pairs to demonstrate that the approach would be compatible for interactions with lower binding affinities. Many carbohydrate-mediated interactions are low affinity (in the µM to mM range) and a more stable binding state is usually achieved with multivalency, when the lectin binds multiple residues at once (the glycoside cluster effect).[220] The BSA conjugate strategy employed for this study readily facilitates multivalent display through the attachment of multiple pendant ligands to the core BSA scaffold. We demonstrated that fluorescently-labeled ConA and RCA$_{120}$ lectins bound to electrodes functionalized with their complementary BSA-carbohydrate conjugates with low background and low nonspecific binding (Figure 21B&C).
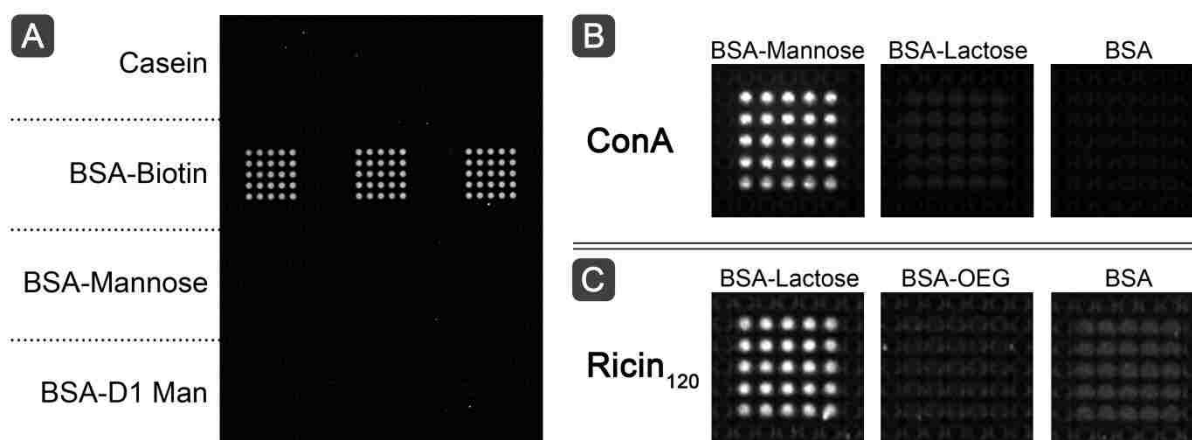
Figure 21. The PPy-BSA conjugate microelectrode array was tested using several ligands and fluorescently-labeled complementary proteins. (A) A representative sector of the microelectrode array functionalized with three different BSA conjugates and blocked with casein was probed with fluorescently-labeled streptavidin. Binding is specific to biotin, as expected. (B & C) Fluorescently-labeled lectins (ConA and Ricin$_{120}$) specifically bind to their complementary glycoconjugate.

3.3.2   Evaluating the MX3120 for high-throughput functionalization

The CFM print head was successfully integrated onto the microelectrode array surface, as demonstrated by fluorescent imaging following flow of AlexaFluor 488 labeled BSA over the microelectrode surface (Figure 22A). BSA preferentially adhered to the silicon oxynitride rings surrounding the microelectrode surface. This and other positive initial results led to the development of the MX3120, which combines a

12-channel CFM print head with the MX300, an instrument capable of depositing Ppy for functionalization with biomolecules. Arrays were functionalized and then probed for bioactivity, demonstrating the versatility of the sensing platform. Fluorescently-labeled ConA was detected only on regions of the chip functionalized with synthetic mannose glycoconjugates and no binding was detected on regions functionalized with non-complementary biomolecules (i.e. Lactose-BSA and BSA) (Figure 22B). Similarly, fluorescently-labeled ricin bound only to regions of the chip functionalized with an anti-ricin antibody (Figure 22C).

Unfortunately, the use of this instrument was curtailed because of issues with its operation instrumentation, and funding to support its repair was not available. Despite the successful binding experiments shown in Figure 22, a majority of experiments attempted on this platform were unsuccessful. Further, the capabilities of the instrument did not enable the multiplexing that we had hoped it would, and the lack of funding to develop the instrument further forced us to abandon this project.
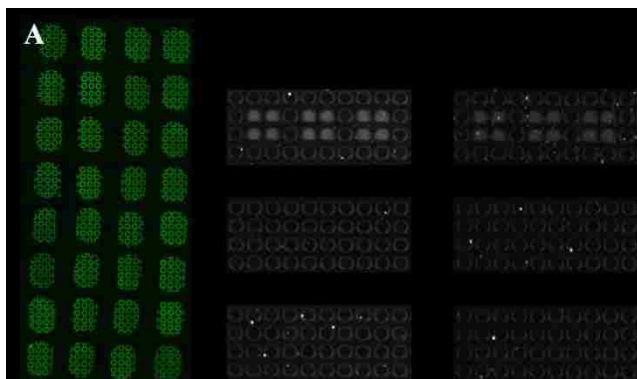
Figure 22. The CFM print head successfully sealed to the non-planar microelectrode surface (A). ConA (B) and ricin (C) bound specifically to functionalized microelectrodes.

3.3.3 Electrochemical detection of ricin

To demonstrate the versatility of the platform, we used ECD to detect RCA_{120} binding to galactose. One of the traditional challenges to ECD with electrode arrays is the technical difficulty of extracting an output signal from each electrode because of the wiring complexity and the need for a multi-channel detector. The integrated microelectronics of CustomArray's chips allows high-throughput electrical readings of the entire array in 15 sec using the ElectraSense®. These signals can be readily analyzed on the computer to which the reader is attached. It has been shown that ECD has equivalent sensitivities as fluorescent detection for genotyping and gene expression assays [207a], and ECD is more attractive for POC applications because the measurement equipment is compact, less expensive, and more robust. In this work, the ElectraSense can be used for both PPy deposition and for acquiring ECD data, thus eliminating the need for additional equipment (e.g. fluorescent microarray scanner). An HRP-mediated redox reaction generated a current that was measured by each electrode (Figure 23A). Measuring these

outputs, the ElectraSense® produced a data file that contains the total current detected on the microelectrode array. This data file was analyzed and converted into a pseudo image where the intensity of each pixel corresponded to measured electrical activity. ECD was successfully applied to detect ricin binding to BSA-galactose, as shown in Figure 23B&C.
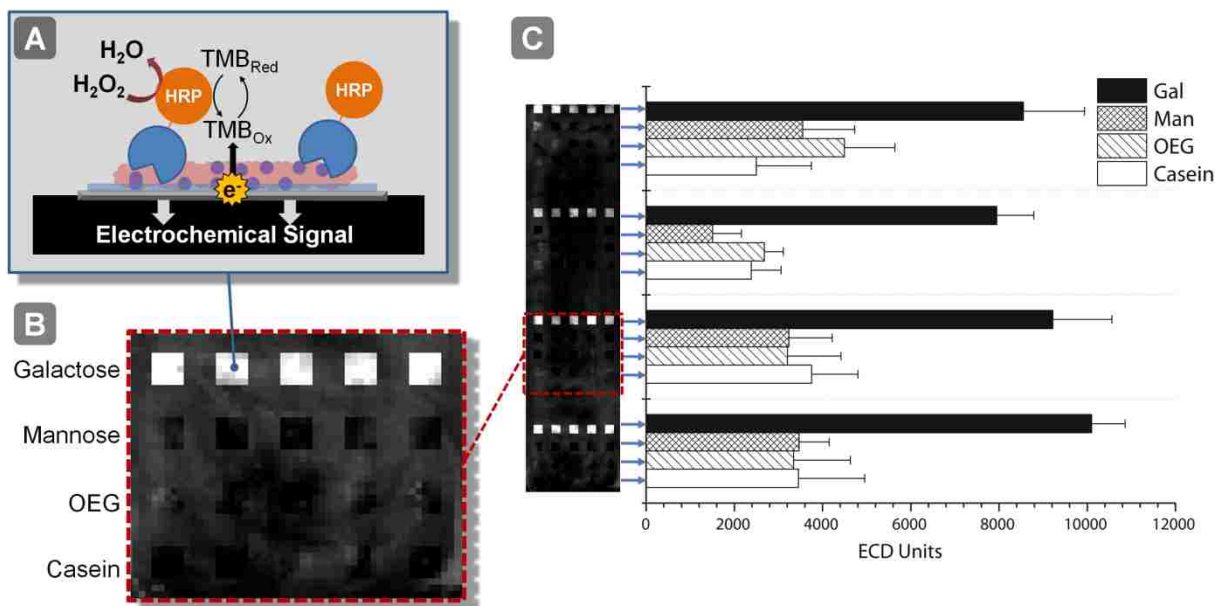
Figure 23. Electrochemical detection of ricin binding to galactose-functionalized electrodes. (A) The reduction of TMB solution by the HRP label on the ricin produces a flow of electrons away from the electrodes. CustomArray instrumentation and software (the ElectraSense®) detects the localized current on each electrode. (B) A pseudo image is generated where the intensity of each pixel corresponds to the electrical activity detected on the microelectrode array. (C) The average signal from each row of electrodes, corresponding to a single glycoconjugate, is shown graphically. (Gal = Galactose; Man = Mannose; OEG = oligoethylene glycol).

3.3.4   Mannose-mediated capture of *E. coli*

Following the validation of the functionalization approach, we investigated the bioactive microelectrode platform for studying whole-cell carbohydrate-mediated bacterial interactions. To test bacterial binding, we used the well-known interaction of type-1 fimbriated K12 *E. coli* and mannose [221]. Type-1 fimbria bind mannose through the FimH lectin domain which is expressed at the fimbrial tip [222]. The array was functionalized with BSA-mannose and BSA-lactose (orthogonal sugar control), BSA-OEG (linker control), and BSA (blocking control). As an additional control, arrays containing BSA-mannose and BSA-blocked electrodes were also probed with *E. coli* FimH-, which lacks the FimH binding lectin. Binding of *E. coli* FimH+ with mannose was verified: *E. coli* FimH+ bound specifically to mannose-coated electrodes (Figure 24A-C) while *E. coli* FimH- did not show an observable binding response (Figure 24D). These binding results were further confirmed using SEM (Figure 24B&C), demonstrating the ability of the

CustomArray microelectrode biosensor to detect specific binding interactions between bacteria and their complementary carbohydrate ligands immobilized on the microelectrodes.
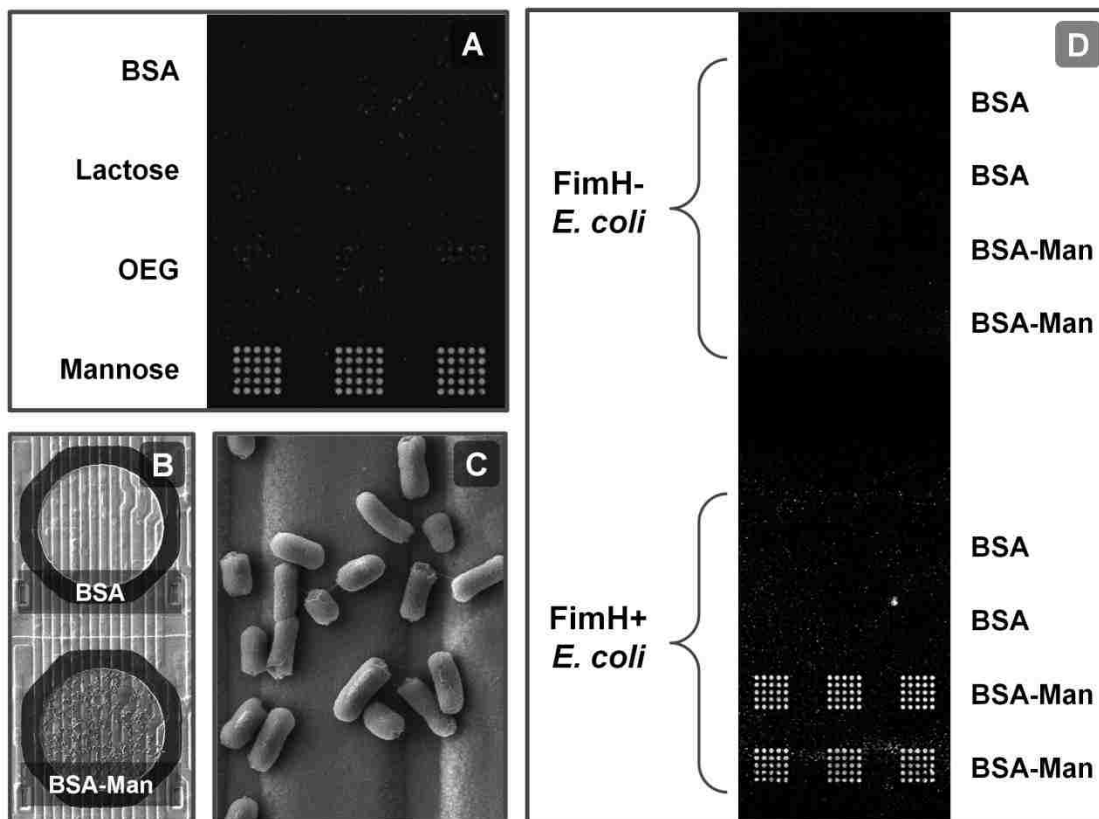
Figure 24. Verification of the platform for detecting carbohydrate-mediated bacterial adhesion using type 1 fimbriated *E. coli* binding to BSA-mannose conjugates. (A) *E. coli* binding visualized using fluorescently-labeled antibodies reveals binding to BSA-mannose with low non-specific binding. (B & C) SEM confirms the binding specificity seen using fluorescence. (D) A FimH knockout strain of *E. coli* (FimH-) does not bind to BSA-mannose, confirming the FimH mediated interaction. FimH- and FimH+ *E. coli* were incubated on the same array using the 4x2k Hyb cap. This chip was stored at room temperature for four months and thus demonstrates an extended shelf-life for pre-functionalized arrays.

A common problem with microarrays and pre-functionalized biosensors is their declining bioactivity over time. In order to test the long-term stability of the modified microelectrodes, we stored a functionalized array for four months at room temperature over desiccant. This array is shown in Figure 24D, which also demonstrates that the *E. coli* binding was FimH-mediated. As can be seen, the BSA-mannose conjugate retained its activity, as indicated by binding of *E. coli* FimH+. Further, non-specific binding remained low and *E. coli* FimH- did not bind to the aged surfaces.

3.3.5   Inhibition of *S. enterica* binding to mannose-functionalized electrodes

Bacterial binding inhibition studies were performed to demonstrate a medically relevant application of the microelectrode biosensor. As previously discussed, anti-adhesive therapies are gaining interest in

the medical community to prevent and treat bacterial infections. High-throughput tools are needed for screening different binding inhibitors for their inhibitory strength prior to their use in *in vivo* experiments. We investigated the use of our bioactive CustomArray platform for studying the inhibition of mannose-binding strain *S. enterica* FimH+ by αMM as a model for screening bacterial anti-adhesives.

As shown in Figure 25, dose-dependent inhibition of *S. enterica* FimH+ was observed using concentrations of αMM ranging from 0.01-1mM. An IC_{50} of 40 µM was determined from these results. The inhibition results were obtained as an average of all electrodes across at least four different arrays (i.e. four different experiments), demonstrating the ability of this functionalization method to obtain reproducible experimental results, a requisite feature for the implementation of this platform for studying bacterial binding inhibition.
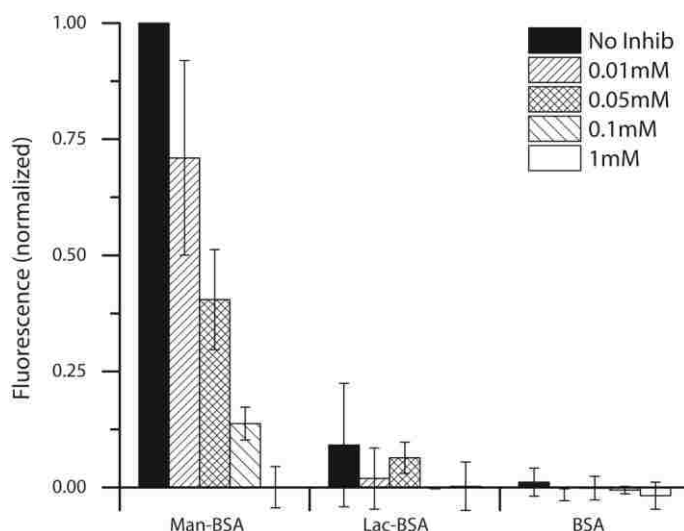
Figure 25. *S. enterica* binding to mannose-BSA is inhibited in a dose-dependent manner. Methyl-α-D-mannopyranoside (αMM) was pre-incubated with the bacteria at concentrations of 0.01, 0.05, 0.1, and 1 mM αMM. Error bars represent one standard deviation from the mean of the fluorescent intensities from at least four different microarrays. Values were normalized to the fluorescent intensity of uninhibited *S. enteric*a on each microarray.

3.4 Conclusions

This study demonstrated the successful application of a functionalized CMOS microelectrode microarray biosensor for use in interrogating carbohydrate-mediated protein and bacterial interactions. The first task was to determine a reliable method for functionalizing the microelectrodes with carbohydrates. Covalent functionalization of thiolated carbohydrates to amine-terminated oligomers built off of the array surface was found to be possible, but unreliable and time consuming. The Ppy functionalization method, on the other hand, was robust and amenable to a variety of biomolecules. Employing this versatile PPy-based strategy capable of selectively modifying individual electrodes within the array, this platform was used to determine the IC_{50} for a specific carbohydrate bacterial binding inhibitor for *Salmonella*. In addition to fluorescent detection, ECD was used to highlight the multimodal detection capabilities of the platform and its potential to be used outside of a traditional laboratory setting. The microelectrode biosensor and the microarray naturally combine to create a single high-throughput platform for identifying bacterial binding specificities and for screening binding inhibitors.

4. CHAPTER 4: SILICON PHOTONIC MICRORING RESONATORS FOR STUDYING BACTERIAL ADHESION

Biosensors based on silicon photonic microring resonators have recently emerged as sensitive and reliable platforms for studying biomolecular interactions. Analogous in many ways to SPR biosensors, the microring resonators show promise for achieving improved sensitivities, higher multiplexing capabilities, and complete device integration than do their optical biosensor counterparts. Much of the early work performed on this platform involved characterizing its capabilities and developing functionalization methods that we could use to deposit carbohydrates onto the microrings. We have successfully demonstrated a variety of functionalization techniques, including covalent attachment via silanization and non-covalent attachment via glycoconjugates. All of these methods have been extended to multiplexing by way of multi-channel flow cells, custom silicone masks, and piezoelectric ink-jet printing. In addition to functionalization with carbohydrates, we also describe the protein-A immobilization of antibodies onto the microrings. Carbohydrate functionalization methods were confirmed using complimentary lectins and antibody functionalization was confirmed using anti-streptavidin/streptavidin. Reliably demonstrating bacterial binding has been difficult, as non-specific binding is common; it is the dominant contributor to the signal for carbohydrate-mediated adhesion. Antibody capture of *Campylobacter jejuni* was successful, however, suggesting that improved methods could enable successful use of this platform for studying carbohydrate-mediated bacterial adhesion.

4.1 Introduction

Silicon photonics is a relatively new and rapidly expanding technology that promises to make significant advances in microelectronics, telecommunications, and biosensing. As was discussed in Chapter 2, silicon photonics has great promise to enable fully-integrated and distributable biosensors. Such devices would have significant impact on the field of POC diagnostics, and a device which could screen for the presence of many different pathogenic organisms can be envisioned. While a silicon photonic device with the source, sensor, detector, and microprocessor has yet to be developed, efforts are underway[160, 185] and the methods for studying whole-cell binding can be developed using existing instruments, such as the microring resonator platform that our lab has been investigating. As applied to biosensors, silicon photonic microring resonators have received much attention due largely to their high sensitivities and the ease with which high densities of devices can be fabricated on inexpensive silicon substrates.

Because of its novelty, impactful research can be performed simply to establish the capabilities of these devices. In addition to the research opportunities, it meets many of the important biosensor criteria outlined in Chapter 2 – it is sensitive, offers multiplexing, and it does not require a label. Although it is not fully integrated, the barriers to achieving such a biosensor using silicon photonics appear to be lower than they are for other sensing modalities. Further, it is similar to SPR from an experimental standpoint, so we are able to refer to the expansive literature using SPR biosensors and perform studies on our SPR instruments to optimize protocols and to run complementary experiments. While the majority of microring resonator biosensors are custom-built by each lab that uses them, we have used the "beta" version and, more recently, a market-ready version of a commercial instrument developed by Genalyte, Inc. (San Diego, CA). Important differences between the two versions of the instrument are noted, but most features are the same.

This chapter describes the silicon photonic microring resonator biosensor and some of the work that we have performed on it. Initial efforts were focused on characterizing the biosensing platform and developing methods to functionalize the microring sensors. Particular attention was given to functionalizing the microrings with carbohydrates, but we have also immobilized antibodies on the microrings. All of this work was done in an effort to eventually utilize this platform for studying carbohydrate-mediated bacterial adhesion. In contrast to the microelectrode array described in Chapter 3, which tests bacterial binding in static conditions, this platform delivers samples under flow. Since many bacteria demonstrate shear-enhanced adhesion,[42b] a flow-based platform broadens the experimental capabilities available to our lab. Further, the growing interest in silicon photonic biosensors and their great potential to become fully integrated platforms encourages this early-stage work.

4.2 Description of the Silicon Photonic Microring Resonator Platform
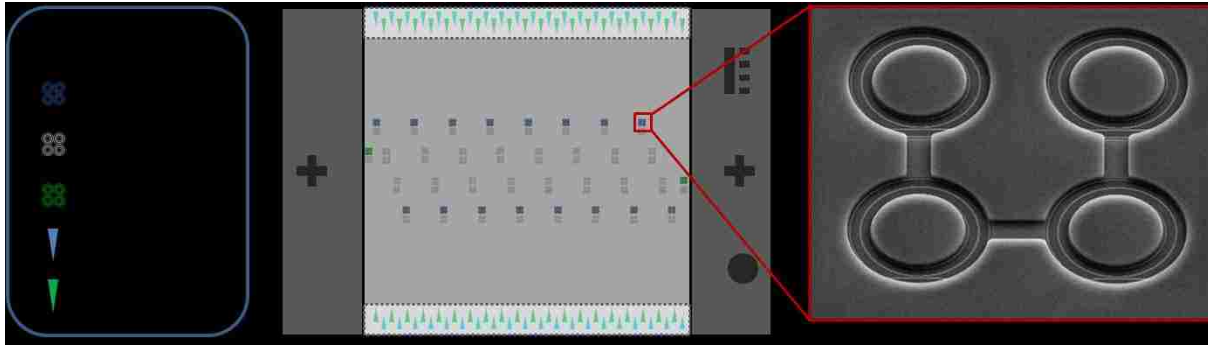
Figure 26. A schematic representation of the microring resonator chips (center) and an SEM of a single group of four microrings (right). There are a total of 72 microrings that can be addressed by the instrument software – 64 of these are exposed for biosensing (blue symbols) and eight of them are covered with CYTOP fluoropolymer to act as references (green symbols). The grey symbols are also microrings, but signals from these rings are not tracked using the current version of the instrument software. Waveguides connecting the input and output grating couplers with the microrings are not depicted for clarity.

 Using silicon-on-insulator (SOI) lithography fabrication, silicon microrings and their corresponding waveguides are defined on a silicon oxide substrate. The sensor chips used in the beta version of the instrument contained 32 addressable microrings, while the new chips contain 72 addressable microrings – 64 microrings are available for biosensing and the eight remaining rings act as temperature and vibration references. A layout of the new chips is shown in Figure 26. Each of the microrings is associated with a waveguide that has an input and an output grating coupler to allow for external interrogation of the microrings. The waveguides pass within 100 nm of the microrings which allows horizontal coupling of the light that travels from the input grating, past the microring, and then to the output grating. The entire chip is covered in a fluoropolymer coating (CYTOP) and annular openings are lithographically etched over all but eight of the microrings to expose them for biosensing (Figure 26, right). The CYTOP fluoropolymer, in addition to covering the reference rings, covers all non-sensing regions of the chip and prevents loss as the light passes through the waveguides. Flow
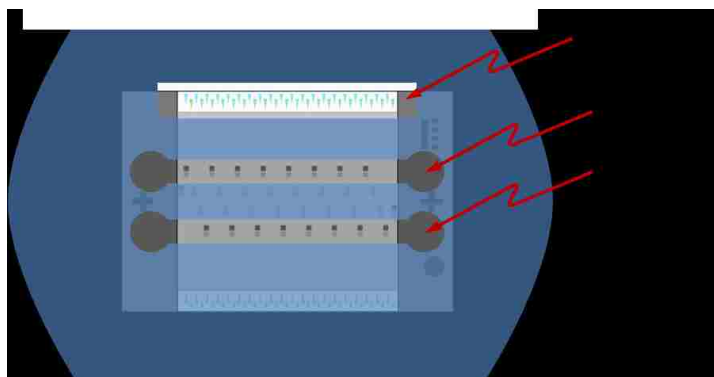
Figure 27. A mylar flow gasket (light blue) defines the two channels used to deliver solutions to two groups of microrings. The floor of the channels is defined by the chip surface, while the roof of the channels is defined by the Teflon lid. There is also an opening in the Teflon lid to allow interrogation of the grating couplers.

cells to deliver solutions to and from the microrings are created by sandwiching a mylar gasket in between the chip and a Teflon lid, to which external tubing is attached. Laser-cut channels in the mylar determine fluidic separation of groups of microrings, with the most commonly-used gasket splitting the microrings into two groups with the same number of rings in each group (Figure 27). Alternating syringe pumps provide a constant negative pressure on the fluidic system, pulling solutions from a 96-well plate on an automated plate sipper. Using custom software, the user is able to control and automate the flow rate and the location on the 96-well plate from which the solution is being pulled. The microrings are interrogated using a focused and linearly-polarized cavity diode laser with a center wavelength of 1560 nm. Two tip-tilt beam steering mirrors control the free-space laser to interrogate one ring at a time. When focused on an input grating coupler, the laser is rapidly swept through a desired spectral range (~20 nm) around the central wavelength. Light is measured at the output grating coupler of the waveguide to generate the transmission spectrum of each ring. This process takes roughly 100 ms for each ring, such that the transmission spectra of all 72 rings can be acquired in less than 10 seconds.
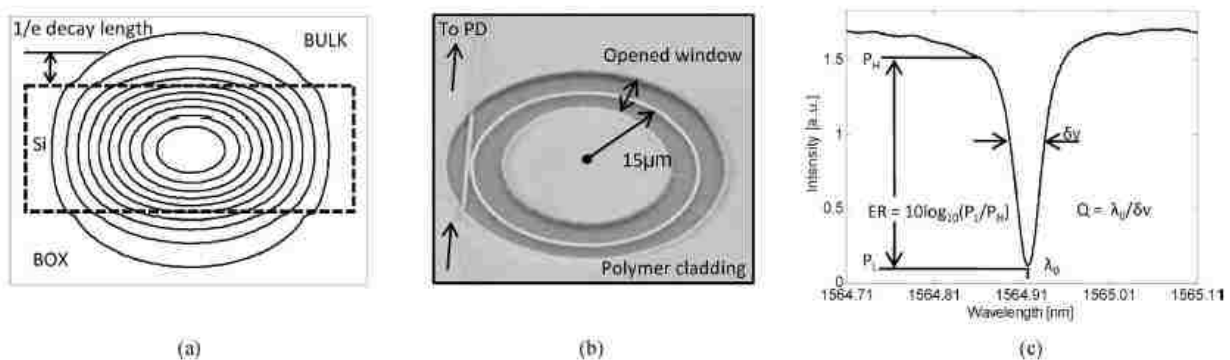
Figure 28. (a) The contour plot reveals the evanescent sensing field that is sensitive to changes in refractive index. (b) A close-up view of one of the rings exposed through the CYTOP. (c) A small portion of a transmission spectrum highlighting the resonant dip. By tracking changes in this dip over time, a sensorgram is produced that describes events at the ring surface. (Credit)[164a]

The dip in the transmission spectrum in Figure 28c represents the wavelength of light that is resonantly coupled with the microrings. These resonant wavelengths are described by the equation $\lambda = 2\pi r n_{eff}/m$, where λ is the wavelength of light, r is the radius of the cavity, n_{eff} is the effective RI of the waveguide mode, and m is an integer. The dependence of the resonant wavelength on n_{eff} is due to the evanescent field that extends and decays exponentially away from the surface of the waveguide and into the dielectric (Figure 28a). By changing n_{eff}, biomolecules binding to the microring induce shifts in the resonant wavelengths supported by the structure, and by tracking these shifts over time, a real-time sensorgram of biomolecule binding is produced.

4.3 Previous Applications

The microring resonator platform fits within the more broad classification of resonant cavity biosensors, which also includes microspheres,[158] microtoroids,[161] and microcapillaries.[223] Research performed using platforms other than the specific microring resonator biosensor that we use was described in the background. Published research using the instrument used by our lab and by the Bailey group at the University of Illinois Urbana Champagne is described here. Bailey's group has reported on detection of carcinoembryonic antigen (CEA) in undiluted serum down to 2 ng/ml,[168c] detection of Jurkat T lymphocyte secretions of IL-2 and IL-8,[224] detection of multiple micro RNAs with the ability to distinguish between single nucleotide polymorphisms,[225] and quantitative detection of five protein biomarkers in mixed samples.[171] This group also did a thorough theoretical and empirical analysis to characterize the mass sensitivity and the evanescent sensing field of the microrings, finding a mass sensitivity of 1.5pg/mm^2 and a 1/e evanescent decay distance of 63nm.[226] Such characterization is rare within the field of biosensors, yet this information is critical for experimental design and interpretation of results. For multiplexed functionalization, Bailey has employed a six-channel microfluidic device to differentially functionalize groups of microrings.[171] Using the same microring-based biosensor, our group has implemented a piezoelectric spotter to differentially functionalize microrings on multiple chips in a single run, thus demonstrating a rapid and scalable approach.[170b] We have also used a thin silicone material in which we define regions for functionalization by cutting openings that correspond to different groups of rings; when applied to the sensing chips, functionalization solutions can be pipetted into the openings for multiplexed deposition of biomolecules. It is clear that microring resonators are gaining favor within the biosensing community, and the Ratner lab has been established as one of the first groups routinely using this platform for biosensing.

4.4 Materials and Methods

4.4.1 Materials

All reagents, other than those specifically noted below, were purchased from Sigma-Aldrich (St. Louis, MO). Sulfosuccinimidyl-4-(N-maleimidomethyl)cyclohexane-1-carboxylate (Sulfo-SMCC), Tris(2-carboxyethyl)phosphine hydrochloride (TCEP-HCl), Zeba spin desalting columns with 7,000 MWCO, Slide-A-Lyzer dialysis cassettes with 10,000 MWCO, and Protein A were purchased from Thermo Fisher Scientific (Rockford, IL). Fraction V BSA was purchased from EMD Chemicals (Darmstadt, Germany). Goat anti-Campylobacter antibodies and goat anti-steptavidin antibodies were purchased from Meridian Life Science, Inc. (Memphis, TN) and Vector Laboratories, Inc. (Burlingame, CA), respectively. 1 µm polystyrene streptavidin-coated microbeads were purchased from Bangs Laboratories, Inc. (Fishers, IN). The silicone material ("Press-to-Seal-Silicone") used to make custom multiplexed functionalization masks was purchased from Grace Bio-Labs (Bend, OR). Concanavalin A (ConA) was obtained from MP Biomedicals (Sodon, OH) and diluted into HEPES buffer containing divalent cations (1 mM $CaCl_2$ and 1 mM $MnCl_2$) to maintain the tetrameric structure of the lectin. Pure ricin agglutinin (RCA_{120}) was purchased from EY Labs (San Mateo, CA) and was diluted into PBS. Campy CVA Agar and GasPak™EZ Campy Container System Sachets were acquired from BD (Franklin Lakes, NJ).

All buffers were made with ultrapure DI water (Barnstead Nanopure; ThermoFisher Scientific) and brought to the correct pH using 1 M HCl or 1 M NaOH. Phosphate buffered saline (PBS, pH 7.4) contained 10 mM phosphate (1.9 mM KH_2PO_4 and 8.1 mM Na_2HPO_4) with 150 mM NaCl. HEPES buffer (pH 7.3) with divalent cations was composed of 20 mM HEPES, 150 mM NaCl, 1 mM $CaCl_2$, and 1 mM $MnCl_2$. Thiolated and aminated sugars with oligoethylene glycol spacers (HS/NH_2-OEG_3-sugar) and thiolated OEG (HS-OEG_3) were synthesized in the Ratner laboratory as previously described.[77c]

4.4.2 BSA Conjugate Synthesis

BSA conjugates used in experiments on the microring resonators were made using two different methods. The first method was described in Chapter 3, whereby sugars containing a thiol functional group were added to the free amines of BSA via the heterobifunctional cross-linker sulfo-SMCC. These conjugates were used in the piezoelectric microspotting experiments. The second method utilized sugars containing an amine reactive group which were conjugated to the amines of BSA via divinyl sulfone (DVS). These conjugates were used in all other experiments where non-specific adsorption was chosen as the functionalization method. In the DVS conjugation method, BSA was dissolved in sodium carbonate buffer (50 mM, pH 10) at a concentration of 20 mg/ml. DVS was added to the BSA solution to

a final concentration of 10% (v/v) and allowed to react at room temperature for one hour, at which point 3 ml of the solution was dialyzed against PBS (pH 7.0) to stop the reaction and prevent widespread cross-linking. After 24 hours of dialysis at 4°C (4L dialysis volume, including one buffer exchange), the DVS-activated BSA was lyophilized and stored at -20°C. To react the aminated galactose and mannose with the DVS-activated BSA, the lyophilized powder was resuspended in carbonate buffer (50 mM, pH 10) and mixed with the aminated carbohydrates (final concentrations of 10 mg/ml for the DVS-activated BSA and 4 mM for the aminated carbohydrates) and left to react for 24 hours at room temperature. Finally, the mixture was buffer exchanged into PBS (pH 7.4) using desalting columns. The final concentration of BSA was determined with a BCA assay and the conjugates were diluted to 5 mg/ml, aliquotted, and stored at -20°C until use. Unless otherwise noted, BSA glycoconjugates were diluted to 0.5 mg/ml in PBS prior to use. The bioactivity of the conjugates was verified using lectin binding assays on an SPRi instrument (GWC SPRi II) before being used on the microring resonators.

4.4.3 Batch Functionalization via Silanization

We first investigated immobilizing glycans to all of the microrings at once (i.e. "batch functionalization") using epoxy-silane chemistries to attach thiolated glycans. This technique is the most straightforward method for initial studies because it requires minimal chip handling. Thus, it was useful for optimizing parameters such as chip cleaning, silanization solvent, glycan preparation, and functionalization times. Because of inconsistencies in the data obtained using our initial functionalization approaches, we underwent an optimization process by changing two variables that we had identified as likely causes of poor functionalization. Specifically, we hypothesized that the chips needed to be rigorously cleaned prior to functionalization and that the choice of silanization solvent was critical for achieving consistent immobilization of glycans. After arriving at a greatly-improved

Table 2. Conditions tested for optimizing cleaning procedure and silanization solvent.

#	Cleaning	Silanization Solvent
1	Piranha	toluene
2	N/A (new)	ethanol
3	N/A (new)	toluene
4	Solvent	ethanol
5	Solvent	toluene

functionalization approach, we performed a series of experiments using a dilution series of analyte (ConA) to show that we could reliably detect different concentrations and to determine the limit of detection using this method.

We tested three different chip preparation (cleaning) methods and two different silanization solvents in order to immobilize D1 mannose to the microrings (Table 2). Initial studies used new, uncleaned chips

and ethanol as the silanization solvent, so we included this condition as a baseline control. The other cleaning approaches were a solvent wash and a piranha soak. For the solvent wash, the chips were washed on a spin coater with solvents in the following sequence: acetone, dichloromethane, acetone, methanol, and isopropyl alcohol. This is a common sequence of solvents used for preparing surfaces for the formation of self-assembled monolayers (SAMs). For piranha cleaning, chips were immersed for 5 minutes in a solution containing 60% sulfuric acid and 40% hydrogen peroxide, followed by two consecutive 10 minute soaks in 18 MΩ filtered DI water. A custom Teflon chip holder was machined in order to safely immerse multiple chips in the piranha solution. The chips were then submerged in isopropyl alcohol, taken out of the Teflon holder one at a time, and dried under a stream of nitrogen. Immediately following washing, the chips were immersed in a 1% (v/v) epoxy-silane (3-glycidoxypropyltrimethoxysilane) solution in individual glass scintillation vials using either anhydrous ethanol or anhydrous toluene as the solvent. After incubating for 6 hours at room temperature on a plate shaker, the silanization solvent was removed and all chips were washed with 5 ml ethanol (2X) and 5 ml water (2X). The chips were transferred to a 96-well plate and incubated on a plate shaker for 12 hours at room temperature with 0.2 mM thiolated D1-mannose in sodium carbonate buffer (pH 8.7). Prior to this step, the thiol groups on the D1-mannose were reduced with TCEP-HCl (Tris(2-carboxyethyl)phosphine hydrochloride) at a 2:1 concentration of sugar:TCEP-HCl. After sugar functionalization, the chips were washed with 400 µl water (5X, each well). Non-specific binding was prevented by blocking the chips with 0.1% BSA in HEPES saline buffer (pH 7.4) containing divalent cations (HEPES 2+: 20mM HEPES, 150 mM NaCl, 1 mM $MnCl_2$, and 1 mM $CaCl_2$). After blocking for 1 hour on a plate shaker at room temperature, the blocking solution was washed off of the chips with 400 µl HEPES 2+ (5X, each well) and the chips were equilibrated in this buffer for at least 8 hours.

4.4.4 Multiplexed Functionalization Techniques

While the batch functionalization methods allow us to optimize conditions and to perform binding experiments, they require that we use completely separate chips for non-specific binding controls and for multi-analyte sensing. In addition to allowing on-chip binding controls, multiplexed functionalization is required to truly take advantage of the fact that there are multiple sensors on each chip as well as the inherent scalability of silicon photonics. Methods that we have investigated include: (1) using a flow cell to separately expose thiolated glycans to epoxy-silane activated chips, (2) using a hand-cut silicone mask to define functionalization regions for physioadsorption of glycoconjugates, and (3) inkjet microspotting of glycoconjugates.

4.4.4.1   Multiplexed Functionalization with the Expoxy-Silane

After batch activation of all microrings with epoxy-silane, the chips were transferred to the experimental

flow chamber using a flow cell that has two channels that run perpendicular to the standard flow cell.

Thiolated glycans (D1-mannose-SH and lactose-SH) at a concentration of 0.2 mM in sodium carbonate

buffer (pH 8.7) were flowed over the chips for 6 hours at 0.5 µl/min using a syringe pump. After

functionalization, the chips were washed extensively with water, blocked with BSA, and equilibrated

with HEPES 2+ buffer using the protocols as were described in the batch functionalization procedure

above. Chips were then tested for ConA binding specificity using 50 nM ConA in HEPES 2+. All binding

responses were normalized to the average response of the thermal reference rings.

4.4.4.2   Multiplexed Functionalization with Custom Silicone Masks

A simple method for multiplexed
functionalization of the microring
resonator sensing chips utilized
custom-cut silicone masks to
separate the rings into different
groups. The silicone acted as a
hydrophobic barrier to aqueous
solutions such that only rings
corresponding to openings in the
mask were functionalized. This
method was used for
multiplexed deposition of BSA
conjugates and antibodies on the
sensor chips.

Figure 29. Schematic of the silicone functionalization mask overlaid on top of the sensor chips. Two openings are cut into the silicone that correspond to groups of rings (24 addressable rings, indicated in blue, in each opening). 16 rings are left covered, and the hydrophobic nature of the silicone prevents aqueous solutions from wicking underneath the mask.

Functionalization masks were
created by cutting openings in a

1 mm thick silicone material. Each opening corresponded to different groups of rings on the microring

resonator sensing chips (Figure 29). Specifically, two separate openings were created in the silicone

masks, each one corresponding to 24 rings; 12 of the rings in each opening are exposed to solutions

pumped through channel 1 of the instrument, and the other 12 rings are exposed to solutions pumped

through channel 2 (see Figure 27 for the layout of the flow channels). Eight rings from each channel (16

total) remain covered by the silicone mask and therefore were not functionalized. Instead, these rings acted as negative controls for the blocking solution applied to the chip after functionalization. Thus, this two-well silicone mask effectively divided the rings into three different groups: two functionalized groups of rings and one blocking control group of rings, and each of these groups existed in duplicate on each chip.

After cutting the silicone masks they were aligned on the sensing chips using a dissection microscope and ~4 µl of functionalization reagent was added to each well. The chips were sealed in 35 mm petri dishes with parafilm in order to prevent the functionalization reagents from evaporating during incubation. For functionalization with BSA conjugates (mannose-BSA and galactose-BSA), the mask was applied to a freshly-cleaned sensor chip and the glycoconjugate solutions were pipetted into the wells (one glycoconjuatge per well, 0.5 mg/ml). The glycoconjugates were allowed to adsorb onto the sensing rings for 2-3 hrs at room temperature. After the incubation, the solutions were carefully wicked out of the wells, the mask was removed, and the chip was rinsed with water and dried under a stream of nitrogen. For antibody functionalization, the chips were first coated with protein A using a 24 hour room temperature incubation of a 0.5 mg/ml protein A solution in PBS. After the protein A adsorbed to the chip surface, chips were washed with water, dried under a stream of nitrogen, and the functionalization mask was aligned. One antibody solution (0.2 mg/ml in PBS) was pipetted into each well and allowed to bind to the protein A-coated surface during a 24 hour incubation at room temperature. The antibody solutions were wicked out of the wells and the mask was removed, but instead of rinsing with water and drying, the antibody-functionalized chips were rinsed with PBS and kept moist while the chip was loaded into the instrument. This was done in order to maintain the bioactivity of the antibodies – when rinsed with water and dried, the antibody binding capacity decreased dramatically. Following functionalization, the chips were loaded into the instrument and blocked by flowing a solution of 0.2% BSA in PBS over the chips for 30-60 min at a flow rate of 10-20 µl/min.

4.4.4.3   Multiplexed Functionalization via Piezoelectric Ink-Jet Printing

In order to achieve high-throughput, multiplexed inkjet functionalization of multiple chips at one time, a 10-chip holder was fabricated (Figure 30a). The holder was designed in Autocad (AutoDesk, Inc., San Rafael, CA), and cut from a single layer of 10 mil polyethylene terephthalate (PET) (Fralock, Valencia, CA) using a 25-watt CO_2 laser (M-360, Universal Laser Systems Inc., Scottsdale, AZ, USA) using previously published specifications.[227] External dimensions are w=165 mm, h= 39mm. Each chip slot is identical, w_1= 10 mm, w_2=6.06 mm, h_1=7 mm, h_2= 3mm. Separation between chip slots is 10 mm.
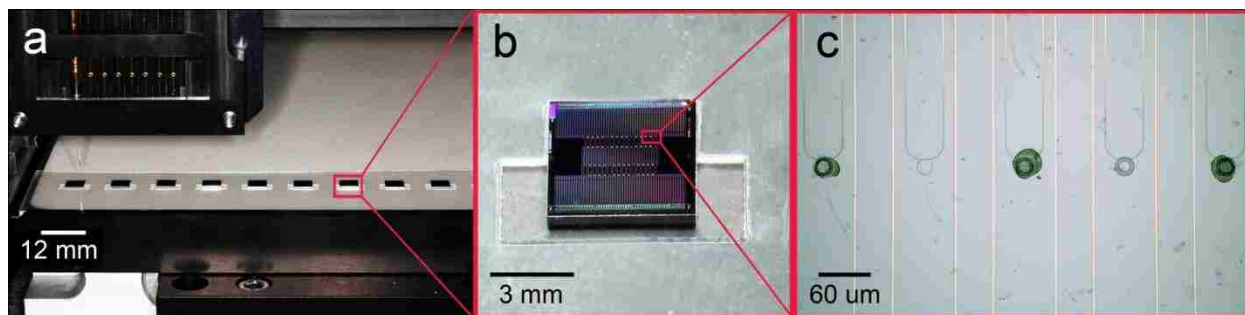
Figure 30. (a) The non-contact printing setup. The multi-chip holder is precisely aligned on the printer's vacuum stage to ensure accurate reagent deposition across ten silicon photonic microring resonator biosensor arrays. (b) Photograph of a single silicon photonic biosensor chip aligned in the multi-chip holder. (c) Brightfield micrograph of an array of microring resonator devices. Following printer calibration, AlexaFluor488 streptavidin was reproducibly printed on specified microrings with a high degree of accuracy and precision. Note that this was done with the previous version of the chips.

Reagents were deposited onto silicon devices using a Scienion S3 Flexarrayer piezoelectric non-contact printer (BioDot, Irvine, CA). Piezo pulse and voltage parameters were set to the manufacturer's recommendations specific to the nozzle used (PDC80; optimized during production). The frequency of droplet release was 500 Hz. This method yielded reproducible and stable droplet formation for a given reagent solution. Droplet volume is dependent on the solution properties such as viscosity and surface tension, and ranged from 350pL to 365pL for the reagents used (as determined using the on-board CCD camera). The multi-chip holder was aligned at the front left corner of the printer substrate support vacuum platform, flush with raised metal stops along the edges (Figure 30a). Using the printer's accompanying software, specific print targets were defined within the pre-established coordinate space (approx. 1µm spatial resolution); print target locations were referenced from the front left corner of the vacuum platform. Coordinates of individual microring resonators were determined using the dimensions of the multi-chip holder and the position of individual ring resonators on each silicon chip. Initially, microspots of AlexaFluor488-conjugated streptavidin (AF488 SA) were printed to calibrate the piezoelectric non-contact printer (Figure 30c). Spotting accuracy was confirmed using a Nikon SMZ1500 fluorescence stereoscopic zoom microscope (Nikon, Inc; Melville, NY).

Following printing, sensor chips were blocked with BSA (0.1% w/v, PBS running buffer, pH=7.4) for one hour and rinsed thoroughly with PBS prior to biosensing experiments. Respective analyte concentrations were as follows: ConA = 200nM, RCA= 500nM, GRFT = 1µM.

4.4.5 Validating the Functionalization Methods

The presence and bioactivity of immobilized carbohydrates and glycoconjugates was assessed with carbohydrate-binding proteins known as lectins. ConA and griffithsin (GRFT) were used to test mannose-

functionalized surfaces and RCA$_{120}$ was used to test lactose- and galactose-functionalized surfaces. In most cases, specific binding of lectins to rings functionalized with complementary carbohydrates validated the functionalization method being used. In the case of optimizing the silanization method, however, we performed a more exhaustive study using various concentrations of ConA to estimate the limit of detection. The specific methods for the optimization studies are listed below.

Antibody functionalization of the microrings was validated using streptavidin to probe for the bioactivity of the immobilized anti-streptavidin antibodies. While this did not directly test the bioactivity of the anti-campylobacter antibodies, retained bioactivity of the anti-streptavidin antibodies served to validate the functionalization method.

4.4.5.1 *Lectin Binding to Optimize the Batch Silanization Method*

The equilibrium binding responses of ConA to the immobilized D1-mannose were used to compare the different functionalization methods. After establishing a stable baseline in buffer, ConA in HEPES 2+ was flowed over the chips at a flow rate of 10 ul/min for 30 minutes, followed by a buffer dissociation wash. All binding responses were normalized to the average response of the thermal reference rings. The equilibrium binding responses (i.e. the difference from the initial baseline signal to the signal at the end of the 30 minute binding step) were extracted for all of the rings in each experiment and plotted in a histogram using Microsoft Excel$^{®}$.

Using the method that was found to produce the highest binding response, we went on to demonstrate that it could be used to generate concentration-dependent binding response with ConA concentrations of 1, 5, 10, 50, and 100 nM. We also used these experiments to get an idea of the lower limits of detection using this functionalization method by finding the lowest concentration of ConA that could be reliably detected over baseline. All binding responses were normalized to the average response of the thermal reference rings.

4.4.6   Bacterial Growth and Preparation

The strains of *E. coli* and *S. enterica* that were used in these experiments were described in Chapter 3 of this document. Two strains of *C. jejuni* subspecies *jejuni* were purchased from American Type Culture Collection (ATCC; Manassas, VA). ATCC #33560 was originally isolated from bovine feces, and ATCC #700819 was isolated from human feces. The freeze-dried stocks sent from ATCC were revived following ATCC's protocols and freezer stocks were made for long-term storage at -80°C.

The primary methods used for culturing all *E. coli* and *S. enterica* can be found in Chapter 3. Due to the difficulties of achieving bacterial binding on the microrings, however, in some cases the *E. coli* and *S. enterica* were grown on a rotating shaker. This method decreased the amount of flagellation of the bacteria, which we hoped would decrease the non-specific binding that we were seeing with the static culture conditions. *C. jejuni* strains were cultured on Campy CVA agar plates at 37°C for 48 hours. Microaerophilic growth conditions were maintained by sealing the inoculated plates in GasPak™ EZ Campy sachets (BD). After being resuspended in PBS, the campylobacter were prepared for experiments following the same protocols as the *E. coli* and the *S. enterica* (see Chapter 3). Unless otherwise noted, bacteria were diluted in buffer to an OD_{600} of 0.8 (+/- 0.05).

4.4.7   Bacterial Binding Experiments

Bacterial binding has been tested using all of the functionalization approaches described above except for the ink-jet printing method. Due to the difficulties in achieving specific bacterial binding, different experimental conditions were tested in an attempt to find the correct experimental conditions.

4.4.7.1   General Bacterial Binding Methods

For binding studies, PBS was flowed until a stable baseline was reached (< 0.5 pm/min drift, ~20 minutes), followed by 30 minutes of bacteria at OD_{600} 0.8 (+/- 0.05) in PBS, and finally a dissociation wash of PBS for 30 minutes. In the case of chips functionalized with antibodies via protein A, the criteria for baseline drift stated above could not be applied, as a constant dissociation of the antibodies from the protein A can be detected. Instead, binding experiments were done after a buffer equilibration period of less than 30 minutes. The flow rate was 10 μl/min in nearly all binding experiments reported herein, as this was found to lead to the best binding data. In most cases, a control strain of bacteria (i.e. one that does not have a known binding specificity to any of the reagents deposited on the chip) was flowed in the channel that did not contain the bacteria of interest. All binding responses were normalized to the average response of the thermal reference rings.

4.4.7.2   Modifications to the General Methods

Many of the modifications to the experimental methods were done prior to the actual binding assay, which include differences in the bacteria, the culture conditions, the functionalization methods, and the functionalization reagents; these are discussed elsewhere. The primary variables that were altered for the binding assays are the blocking method, the running buffer, the concentration of bacteria, and the flow rate. The most common blocking method used was immersing the chips in buffer containing

anywhere from 0.1% BSA up to 2% BSA for periods ranging from 30 minutes up to 24 hours. BSA-containing buffers were also flowed over the chip immediately prior to running the experiments, in which case the deposition of BSA was tracked with the biosensors and blocking was deemed complete when the signals reached a stable state (generally 30-60 minutes). In addition to BSA, we also tested blocking the chips with two proprietary blocking reagents from Thermo-Fisher: the "Protein-Free Blocking Buffer" and "SuperBlock."

Initially, all binding experiments were performed in PBS. On the recommendation of our collaborators in the Sorkurenko lab at UW, we also attempted binding assays with 0.2% BSA in PBS as the running buffer for *E. coli*, *S. enterica*, and *C. jejuni*. Finally, a few binding assays were conducted in unmodified growth medium. When resuspending the bacteria in running buffers, the concentration of bacteria was determined indirectly by checking the optical density of the suspensions at a wavelength of 600 nm. Suspensions of bacteria ranging from an OD_{600} of 0.4 to 1.5 were used in various experiments. At an OD_{600} of 0.4, the presence of bacteria is difficult to detect by eye. At an OD_{600} of 1.5, however, the solution is nearly opaque due to the high concentration of bacteria.

The flow rate that was used for most binding experiments was 10 µl/min – this flow rate was chosen because it is the lowest that the built-in instrument pumps allow, and we wanted to decrease the shear forces exerted on the bacteria by as much as possible. The K12 *E. coli* used in these studies actually bind with higher affinities under shear.[42a] Calculations suggest that flow rates of 10 µl/min should provide the favorable shear conditions for K12 *E. coli* binding, but we also tested other flow rates since the calculations rely on several approximations that may not hold true with the flow cells on this platform. In order to test lower flow rates, we connected an external syringe pump to the instrument that allowed us to test flow rates down to 0.5 µl/min. In all, we tested flow rates ranging from 0.5 to 40 µl/min, which correspond to an average linear velocity range of 0.09 to 7.4 mm/sec, respectively. Binding experiments were also performed in a "stop-flow" flow regime, wherein the pumps were stopped altogether for periods ranging from five to 60 minutes. After the flow was stopped for a given amount of time, flow was restarted for a short period before stopping the flow again – this ensured that the bacteria in the solution were not being depleted by binding to non-sensing portions of the chips. The "stop-flow" experiments were done to allow the bacteria to settle onto the sensor chip surface during the periods when the flow was stopped; although the flow was stopped, the instrument continued monitoring the signal from the microrings.

4.5 Results and Discussion

4.5.1 Validation of Functionalization Approaches

4.5.1.1 Validating Batch Silanization

As can be seen in the histogram (Figure 31), the cleaning method and the silanization solvent have a dramatic effect on the amount of ConA that binds to the microrings, presumably because of the amount of D1-mannose that was functionalized on the surface. In addition to generating a higher binding response, the rings that were cleaned with piranha solution and silanized in toluene showed less ring-to-ring variability.

Using the best method from the optimization study to functionalize rings with D1-mannose, various concentrations of ConA were flowed over the chips and binding sensorgrams were overlaid so that the responses could be compared. Each of the sensorgrams represents the averaged signal from 10-12 different rings from one of two

Figure 31. The combination of piranha cleaning and toluene as the silanization solvent led to the highest degree of ConA binding and the lowest inter-ring variability (as indicated by the error bars). Groups 1, 3, and 5 all used toluene as the solvent, which suggests that this is the more critical change that was made.

channels in each experiment. With the exception of one of the 10 nM concentrations, all of the binding responses show distinguishable sensorgrams based on the concentration of ConA used (Figure 32).

These experiments also indicate that concentrations as low as 1 nM can be distinguished from the reference rings, showing an average relative wavelength shift of 8 pm. Future work is required to test increasingly lower concentrations until the signal can no longer be distinguished from the baseline thermal references.

In addition to determining an improved functionalization method, two other important discoveries were made during this process that influenced all subsequent experiments on this platform. First, chip equilibration is critical to prevent signal drift during the experiment. While this is also true for the SPR experiments that we were already running, the higher sensitivity of the microrings amplified the importance of pre-equilibration. Secondly, the assay sensitivity degrades over time, particularly when the chips are

Figure 32. Various concentrations of ConA binding to chips functionalized with D1-mannose. With the exception of one of the 10 nM sensorgrams, concentration-dependent binding is apparent. 1 nM ConA produces a small signal, which encourages futures studies with even lower concentrations.

stored in the equilibration buffer. We believe that this is due to degradation of the silane anchoring the carbohydrates to the surface. Regardless of the cause, it is recommended that all chips functionalized in this way are used within 48 hours of functionalization and equilibration.

4.5.1.2   Validating Multiplexed Silanization

As mentioned, the two channels in the functionalization gasket run perpendicular to the channels used for binding, which resulted in each channel containing four rings with D1-mannose, four rings with lactose, and four unmodified BSA-blocked rings. As expected, 50 mM ConA bound only to the rings functionalized with D1-mannose and no binding was seen on the control rings (lactose and BSA) (Figure 33). While these results are encouraging, the binding response was lower than what was seen for the same concentration of ConA using the batch functionalization method (~110 pm shift vs. ~175 pm shift), and subsequent applications of this method have found that there is increased variability in signal. The increased number of steps and amount of chip handling that are required for this multiplexing approach are the likely causes of these problems. In the literature, silane functionalization is often done in a dehumidified glove box under an inert gas atmosphere. Neither the batch nor the multiplexed functionalization method were done using a glove box, but since the multiplexed approach exposes the chip surface to standard atmospheric conditions for longer periods of time and it requires chip insertion

into a flow cell, a lower functionalization efficiency is not surprising. Nevertheless, lower functionalization efficiency is not a problem if it can be done reliably; it is clear that it still permits on-chip controls and multi-analyte screening. By not taking advantage of the high densities of sensors that can be fabricated on a single chip through multiplexed functionalization, we would negate one of the most compelling reasons for using silicon photonic microring resonators. Indeed, the Bailey group routinely implements multiplexed functionalization on these chips using a 6-channel PDMS flow cell.[170a, 171, 225]
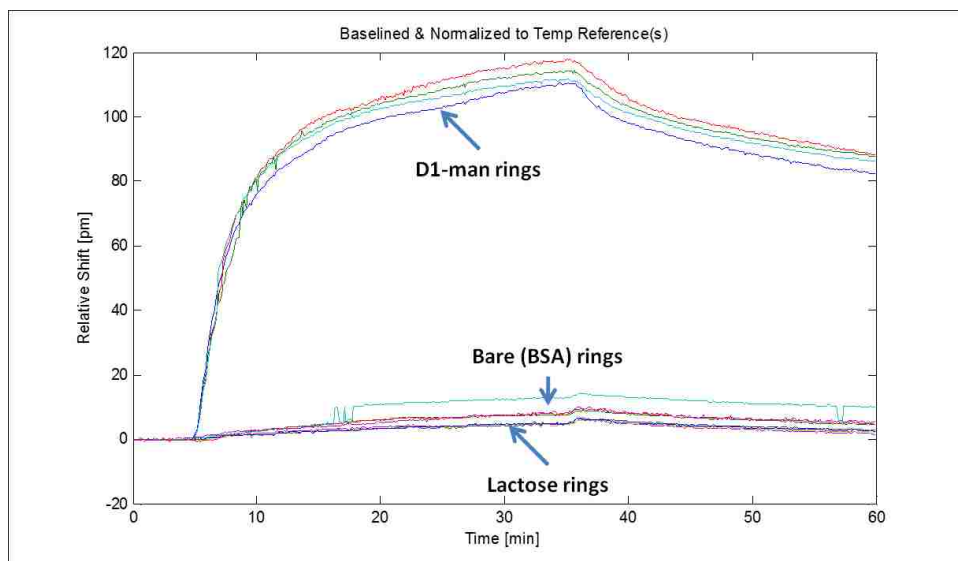
Figure 33. Multiplexed functionalization via epoxy-silane was evaluated using ConA binding to D1-mannose.

4.5.1.3   Validating Multiplexed Functionalization with Silicone Masks

Probing for the bioactivity of anti-streptavidin antibodies immobilized via protein A served to validate the functionalization approach. Streptavidin (50 nM in PBS) was flowed over the chips at 10 µl/min resulted in an average shift of ~60 pm for anti-streptavidin coated microrings. Streptavidin did not bind to either BSA-blocked rings or anti-campylobacter rings, showing that the multiplexed functionalization method worked as intended (Figure 34). The tight grouping of the signals based on the functionalization reagent indicates uniform functionalization on each set of microrings.
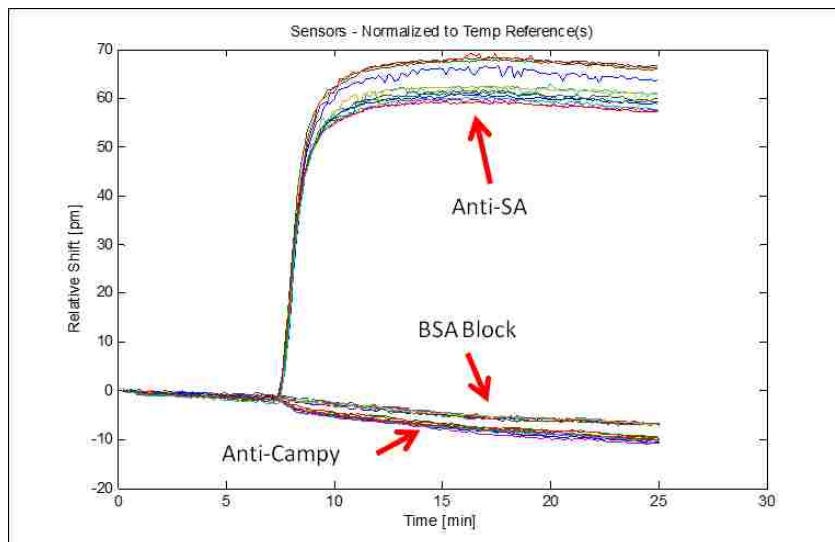
Figure 34. Multiplexed functionalization of antibodies using silicone masks on top of protein A-coated chips was evaluated by flowing streptavidin (50 nM in PBS) over the chip. The labels in the figures refer to the functionalization reagent used. As can be seen, streptavidin bound specifically to rings coated with anti-streptavidin antibodies (Anti-SA) and not to rings coated with anti-campylobacter antibodies (Anti-Campy) or BSA blocked rings.

All chips used for campylobacter binding were probed with streptavidin immediately after the bacterial binding assay was finished in order to ensure that the functionalization process was successful and as a chip quality control. Similar results were obtained on carbohydrate-functionalized rings when complementary lectins were used as the probe (data not shown).

4.5.1.4   *Piezoelectric Ink-Jet Printing*

The piezoelectric printer was initially calibrated using fluorescent protein conjugates to ensure reliable, efficient, and precise reagent deposition onto select microring resonators. Subsequently, we tested the bioactivity of printed BSA-glycoconjugates using the model carbohydrate-binding protein, concanavalin A (ConA) and went on to demonstrate a multiplexed silicon photonic-based biosensor capable of detecting two lectins of interest, griffithsin (GRFT) and ricin (RCA). GRFT is a potent antiviral lectin isolated from the red algae *Griffithsia* sp. and has shown promising activity against human immunodeficiency virus (HIV) and severe acute respiratory syndrome (SARS)--these antiviral properties are attributed to its multivalent mannose-dependent binding capability.[228] RCA is a highly toxic galactose- and lactose-binding lectin[229] and is considered a potential biothreat agent.[230]

Printing of fluorescently labeled proteins on individual microring resonators allowed visual verification of spotting accuracy using fluorescence microscopy. Positional inaccuracies in print location were corrected manually within the printer's software settings. These 'sighting in,' or calibration, results

demonstrate that piezoelectric non-contact printers are suitable for printing reagents on individual microrings, and that print location can be calibrated by visual inspection and subsequent software-based adjustments. This process requires that the printer's piezo settings be optimized to yield stable and uniform droplet formation prior to printer calibration. Additionally, biosensor chips must be carefully positioned on the printer's vacuum stage, as inconsistencies in device placement can introduce large errors in the location of printed reagents on the silicon chip, possibly even missing the sensing devices entirely. Therefore, precise machining and optimization of the multi-chip holder are necessary to ensure that all devices are positioned on the printer stage.

To demonstrate the high-throughput capabilities for the deposition of biomolecules via this method, we concurrently printed ten chips with AF488 SA using the multi-chip holder. The printing nozzle was scanned across all ten chips while depositing AF488 SA—approximately 350pL per spot—on six evenly-spaced microrings per chip. Print accuracy and precision were confirmed using fluorescence microscopy, establishing that all chips were properly printed. Remarkably, all ten silicon microring array chips were printed in a total of 9 seconds and consumed less than 25nL of reagent. These results conclusively demonstrate the suitability of this printing method for rapid and efficient mass-production of highly multiplexed microring resonator arrays. Furthermore, the efficiency can be increased with additional printing nozzles for simultaneous deposition of multiple biomolecules.

To establish this approach for multiplexed printing of bioactive molecules onto a microring resonator array, we have initially elected to explore several carbohydrate-protein interactions on a single chip. This category of glycan-mediated interactions is particularly relevant to the growing field of glycomics, which is making extensive use of the carbohydrate microarray to unravel the biological roles played by glycans in nature.
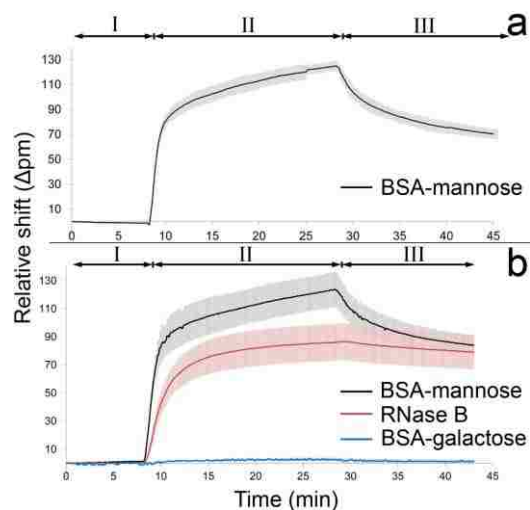
Figure 35. (a) ConA (200nM) binding to BSA-mannose-functionalized microring resonators, demonstrating the bioactivity of printed glycoconjugates. (b) ConA (200nM) was flowed over an array of microring resonators functionalized with BSA-mannose, BSA-galactose, and RNase B. The binding responses show specific ConA binding to mannose-presenting biomolecules with no contamination of adjacent microrings. All data are presented as the average ± standard deviation, n=3. BSA-mannose and RNase B binding data are normalized to unmodified microrings. BSA-galactose microrings are normalized to temperature reference control microrings.

Extending the potential sensitivity and scalability of silicon photonics arrays towards glycomics investigation will be particularly useful to glycan-based drug discovery and vaccine design.

To assess this printing technique for biosensing, we evaluated the bioactivity of printed BSA-glycoconjugates using a number of carbohydrate-binding proteins (lectins). After "sighting in" the non-contact printer, BSA-mannose was deposited on non-adjacent microring resonators. The bioactivity of mannose-functionalized microrings was probed using the lectin ConA (Figure 35a). ConA binding to BSA-mannose-functionalized microrings resulted in a maximum resonance shift of approximately 124.9 ± 3.8pm (n=3). These results indicate that BSA-glycoconjugates were specifically deposited on microring resonators and retained their intrinsic biological activity, validating the printing technique for high-throughput biosensor surface modification.

A major challenge for multiplexed biosensor printing is the accurate deposition of reagent onto specific sensing elements within the array – in this case, individual microring resonators – without mislabeling neighboring devices. Any significant inaccuracy during printing will result in poor array performance due to cross-reactivity of adjacent microrings. To ascertain whether our printing method can address this challenge, we printed three different glycoconjugates onto alternating devices. Again, we utilized the mannose-binding lectin ConA to probe the bioactivity of the printed biomolecules, as shown in (Figure 35b). As expected, microrings functionalized with BSA-mannose and the natural mannosylated protein RNase B showed substantial relative shifts of 123.8

Figure 36. (a) GRFT (1µM) binding to BSA-mannose functionalized microring resonators. BSA-lactose functionalized microrings show minimal non-specific binding. (b) Specific RCA (500nM) binding to BSA-lactose functionalized microrings. All data are presented as the average ± standard deviation, n=3 and are normalized to BSA-OEG functionalized microring resonators.

± 12.7pm (n=3) and 86.6 ± 13.0pm (n=3), respectively. The BSA-galactose control microrings displayed a negligible binding response to ConA, as predicted by ConA's carbohydrate specificity.

Having confirmed the functionality of the printed glycan array using ConA, we prepared a model array to examine the carbohydrate-mediated interactions of GRFT and RCA. Microrings were printed with BSA-mannose and BSA-lactose. Subsequent binding was normalized to inert BSA-OEG functionalized

microrings to control for non-specific protein interactions to the surface and the linker used for glycan/BSA conjugation.

GRFT binding to BSA-mannose modified microrings resulted in a maximum relative shift of 26.1 ± 10.3pm (n = 3, Figure 36a). While GRFT-binding to BSA-mannose is considerably lower than that of ConA, it is easily resolvable from the non-specific interactions to BSA-lactose printed as a control (2.6 ± 2.7pm, n=3). RCA binding was specific to BSA-lactose functionalized microrings, resulting in a relative shift of 15.5 ± 0.5pm (n=3; Figure 36b). These promising results demonstrate excellent ring-to-ring selectivity based on printed glycoconjugates and strongly support the application of multiplexed silicon photonic biosenor arrays for glycomics applications.

4.5.2   Bacterial Binding Experiments

4.5.2.1   Carbohydrate-Mediated Capture of Bacteria

Experiments on *E. coli* binding using the batch functionalized chips show that K12 *E. coli* – regardless of whether binding is specific for D1 mannose or non-specific – can be detected using the microring resonators (Figure 37). Compared to the KB2 *E. coli* control strain, which generated a post-wash signal around 10 pm shift, K12 *E. coli* binding generated a signal that was roughly ten times higher.

Unfortunately, subsequent experiments that included on-chip controls, made possible when the multiplexed functionalization method was developed, revealed that the K12 *E. coli* also bound to lactose- and BSA-coated microrings. The differential functionality of the chip was verified after *E. coli* binding using ConA to probe for mannose – specific binding of ConA to the mannose-coated rings revealed that the non-specific binding of *E. coli* was not due to faulty multiplexed functionalization. A potential reason for the non-specific
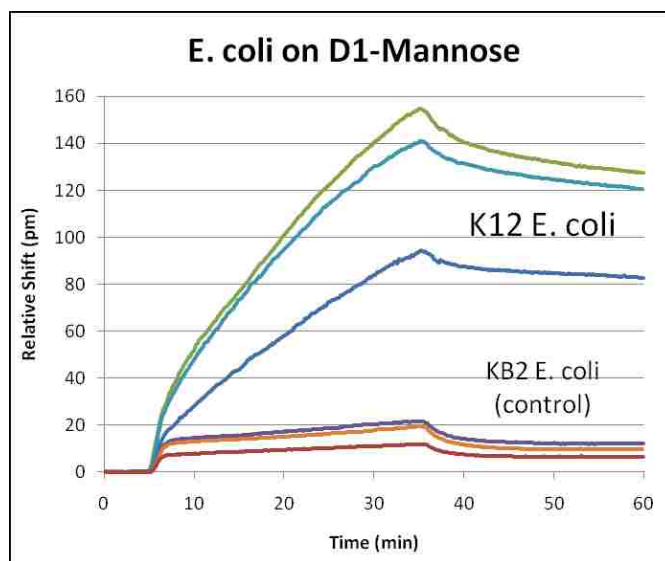
Figure 37. E. coli binding to microrings functionalized with D1-mannose. The control strain did not show appreciable binding. Each line is the average signal from 10-12 rings in a given experiment.

binding is that the bacteria are flagellated; our collaborators in the Thomas and Sokurenko labs, who work with this strain of bacteria often, cite flagella as a common reason for non-specific binding.

In an effort to prevent non-specific binding, different bacterial culture conditions were used to prevent the *E. coli* from expressing flagella. We found that culturing the bacteria on a rotating shaker, rather than under static conditions, resulted in far less flagellation of the bacteria (as determined via microscopy). Binding experiments using *E. coli* grown under these conditions, however, simply saw a reduced amount of non-specific binding with no relative increase in specific binding. Experiments using SPRi revealed that the *E. coli* are able to bind specifically to mannose-containing reagents deposited on the chip (Figure 38A). Not only does this act as an additional demonstration of the K12 *E. coli* binding specificity to mannose, but it confirmed that they are able to bind under flow conditions.

The same strain of *S. enterica* that was used in the experiments on the microelectrode arrays (Chapter 3) has a higher reported binding affinity for mannose than does the *E. coli*, so we also performed binding experiments using this strain. Again, no specific binding was seen in any of the binding assays. Since the binding on the microelectrode arrays is done under static conditions, we also tested *S. enterica* binding to the mannose-BSA conjugates using SPRi, another flow-based platform. The *S. enterica* bound specifically to mono-mannose and RNaseB (a glycoprotein that expresses various terminal mannose residues), demonstrating that it also binds under flow conditions (Figure 38B).
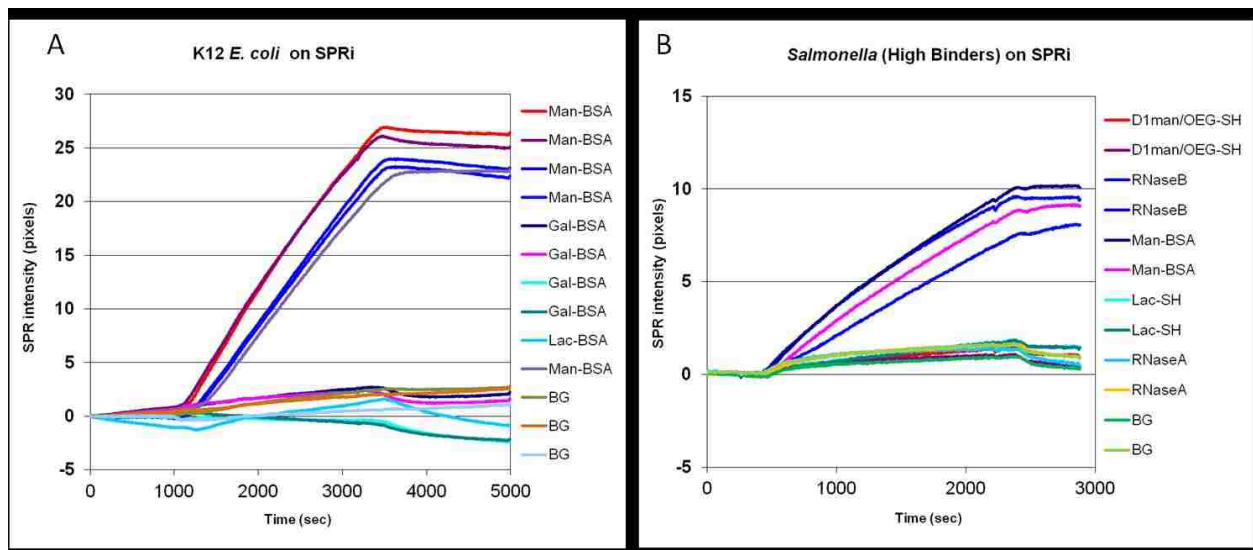
Figure 38. K12 *E. coli* and *Salmonella* binding specifically to mannose-functionalized regions of the SPRi chip, confirming both the bacterial binding specificity and binding under flow. It is known that *S. enterica* does not bind to D1-mannose, so the lack of binding to those spots was expected. BG = background regions of the chip that were blocked with BSA.

In addition to testing different strains of bacteria and different growth conditions, we tested different blocking conditions, different flow rates (ranging from 0 µl/min to 40 µl/min), and different running buffers (PBS and PBS with 0.2% BSA (w/v)). None of these changes improved the binding specificity.

As has been communicated, none of the carbohydrate-mediated bacterial binding experiments on the microring resonator platform led to specific binding. In all chips tested for bacterial binding, the bioactivity of the mannose-BSA-coated microrings was confirmed using ConA, and bacterial binding to the mannose-BSA reagent was confirmed using SPRi and the microelectrode arrays. Thus, there is a specific feature of using the microring resonator platform for carbohydrate-mediated capture of bacteria that prevents binding. As was discussed in Chapter 1, protein binding affinities for carbohydrates are relatively low (K_d = 1-1000 µM)[72]; this includes the carbohydrate-binding proteins that decorate the surfaces of the bacteria used in these experiments. Since binding between the mannose-BSA reagent and the bacteria was confirmed using both static binding assays and another flow-based platform (i.e. SPRi), it is difficult to identify the reason that binding does not work on this platform.

A possible explanation is that mass transport of the bacteria to the microrings is too low to achieve detectable binding. Additional experiments were performed to increase the mass transport of the bacteria, including stopping the flow to allow the bacteria to settle on the microring surfaces. Indeed, it has been shown that sedimentation is the primary factor in bacterial transport to the bottom surface of parallel plate flow chamber (PPFC) experiments,[231] so it was surprising that this method did not generate any specific binding.

Another possibility is that there is charge repulsion between the bacteria and the sensing chip surfaces, whereby the bacteria are prevented from getting close enough to the microring surfaces to form the multivalent bonds that are required for adhesion.[73] Importantly, different functionalization methods yield different results in bacterial binding – although there is not specific binding, chips functionalized via silanization show much higher non-specific binding than those functionalized via adsorption of the BSA glycoconjugates. This observation supports the idea that charge interactions could be influencing the transport of bacteria to the surface, but more detailed studies are needed to determine if this is responsible for the lack of binding that has been observed. Experiments aimed at testing this are outlined in Chapter 5.

4.5.2.2 Antibody Capture of Bacteria

Antibody-bacteria interactions are stronger and more specific than are carbohydrate-bacteria interactions; in order to demonstrate some form of bacterial binding on the microring resonator biosensor, we conducted a series of experiments to the capture *C. jejuni* using antibody-functionalized microrings. As described, each chip was functionalized with antibodies against *C. jejuni* and streptavidin, and rings that were not functionalized were blocked with BSA. After validating the functionalization approach with streptavidin binding, both strains of *C. jejuni* (ATCC 33560 and ATCC 700819) were tested. Though there was non-specific binding to anti-streptavidin and BSA-coated microrings, both strains were found to bind more strongly to microrings functionalized with anti-campylobacter antibodies (Figure 39). In addition to this, the binding to both sets of the negative control microrings was roughly equal, further supporting the belief that *C. jejuni* binding to the anti-campylobacter antibodies is at least partly due to specific capture.
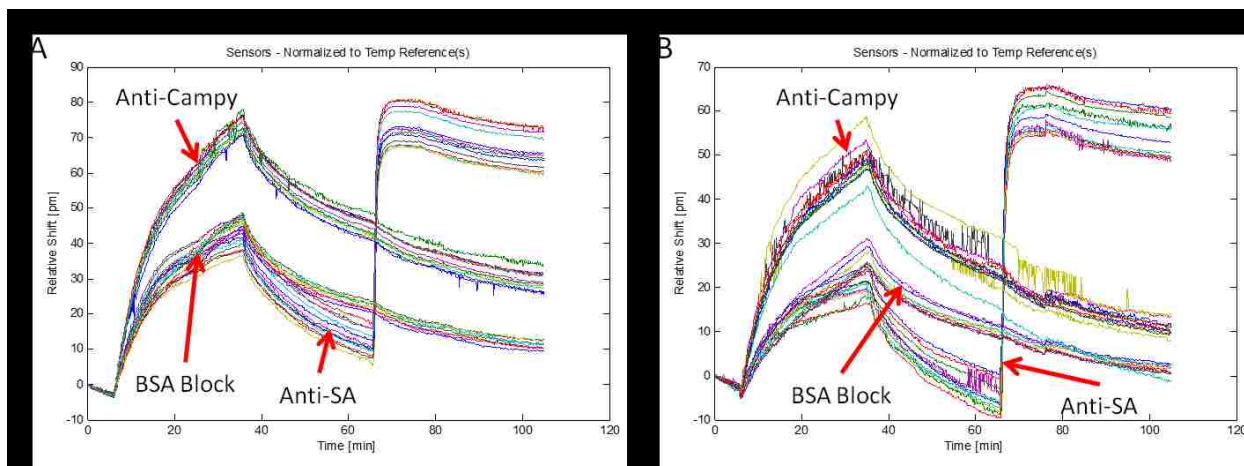
Figure 39. Two strains of *C. jejuni* binding to microrings functionalized with anti-campylobacter antibodies (Anti-Campy). ATCC strain 700819 (A) and ATCC strain 33560 (B). Following the buffer wash after bacteria were flowed over the chip, streptavidin (50 nM in PBS) was flowed over the chip (@ t = ~65 minutes) to test for the bioactivity of anti-streptavidin antibodies (Anti-SA). Streptavidin bound with high specificity to the expected microrings. Non-specific binding of *C. jejuni* to BSA-blocked and anti-streptavidin microrings was lower than the binding to the microrings functionalized with anti-campylobacter antibodies. The labels in the figures refer to the functionalization reagent used for that group of microrings.

4.6 Conclusions

As a relatively new biosensing platform, the silicon photonic microring resonator biosensor has performed exceptionally well in all of the experiments that we have performed on protein-carbohydrate interactions. We have demonstrated a variety of functionalization methods – both covalent and non-covalent, as well as batch functionalization and multiplexed functionalization – that have enabled the characterization of this platform. Unfortunately, this success has not translated well to studying carbohydrate-mediated bacterial adhesion. The binding results with K12 *E. coli* appeared successful initially, but incorporating the appropriate controls revealed that the binding was largely non-specific. These experiments did reveal, however, that bacterial binding could be detected. Subsequent experiments using antibody capture of *C. jejuni* confirmed that binding could be detected, but in this case the binding was specific. There was still non-specific binding to control sensors, so strategies for addressing this will have to be developed. Despite successfully detecting *C. jejuni* binding using antibody functionalization, developing methods to achieve carbohydrate-mediated bacterial binding remains a primary goal. Some of the potential causes of the difficulties that we had in achieving carbohydrate-mediated bacterial binding on this platform are discussed in Chapter 5, as well as recommended avenues to pursue to achieve this goal.

5. CHAPTER 5: CONCLUSIONS AND FUTURE DIRECTIONS

This document has detailed the work performed toward developing biosensing platforms for studying carbohydrate-mediated bacterial adhesion. Significant advancements were made in functionalizing, characterizing, and operating two biosensor platforms: a commercial microelectrode array and a new silicon photonic microring resonator biosensor. The research performed on these biosensors, described in Chapters 3 and 4, was prefaced with a chapter on the significance of carbohydrate-mediated bacterial adhesion and a chapter that provided an overview of biosensing technologies.

The microelectrode array biosensor proved to be the most successful platform for studying bacterial adhesion to carbohydrate-modified electrodes. We determined a reliable and versatile functionalization strategy of immobilizing glycoconjugates to polypyrrole-coated microelectrodes, and demonstrated its effectiveness for detecting specific interactions between lectins and bacteria with their carbohydrate binding targets. Both fluorescence and electrochemical detection were used to detect binding events, with fluorescence being the primary and most effective method. Further, we validated its use for studying carbohydrate anti-adhesives through the dose-dependent inhibition of *S. enterica* binding. Unfortunately, the future availability of this platform is uncertain due to business decisions made by CustomArray, Inc., the company that designed and built the arrays and the supporting instrumentation. The methods developed for this platform, however, should translate well to other technologies, including glass-slide carbohydrate microarrays, which are discussed in more detail later in this chapter.

The microring resonator biosensor has great promise for studying carbohydrate-mediated bacterial adhesion, although achieving this proved elusive in the course of these studies. From a platform development standpoint, we have made great strides in leveraging this instrument, particularly for studying protein-carbohydrate interactions. As one of the early adopters of this technology, and one of just three labs using Genalyte's microring resonator biosensing platform, much work was done to develop experimental protocols and to characterize the capabilities of the device. We have successfully demonstrated multiple functionalization methods, including a scalable, high-throughput piezoelectric ink-jet spotting method. Other functionalization methods include covalent attachment of thiolated carbohydrates via epoxy-silane and non-covalent physioadsorption of glycoconjugates. Both of these methods have also been adapted for multiplexed functionalization. Although we were unable to demonstrate specific carbohydrate-mediated bacterial binding on this platform – potential reasons are discussed later in this chapter – we did achieve specific binding of *C. jejuni* to microrings functionalized

with antibodies. These promising results warrant further efforts dedicated to realizing the goal of using this platform for studying bacterial adhesion to carbohydrates, and a section of this chapter is dedicated to recommendations for how the Ratner lab should proceed.

Importantly, many of the methods developed for these platforms are not limited to these specific platforms. For instance, using glyconconjugates for functionalizing biosensors for bacterial binding studies was established as an effective way to present the multivalent interactions that these bacteria require for adhesion. The methods for culturing and preparing the bacteria for experiments can also be widely applied, although I will argue in this chapter that it is still imperative to establish close collaborations with people who are expertly familiar with each of the bacterial strains that are used in future research.

In addition to the accomplishments achieved and the progress made toward developing reliable biosensing platforms for studying carbohydrate-mediated bacterial adhesion, a number of challenges emerged through the process of this work. Developing biosensing platforms for whole-cell binding assays necessitates a deep understanding of the biosensor instrumentation as well as the biological components that are involved; thus, it seems appropriate for a bioengineer to address these challenges. Importantly, these challenges present opportunities for the Ratner lab to make significant contributions to the field through future research.

5.1 Replacing the Microelectrode Arrays

The microelectrode array described in Chapter 3 embodies many of the desired features of a biosensor for studying carbohydrate-mediated interactions. It is a versatile platform that can be multiplexed, it has a suite of support instrumentation specifically developed for its various uses, and the technology has potential to be translated for POC applications. The polypyrrole (Ppy) functionalization method combined with the experimental protocols that we developed to study bacterial adhesion enabled the most reliable and impactful binding studies that were performed in this project. The functionalization method, in particular, is attractive because it allows the immobilization of a diverse set biomolecules and the presentation of carbohydrate binding epitopes in a multivalent fashion, both of which are critical for studying bacterial binding. Further, it fits in well with our approach of biosensor development, in that it represents the method that we would use for conducting static bacterial binding assays (as opposed to flow-based platforms, which are covered by the microring resonator and SPR

platforms). Unfortunately, the company that we were collaborating with on this project, CombiMatrix, cut all of its research efforts and the associated microarray development, instead deciding to focus on their commercial diagnostics.[232] The portion of the company that we were working with was purchased, downsized, and renamed CustomArray. While we were able to secure instrumentation and materials that allow us to functionalize the microarrays via Ppy deposition, our supply of microarrays is diminished and our ability to purchase additional arrays in the future remains uncertain. Indeed, the microarrays are expensive, as they have not yet reached a point where the economies of scale apply, and there is no indication that this point will ever be reached. With this in mind, the Ratner lab should identify one or more reliable experimental platforms to replace the microelectrode array. Important to these platforms will be their ability to perform static bacterial binding assays on a variety of carbohydrate-containing biomolecules that present the carbohydrate binding epitopes in a multivalent fashion. Further, it is imperative that the functionalization method or methods amenable to this platform consume minimal amounts of precious carbohydrate reagents. For this reason, methods such as whole-cell ELISAs are not ideal. The best candidate for such a platform is the glass slide microarray.

5.1.1   Glass Slide Microarrays

Carbohydrate microarrays have gained considerable support from the glycomics community because they conserve reagents and they allow high throughput binding experiments. These tools were discussed briefly in Chapter 1 as an existing method for studying protein and whole cell interactions with carbohydrates. There are a few examples in the literature of carbohydrate microarrays being used for studying bacterial adhesion,[79, 233] but given the importance of understanding carbohydrate-mediated bacterial binding and the growing popularity of carbohydrate microarrays, surprisingly few research articles exist.

Some of the most appealing features of glass slide microarrays are the low cost of the glass substrates and the wealth of knowledge about modifying glass surfaces with chemistries for facilitating functionalization. In addition to the vast number of silane chemistries available,[234] the glass surface can be modified with a wide range of materials,[72, 74, 235] including Ppy.[236] Unlike optical biosensors, which require particular material properties to efficiently couple the light that is used for detecting binding events, glass slide microarrays are far more tolerant to changes in the surface material. Therefore, the Ppy functionalization method used for the microelectrodes could be translated to glass slide microarrays if it is discovered that the Ppy was a key component of the effectiveness of the microelectrode platform.

Such modifications may not be necessary, however, as the glycoconjugates successfully applied for most binding studies in this work also adsorb to unmodified glass surfaces.

There are drawbacks to carbohydrate microarrays as applied to the study of bacterial adhesion, which could help to explain the lack of research in this area. For one, the fabrication of microarrays is often done using expensive equipment such as the piezoelectric ink-jet array that was used to functionalize the microring resonators (see Chapter 4). Unfortunately, this instrument is no longer available to us, and it is likely that very few researchers have such tools at their disposal. Such expensive equipment is not needed, however, as our lab has utilized a low-cost, manual, contact microarray printer from V&P Scientific (San Diego, CA). Using this tool, we have demonstrated the printing of up to 100 spots within a 0.5 cm^2 region on a gold-coated glass chip. These chips are routinely used for SPRi experiments and have yielded reliable binding data for proteins with printed milk oligosaccharides. This instrument has also been used for depositing BSA glyconjugates, so it would translate directly to the materials that have already been made for this project.

Another possible limitation for using microarrays for studying bacterial adhesion is that the experimental protocols are not ideally suited for such interactions, as the technology was originally developed for use with nucleic acids. The modification of these protocols so that they are better suited for studying bacterial adhesion, however, does not seem to be a significant barrier. Specifically, similar methods that were used to perform experiments on the microelectrode arrays could be easily translated to glass slides. As was described in Chapter 3, the microelectrode arrays were embedded in a 1"x3"ceramic support, the same size as the standard glass slide. The same flow cells that were used for functionalization and bacterial binding could therefore be directly applied to glass slides, and the GenePix 4000B scanner could be used for imaging fluorescently-labeled bacteria.

The requirement of a fluorescent label is another one of the drawbacks of the glass slide microarrays because it does not translate well to POC-ready devices and because one is limited by the wavelengths of light that the scanning instrumentation is able to detect. For use in basic research, however, such as indentifying bacteria-carbohydrate binding pairs or for testing binding inhibitors, using a fluorescent label is actually advantageous. Not only are fluorescent nucleic acid stains relatively cheap and easy to use, they also act as a built-in signal amplification method, which itself can be tuned by changing the gain on the imaging instrument or by altering the labeling conditions.

The most important challenge for the Ratner lab to replace the microelectrode arrays with glass slide microarrays is developing a reliable functionalization method. However, with the plethora of glass-modification chemistries available, the microarray spotting equipment that is already in place in the Ratner lab, and the functionalization methods reported here, functionalizing these arrays should not be difficult. With a reliable functionalization method, it seems that all of the binding experiments that were performed on the microelectrode arrays could be directly translated to glass slide microarrays. The ability to perform electrochemical detection and the promise of using label-free sensing methods would both be lost, but these aspects of the microelectrodes were not important in the bacterial binding studies that we performed. Further, the relative simplicity of glass slide microarrays compared to the microelectrodes and the optical biosensors used in the Ratner lab is actually another attractive feature of this platform; given the complexity of the biological component of studying bacterial binding interactions, reducing the technical complexity eliminates potentially confounding variables from the experiments. Take, for example, the many experimental variables that we had to consider when we were trouble-shooting the covalent attachment of glycans to the microelectrode arrays (see Chapter 3). For the purposes of identifying bacteria-carbohydrate binding partners and testing the relative inhibition strength of carbohydrate binding inhibitors, the glass slide microarray is an attractive platform.

5.2   Carbohydrate-Mediated Bacterial Adhesion on the Microring Resonators

Numerous obstacles have been encountered in the pursuit of developing experimental methods to study carbohydrate-mediated bacterial adhesion on the microring resonator biosensing platform. We have demonstrated that bacterial binding interactions can be detected by functionalizing the microrings with antibodies specific to the bacteria, but specific binding between bacteria and their carbohydrate ligands has yet to be accomplished. It is important to note that, in all cases, functionalization reagents were tested for bioactivity prior to and following binding experiments using complementary lectins. Possible reasons for these difficulties abound, and we have performed numerous experiments to test some of the hypotheses for why we were not able to demonstrate carbohydrate-mediated bacterial adhesion on the microrings. While we are able to rule out some possible deterrents to binding with these trouble-shooting experiments, it is likely that a combination of factors – both those that we have identified as well as additional unknown factors – contributes to the challenges we have faced.

First, as has been discussed, protein binding affinities for carbohydrates are relatively low, so carbohydrate-binding proteins and carbohydrate-binding bacteria rely on multivalent interactions for adhesion.[72-73] Bacteria experiencing shear forces, as they do in the microring resonators, may not have sufficient exposure to the glycans to form these multivalent interactions. This is almost certainly not the only reason for the lack of binding, as we have demonstrated that the glyconjugates synthesized for these experiments present sufficiently high densities of glycans to achieve binding in multiple biosensing platforms, including SPRi, which is also a flow-based platform. Additionally, the K12 *E. coli* that has been tested on the microring resonators actually experiences higher binding affinities for its mannose ligand under specific shear conditions.[42a] We have tested the K12 *E. coli* using flow rates ranging from 0 ul/min to 40 ul/min – a range which encompasses the shear-enhanced binding regime of this bacteria – with negative results.

A second challenge for detecting specific carbohydrate-mediated bacterial adhesion under flow is the mass transport limitation of the bacteria to the sensors themselves. As discussed, we performed experiments with K12 *E. coli* and *S. enterica* under a wide range of flow rates, including no flow at all, without seeing any significant improvements in binding to carbohydrate-functionalized microrings. The fluid dynamics of particles (e.g. bacteria) under laminar flow conditions is still poorly understood, but studies on solid-liquid two-phase flows have demonstrated that the particles tend to aggregate away from the walls of flow channels.[237] Conventional wisdom in the field has treated bacterial mass transport to be absent of gravitational, colloidal, and hydrodynamic interactions, instead suggesting that bacteria should be treated as neutrally buoyant particles that are dominated by convective transport.[238] This assumption has been proven incorrect, however, as it has been demonstrated that in parallel plate flow chambers, sedimentation is the dominant factor influencing bacterial transport to the bottom surface of the flow cell.[231, 238b] The amount of sedimentation is inversely related to the flow rate, and an increased number of bacteria reach the surface of the flow chamber at positions farthest from the channel entrance.[231, 239] This validates our use of low flow rates in the majority of bacterial binding experiments. On the other hand, carbohydrate-mediated bacterial binding was successfully accomplished with SPRi, and the Thomas lab routinely performs similar experiments in their parallel plate flow chamber. Lastly, we did observe binding, albeit non-specific binding, using the original microring resonator biosensor. Together, these observations seem to rule out mass transport limitations as the main reason that we have not been able to accomplish specific carbohydrate-mediated bacterial capture on the new instrument. Surely, the transport of large particles such as bacteria to the biosensor surface is limited, so it remains an important consideration in flow-based binding assays.[184a]

Perhaps the most surprising observation from the trouble-shooting experiments that we have performed is that we did not see binding when the flow was stopped completely. At the very least, accumulation of bacteria on the sensor surface should have elicited a detectable signal, even if they were not biding specifically. Although seemingly unrelated to this, the nonspecific binding observed with the K12 *E. coli* using silane functionalization techniques (see Chapter 4 and Figure 38) is not seen to the same degree when chips are functionalized using BSA glycoconjugates. In the latter case, the bacteria still bind non-specifically to the surface, but far less than the chips functionalized via epoxy-silane. The combination of these observations has led to the most recent hypothesis for the difficulties we have encountered, which is that electrostatic repulsion between the bacteria and the surface of the microring resonator chips is preventing the bacteria from reaching the microring sensors. This theory is currently untested, but it represents an important avenue of exploration.

A few small changes to the experimental protocols could shed some light on whether electrostatic repulsion between the surface of the microring resonator chips and the bacteria is involved. Namely, changing both the pH and the ionic strength of the running buffer should lead to changes in bacterial binding if electrostatic repulsion is occurring. Both the surface of the chips and most bacteria are negatively charged at a neutral pH, so by lowering the pH incrementally, a point should be reached where the repulsion forces are no longer as high. It is more difficult to predict the effect of changing the ionic strength of the buffer due to the combination of electrostatic and hydrophobic interactions that are involved,[240] but it is likely that there exists an optimal salt concentration in the buffer to minimize the repulsion effects, if they exist.

Should these experiments suggest that electrostatic repulsion is preventing the bacteria from reaching the sensors, more detailed experiments could be undertaken to quantify the charge (i.e. the zeta potential) on the chip surface in the experimental buffers. These experiments would need to determine the zeta potential at each stage of functionalization and for different functionalization methods (e.g. epoxy-silane vs. glyconjugate physioadsorption). Further, since the sensing chips themselves would not likely be amenable to the analytical methods, a representative model would have to be developed. Both bare silicon chips and CYTOP-coated chips should be investigated, since either or both may contribute to the hypothesized electrostatic repulsion. The results of such investigations would help choose the optimal functionalization conditions as well as the buffers that should be used for bacterial adhesion experiments.

5.3 The Inherent Challenges of Bacterial Binding Experiments: Biological Complexity

The biological complexity of carbohydrate-mediated bacterial binding has been another significant challenge to the work described in this document. Carbohydrate-mediated binding aside, the complexity of bacteria themselves is a difficult obstacle to overcome. In addition to the carbohydrate-binding bacteria that were used for the biosensor platform development described in this dissertation, both *Campylobacter jejuni* and F18 *E. coli* were also tested for their binding to 2'fucosyllactose (2'FL). As has been discussed, glycans with terminal α1,2-linked fucose play an important role in the pathogenesis of a variety of pathogens, including *C. jejuni*.[2] Fucosylated epitopes found on the lining of the GI tract are recognized by enteropathogens and this binding constitutes the first step in pathogenesis. 2'FL (Fucα2Galβ4Glc) is an example of an glycan that has a terminal α1,2-linked fucose and it has been identified as a likely candidate for bacterial binding because of its abundance in breast milk and on the intestinal lumen. It is believed that breast milk containing 2'FL acts as an anti-adhesive for enteropathogens; infants consuming milk with high quantities of fucosylated sugars and glycoproteins are resistant to diarrheal diseases.[1, 68] F18 *E. coli* is a porcine enteropathogen that causes edema disease and diarrhea in piglets. Piglet morbidity and mortality associated with infection is a significant cost-burden on the pig breeding industry.[241] Interestingly, F18 *E. coli* also binds to structures containing terminal α1,2-fucose;[242] as is the case in human infants, piglets that do not express these structures have a significantly lower incidence of enteric disease.[241a]

With the support of this previous research showing the involvement of terminal α1,2-fucose epitopes in *C. jejuni* and F18 *E. coli* adhesion, both strains of bacteria were tested using the microelectrode arrays, SPRi, and static adhesion assays on polystyrene. The biosensors were functionalized with a 2'FL BSA glycoconjugate that we synthesized using reductive amination to attach the 2'FL to the BSA.[243] Unfortunately, no specific binding was seen in any of these assays. In the process of trouble-shooting these experiments, we identified several important assumptions that were implicit to our investigations. These are now discussed in detail since they demonstrate the challenges of developing biosensor platforms for studying carbohydrate-mediated adhesion; detailed understanding of these challenges should help alleviate these problems in the future by informing experimental design.

The first important assumption that we made is that the terminal α1,2-fucose present in the 2'FL was the important binding epitope for the *C. jejuni* and F18 *E. coli*. While we cannot rule 2'FL out as a binding target for these bacteria (see the discussion on the environmental conditions below), a more in-depth literature analysis reveals a more complex picture than what we had originally imagined. The research

which formed the basis of *C. jejuni* specificity to terminal α1,2-fucose did not directly test a synthetic or purified version of the α1,2-fucose monosaccharide or of 2'FL.[2] Instead, they utilized Chinese hamster ovary (CHO) cells and mice that had been transfected with a human α1,2-fucosyltransferase gene so that they would overexpress the H-2 antigen (Fucα2Galβ4GlcNAc…) to conduct their binding assays. Not only is the H-2 antigen attached to additional proximal glycans, but it is slightly different than the 2'FL glycan that we were using (instead of N-acetyl glucosamine, 2'FL has glucose). While this difference may seem subtle, such specificity is widely seen in biological interactions.[205b] We have observed such a case with the *S. enterica* binding experiments that we performed, finding that this strain of bacteria does not bind to D1-mannose, a tri-mannose structure in which all of the residues have an α1,2 linkage, even though it binds strongly to mono-mannose which is linked to the oligo(ethylene glycol) spacer in an α1,2 fashion. The K12 *E. coli*, on the other hand, binds to both mannose structures. A similar nuance has also been reported with the F18 *E. coli* binding specificity.[244] In this paper, the authors identify a minimal binding epitope – meaning that all of the monosaccharides present in the epitope are critical for binding – which is the H-1 blood group antigen (Fucα2Galβ3GlcNAc). They also identified an "optimal" binding epitope, which has an additional galactose residue attached to the distal end of the glycan (Galα3(Fucα2)Galβ3GlcNAc). All of these examples demonstrate both the high specificity of these interactions as well as the complexity involved with studying them.

Despite our experimental observations and the contrary evidence in the literature, it is still possible that the bacteria bind to 2'FL, since the second major assumption that we made is that we were providing the appropriate conditions for bacterial binding to occur. An important consideration is that enteropathogens are exposed to and exist in a dynamic progression of environments prior to reaching the intestinal surfaces where they bind. For instance, after being ingested, the pathogens experience the highly acidic conditions in the stomach (pH ~2.0) prior to reaching the intestine, where the pH is then raised to promote enzymatic digestion. In addition to the dramatic shifts in the pH, the bacteria are exposed to various digestive juices and environmental conditions that they do not experience in the binding assays that we perform in the lab. It is well known that bacteria respond to changes in their environment,[29, 40] including their expression of flagella and fimbria, so it is quite possible that the necessary conditions for bacterial adhesion were not met in our experiments. A simple demonstration of the importance of environmental conditions on bacterial behavior is the severe decrease in the degree of flagellation that we observed when we changed the K12 *E. coli* culture conditions from static to rotating. For *S. enterica* binding studies, we were instructed by the Sokurenko lab that the bacteria must be cultured in broth, rather than on agar plates, in order to express the fimbria that bind to mannose.

Another research group has reported on the culture condition-dependent binding of *C. jejuni*, which found that the incubation temperature influenced whether the bacteria would adhere to their carbohydrate binding targets.[233c] Thus, both the bacterial culture conditions and the experimental conditions need to be tuned to ensure that the bacteria are properly expressing their carbohydrate-binding receptors.

The third assumption implicit in the experiments that we performed is that the bacteria stocks that we were using in our experiments behave as they do in nature, or at least as they have in the previous research that guides our studies. Bacteria are notoriously good at evolving – it is one of the reasons that they are ubiquitous in nature, inhabiting even the most inhospitable environments. The plasticity of these organisms, however, severely complicates research endeavors, wherein the experimental variables need to be minimized in order to test the variables of interest. A striking and relevant example of how a strain of bacteria can change over time was reported for a clinical strain of *C. jejuni* that has been made available through the National Collection of Type Cultures (NCTC).[233c, 245] In this study, the researchers were able to obtain the original clinical isolate of *C. jejuni* which had not been passaged multiple times as the NCTC strain had been. The researchers found that the two strains differed significantly in colonization, gene expression, and virulence-associated phenotypes.[245] Not surprisingly, additional studies found that their carbohydrate-binding specificities also changed – the NCTC strain was far more promiscuous.[233c] The Sorkuenko and Thomas labs have experienced similar phenotypic shifts in their freezer stocks, and they routinely discard stocks of bacteria because a strain previously not expressing flagella starts to express them, even when all of the growth conditions are held constant.

These examples demonstrate the importance of having a deep understanding of the biological components of these assays. Such an understanding requires specific expertise, which members of the Ratner lab may not possess, so emphasis should be placed on establishing close collaborations with specialists for each strain of bacteria that is tested for carbohydrate binding. Indeed, we had the support of the Sokurenko and Thomas labs for the bacteria with which we were able to achieve specific carbohydrate binding (i.e. K12 *E. coli* and *S. enterica*). In the case of *C. jejuni* and F18 *E. coli*, however, support from the microbiologists who routinely work with these strains of bacteria was not as reliable.

Despite the challenges encountered, the lack of current tools available and the biological complexity of bacteria emphasize the need for developing biosensing platforms that are able to identify and characterize these interactions.

6. REFERENCES

1.   Newburg, D. S.; Ruiz-Palacios, G. M.; Morrow, A. L., Human milk glycans protect infants against enteric pathogens. *Annual Review of Nutrition* **2005,** *25*, 37-58.

2.   Ruiz-Palacios, G. M.; Cervantes, L. E.; Ramos, P.; Chavez-Munguia, B.; Newburg, D. S., Campylobacter jejuni binds intestinal H(O) antigen (Fuc alpha 1, 2Gal beta 1, 4GlcNAc), and fucosyloligosaccharides of human milk inhibit its binding and infection. *J. Biol. Chem.* **2003,** *278* (16), 14112-14120.

3.   Lehninger, A. L.; Nelson, D. L.; Cox, M. M., *Lehninger principles of biochemistry*. 5th ed.; W.H. Freeman: New York, 2008; p 1 v. (various pagings).

4.   Vollmer, F.; Arnold, S.; Braun, D.; Teraoka, I.; Libchaber, A., Multiplexed DNA quanti. cation by spectroscopic shift of two microsphere cavities. *Biophysical Journal* **2003,** *85* (3), 1974-1979.

5.   Vahala, K. J., Optical microcavities. *Nature* **2003,** *424* (6950), 839-846.

6.   McMillan, S. J.; Crocker, P. R., CD33-related sialic-acid-binding immunoglobulin-like lectins in health and disease. *Carbohyd Res* **2008,** *343* (12), 2050-2056.

7.   Sacchettini, J. C.; Baum, L. G.; Brewer, C. F., Multivalent protein-carbohydrate interactions. A new paradigm for supermolecular assembly and signal transduction. *Biochemistry* **2001,** *40* (10), 3009-3015.

8.   (a) Karlsson, K. A., Bacterium-host protein-carbohydrate interactions and pathogenicity. *Biochem Soc T* **1999,** *27* (4), 471-474; (b) Kumari, K.; Gulati, S.; Smith, D. F.; Gulati, U.; Cummings, R. D.; Air, G. M., Receptor binding specificity of recent human H3N2 influenza viruses. *Virol J* **2007,** *4*, -; (c) Taylor, M. E.; Drickamer, K., *Introduction to glycobiology*. Oxford University Press: Oxford ; New York, 2003; p xv, 207 p.

9.   (a) WHO, The World Health Report 2004. **2005**; (b) Morens, D. M.; Folkers, G. K.; Fauci, A. S., The challenge of emerging and re-emerging infectious diseases (vol 430, pg 242, 2004). *Nature* **2010,** *463* (7277), 122-122.

10.   (a) Scallan, E.; Hoekstra, R. M.; Angulo, F. J.; Tauxe, R. V.; Widdowson, M. A.; Roy, S. L.; Jones, J. L.; Griffin, P. M., Foodborne Illness Acquired in the United States-Major Pathogens. *Emerg Infect Dis* **2011,** *17* (1), 7-15; (b) Cheng, A. C.; McDonald, J. R.; Thielman, N. M., Infectious diarrhea in developed and developing countries. *J Clin Gastroenterol* **2005,** *39* (9), 757-773; (c) Garthright, W. E.; Archer, D. L.; Kvenberg, J. E., Estimates of Incidence and Costs of Intestinal Infectious-Diseases in the United-States. *Public Health Rep* **1988,** *103* (2), 107-115.

11.   CDC 2011 Estimates of Foodborne Illness in the United States. http://www.cdc.gov/Features/dsFoodborneEstimates/.

12.   (a) Bavington, C.; Page, C., Stopping bacterial adhesion: A novel approach to treating infections. *Respiration* **2005,** *72* (4), 335-344; (b) Sharon, N., Carbohydrates as future anti-adhesion drugs for infectious diseases. *Biochim. Biophys. Acta-Gen. Subj.* **2006,** *1760* (4), 527-537; (c) Klemm, P.; Vejborg, R. M.; Hancock, V., Prevention of bacterial adhesion. *Appl. Microbiol. Biotechnol.* **2010,** *88* (2), 451-459.

13.   Berg, R. D., The indigenous gastrointestinal microflora. *Trends Microbiol* **1996,** *4* (11), 430-435.

14.   Hooper, L. V.; Gordon, J. I., Commensal host-bacterial relationships in the gut. *Science* **2001,** *292* (5519), 1115-1118.

15.   (a) Lindhorst, T. K., *Essentials of carbohydrate chemistry and biochemistry*. 2nd, rev. and updated ed.; Wiley-VCH: Weinheim, 2003; p xiii, 219 p; (b) Davis, B. G.; Fairbanks, A. J., *Carbohydrate chemistry*. Oxford University Press: Oxford ; New York, 2002; p 100 p.

16.   Brooks, S. A.; Dwek, M. V.; Schumacher, U., *Functional and molecular glycobiology*. BIOS Scientific ;

Distributed exclusively in the United States of America, its dependedent territories and ... by Springer-
        Verlag: Oxford
New York, 2002; p xvi, 354 p.
17.   (a) Newburg, D. S.; Ruiz-Palacios, G. M.; Altaye, M.; Chaturvedi, P.; Guerrero, M. D.; Meinzen-
Derr, J. K.; Pickering, L. K.; Morrow, A. L., Innate variation of fucosylated oligosaccharides in human milk
is associated with protection against diarrhea in breast-fed infants. *Glycobiology* **2001,** *11* (10), 901-901;
(b) Newburg, D. S.; Walker, W. A., Protection of the neonate by the innate immune system of developing
gut and of human milk. *Pediatric Research* **2007,** *61* (1), 2-8; (c) Morrow, A. L.; Ruiz-Palacios, G. M.;
Altaye, M.; Jiang, X.; Guerrero, M. L.; Meinzen-Derr, J. K.; Farkas, T.; Chaturvedi, P.; Pickering, L. K.;
Newburg, D. S., Human milk oligosaccharides are associated with protection against diarrhea in breast-
fed infants. *J Pediatr* **2004,** *145* (3), 297-303; (d) Sharon, N.; Ofek, I., Safe as mother's milk:
carbohydrates as future anti-adhesion drugs for bacterial diseases. *Glycoconj J* **2000,** *17* (7-9), 659-64.
18.   Mann, M.; Jensen, O. N., Proteomic analysis of post-translational modifications. *Nature
Biotechnology* **2003,** *21* (3), 255-261.
19.   Voet, D.; Voet, J. G.; Pratt, C. W., *Fundamentals of biochemistry : life at the molecular level*. 3rd
ed.; Wiley: Hoboken, NJ, 2008; p xxx, 1099, 30, 31, 11.
20.   Lairson, L. L.; Henrissat, B.; Davies, G. J.; Withers, S. G., Glycosyltransferases: Structures,
functions, and mechanisms. *Annu Rev Biochem* **2008,** *77*, 521-555.
21.   Hakomori, S.; Zhang, Y. M., Glycosphingolipid antigens and cancer therapy. *Chem Biol* **1997,** *4*
(2), 97-104.
22.   (a) Karlsson, K. A., Microbial recognition of target-cell glycoconjugates. *Curr Opin Struct Biol*
1995, *5* (5), 622-35; (b) Whitesides, G. M.; Mammen, M.; Choi, S. K., Polyvalent interactions in biological
systems: Implications for design and use of multivalent ligands and inhibitors. *Angewandte Chemie-
International Edition* **1998,** *37* (20), 2755-2794.
23.   Varki, A., Biological Roles of Oligosaccharides - All of the Theories Are Correct. *Glycobiology*
1993, *3* (2), 97-130.
24.   Huber, R. http://www.utm.utoronto.ca/~w3bio315/lecture2.htm.
25.   Roseman, S., Reflections on glycobiology. *J. Biol. Chem.* **2001,** *276* (45), 41527-41542.
26.   Moran, A. P.; Gupta, A.; Joshi, L., Sweet-talk: role of host glycosylation in bacterial pathogenesis
of the gastrointestinal tract. *Gut* **2011,** *60* (10), 1412-1425.
27.   Varki, A., *Essentials of glycobiology*. 2nd ed.; Cold Spring Harbor Laboratory Press: Cold Spring
Harbor, N.Y., 2009; p xxix, 784 p.
28.   (a) Nanthakumar, N. N.; Dai, D. W.; Newburg, D. S.; Walker, W. A., The role of indigenous
microflora in the development of murine intestinal fucosyl- and sialyltransferases. *Faseb J* **2002,** *16* (13),
44-+; (b) Robbe, C.; Capon, C.; Coddeville, B.; Michalski, J. C., Structural diversity and specific distribution
of 0-glycans in normal human mucins along the intestinal tract. *Biochemical Journal* **2004,** *384*, 307-316.
29.   (a) Deplancke, B.; Gaskins, H. R., Microbial modulation of innate defense: goblet cells and the
intestinal mucus layer. *Am J Clin Nutr* **2001,** *73* (6), 1131s-1141s; (b) Linden, S. K.; Florin, T. H. J.;
McGuckin, M. A., Mucin Dynamics in Intestinal Bacterial Infection. *PLoS One* **2008,** *3* (12).
30.   Mirelman, D., *Microbial lectins and agglutinins : properties and biological activity*. Wiley: New
York, 1986; p xv, 443 p.
31.   (a) Yatsunenko, T.; Rey, F. E.; Manary, M. J.; Trehan, I.; Dominguez-Bello, M. G.; Contreras, M.;
Magris, M.; Hidalgo, G.; Baldassano, R. N.; Anokhin, A. P.; Heath, A. C.; Warner, B.; Reeder, J.; Kuczynski,
J.; Caporaso, J. G.; Lozupone, C. A.; Lauber, C.; Clemente, J. C.; Knights, D.; Knight, R.; Gordon, J. I.,
Human gut microbiome viewed across age and geography. *Nature* **2012,** *486* (7402), 222-+; (b)
Greenblum, S.; Turnbaugh, P. J.; Borenstein, E., Metagenomic systems biology of the human gut
microbiome reveals topological shifts associated with obesity and inflammatory bowel disease. *P Natl*

Acad Sci USA **2012,** *109* (2), 594-599; (c) Kinross, J. M.; Darzi, A. W.; Nicholson, J. K., Gut microbiome-host interactions in health and disease. *Genome Med* **2011,** *3* (3), 14.

32.   Patsos, G.; Corfield, A., Management of the human mucosal defensive barrier: evidence for glycan legislation. *Biol. Chem.* **2009,** *390* (7), 581-590.

33.   Clayton, T. A.; Lindon, J. C.; Cloarec, O.; Antti, H.; Charuel, C.; Hanton, G.; Provost, J. P.; Le Net, J. L.; Baker, D.; Walley, R. J.; Everett, J. R.; Nicholson, J. K., Pharmaco-metabonomic phenotyping and personalized drug treatment. *Nature* **2006,** *440* (7087), 1073-7.

34.   Clarke, T. B.; Davis, K. M.; Lysenko, E. S.; Zhou, A. Y.; Yu, Y. M.; Weiser, J. N., Recognition of peptidoglycan from the microbiota by Nod1 enhances systemic innate immunity. *Nat Med* **2010,** *16* (2), 228-U137.

35.   Arumugam, M.; Raes, J.; Pelletier, E.; Le Paslier, D.; Yamada, T.; Mende, D. R.; Fernandes, G. R.; Tap, J.; Bruls, T.; Batto, J. M.; Bertalan, M.; Borruel, N.; Casellas, F.; Fernandez, L.; Gautier, L.; Hansen, T.; Hattori, M.; Hayashi, T.; Kleerebezem, M.; Kurokawa, K.; Leclerc, M.; Levenez, F.; Manichanh, C.; Nielsen, H. B.; Nielsen, T.; Pons, N.; Poulain, J.; Qin, J.; Sicheritz-Ponten, T.; Tims, S.; Torrents, D.; Ugarte, E.; Zoetendal, E. G.; Wang, J.; Guarner, F.; Pedersen, O.; de Vos, W. M.; Brunak, S.; Dore, J.; Consortium, M.; Weissenbach, J.; Ehrlich, S. D.; Bork, P.; Antolin, M.; Artiguenave, F.; Blottiere, H. M.; Almeida, M.; Brechot, C.; Cara, C.; Chervaux, C.; Cultrone, A.; Delorme, C.; Denariaz, G.; Dervyn, R.; Foerstner, K. U.; Friss, C.; van de Guchte, M.; Guedon, E.; Haimet, F.; Huber, W.; van Hylckama-Vlieg, J.; Jamet, A.; Juste, C.; Kaci, G.; Knol, J.; Lakhdari, O.; Layec, S.; Le Roux, K.; Maguin, E.; Merieux, A.; Melo Minardi, R.; M'Rini, C.; Muller, J.; Oozeer, R.; Parkhill, J.; Renault, P.; Rescigno, M.; Sanchez, N.; Sunagawa, S.; Torrejon, A.; Turner, K.; Vandemeulebrouck, G.; Varela, E.; Winogradsky, Y.; Zeller, G., Enterotypes of the human gut microbiome. *Nature* **2011**.

36.   Turnbaugh, P. J.; Ley, R. E.; Mahowald, M. A.; Magrini, V.; Mardis, E. R.; Gordon, J. I., An obesity-associated gut microbiome with increased capacity for energy harvest. *Nature* **2006,** *444* (7122), 1027-31.

37.   Holmes, E.; Loo, R. L.; Stamler, J.; Bictash, M.; Yap, I. K.; Chan, Q.; Ebbels, T.; De Iorio, M.; Brown, I. J.; Veselkov, K. A.; Daviglus, M. L.; Kesteloot, H.; Ueshima, H.; Zhao, L.; Nicholson, J. K.; Elliott, P., Human metabolic phenotype diversity and its association with diet and blood pressure. *Nature* **2008,** *453* (7193), 396-400.

38.   Marchesi, J. R.; Holmes, E.; Khan, F.; Kochhar, S.; Scanlan, P.; Shanahan, F.; Wilson, I. D.; Wang, Y., Rapid and noninvasive metabonomic characterization of inflammatory bowel disease. *J Proteome Res* **2007,** *6* (2), 546-51.

39.   (a) Meng, D.; Newburg, D. S.; Young, C.; Baker, A.; Tonkonogy, S. L.; Sartor, R. B.; Walker, W. A.; Nanthakumar, N. N., Bacterial symbionts induce a FUT2-dependent fucosylated niche on colonic epithelium via ERK and JNK signaling. *Am J Physiol Gastrointest Liver Physiol* **2007,** *293* (4), G780-7; (b) Staubach, F.; Kunzel, S.; Baines, A. C.; Yee, A.; McGee, B. M.; Backhed, F.; Baines, J. F.; Johnsen, J. M., Expression of the blood-group-related glycosyltransferase B4galnt2 influences the intestinal microbiota in mice. *Isme J* **2012,** *6* (7), 1345-55.

40.   (a) Sharma, R.; Schumacher, U., Carbohydrate expression in the intestinal mucosa. *Adv Anat Embryol Cell Biol* **2001,** *160*, III-IX, 1-91; (b) Comelli, E. M.; Simmering, R.; Faure, M.; Donnicola, D.; Mansourian, R.; Rochat, F.; Corthesy-Theulaz, I.; Cherbut, C., Multifaceted transcriptional regulation of the murine intestinal mucus layer by endogenous microbiota. *Genomics* **2008,** *91* (1), 70-7.

41.   Dai, D. W.; Nanthkumar, N. N.; Newburg, D. S.; Walker, W. A., Role of oligosaccharides and glycoconjugates in intestinal host defense. *J Pediatr Gastr Nutr* **2000,** *30*, S23-S33.

42.   (a) Thomas, W. E.; Nilsson, L. M.; Forero, M.; Sokurenko, E. V.; Vogel, V., Shear-dependent 'stick-and-roll' adhesion of type 1 fimbriated Escherichia coli. *Molecular Microbiology* **2004,** *53* (5), 1545-1557; (b) Thomas, W., Catch bonds in adhesion. *Annual Review of Biomedical Engineering* **2008,** *10*, 39-57.

43.	Blaser, M. J., Not all Helicobacter pylori strains are created equal: Should all be eliminated? *Lancet* **1997,** *349* (9057), 1020-1022.

44.	Wyatt, J. I.; Dixon, M. F., Chronic gastritis--a pathogenetic approach. *J Pathol* **1988,** *154* (2), 113-24.

45.	Graham, D. Y., Helicobacter pylori: its epidemiology and its role in duodenal ulcer disease. *J Gastroenterol Hepatol* **1991,** *6* (2), 105-13.

46.	Forman, D.; Coleman, M.; Debacker, G.; Eider, J.; Moller, H.; Damotta, L. C.; Roy, P.; Abid, L.; Debacker, G.; Tjonneland, A.; Boeing, H.; Haubrich, T.; Wahrendorf, J.; Manousos, O.; Tulinius, H.; Ogmundsdottir, H.; Palli, D.; Cipriani, F.; Fukao, A.; Tsugane, S.; Miyajima, Y.; Zatonski, W.; Tyczynski, J.; Calheiros, J.; Zakelj, M. P.; Potocnik, M.; Webb, P.; Knight, T.; Wilson, A.; Kaye, S.; Potter, J., An International Association between Helicobacter-Pylori Infection and Gastric-Cancer. *Lancet* **1993,** *341* (8857), 1359-1362.

47.	Gori, A. H.; Ahmed, K.; Martinez, G.; Masaki, H.; Watanabe, K.; Nagatake, T., Mediation of attachment of Burkholderia pseudomallei to human pharyngeal epithelial cells by the asialoganglioside GM1-GM2 receptor complex. *Am J Trop Med Hyg* **1999,** *61* (3), 473-475.

48.	Lacy, D. B.; Stevens, R. C., Sequence homology and structural analysis of the clostridial neurotoxins. *J Mol Biol* **1999,** *291* (5), 1091-1104.

49.	(a) Naaber, P.; Lehto, E.; Salminen, S.; Mikelsaar, M., Inhibition of adhesion of Clostridium difficile to Caco-2 cells. *Fems Immunol Med Mic* **1996,** *14* (4), 205-209; (b) Karjalainen, T.; Barc, M. C.; Collignon, A.; Trolle, S.; Boureau, H.; Cottelaffitte, J.; Bourlioux, P., Cloning of a Genetic Determinant from Clostridium-Difficile Involved in Adherence to Tissue-Culture Cells and Mucus. *Infect Immun* **1994,** *62* (10), 4347-4355; (c) Eveillard, M.; Fourel, V.; Barc, M. C.; Kerneis, S.; Coconnier, M. H.; Karjalainen, T.; Bourlioux, P.; Servin, A. L., Identification and Characterization of Adhesive Factors of Clostridium-Difficile Involved in Adhesion to Human Colonic Enterocyte-Like Caco-2 and Mucus-Secreting Ht29 Cells in Culture. *Molecular Microbiology* **1993,** *7* (3), 371-381; (d) Drudy, D.; O'Donoghue, D. P.; Baird, A.; Fenelon, L.; O'Farrelly, C., Flow cytometric analysis of Clostridium difficile adherence to human intestinal epithelial cells. *J Med Microbiol* **2001,** *50* (6), 526-534.

50.	Capo, C.; Lindberg, F. P.; Meconi, S.; Zaffran, Y.; Tardei, G.; Brown, E. J.; Raoult, D.; Mege, J. L., Subversion of monocyte functions by Coxiella burnetii: Impairment of the cross-talk between alpha(v)beta(3) integrin and CR3. *J Immunol* **1999,** *163* (11), 6078-6085.

51.	Ashkenazi, S., Review of the Effect of Human-Milk Fractions on the Adherence of Diarrheogenic Escherichia-Coli to the Gut in an Animal-Model. *Israel J Med Sci* **1994,** *30* (5-6), 335-338.

52.	(a) Cravioto, A.; Tello, A.; Villafan, H.; Ruiz, J.; Delvedovo, S.; Neeser, J. R., Inhibition of Localized Adhesion of Enteropathogenic Escherichia-Coli to Hep-2 Cells by Immunoglobulin and Oligosaccharide Fractions of Human Colostrum and Breast-Milk. *J Infect Dis* **1991,** *163* (6), 1247-1255; (b) Idota, T.; Kawakami, H.; Murakami, Y.; Sugawara, M., Inhibition of Cholera-Toxin by Human-Milk Fractions and Sialyllactose. *Biosci Biotech Bioch* **1995,** *59* (3), 417-419.

53.	(a) Virkola, R.; Parkkinen, J.; Hacker, J.; Korhonen, T. K., Sialyloligosaccharide Chains of Laminin as an Extracellular-Matrix Target for S Fimbriae of Escherichia-Coli. *Infect Immun* **1993,** *61* (10), 4480-4484; (b) Stins, M. F.; Prasadarao, N. V.; Ibric, L.; Wass, C. A.; Luckett, P.; Kim, K. S., Binding Characteristics of S-Fimbriated Escherichia-Coli to Isolated Brain Microvascular Endothelial-Cells. *Am J Pathol* **1994,** *145* (5), 1228-1236; (c) Schroten, H.; Hanisch, F. G.; Plogmann, R.; Hacker, J.; Uhlenbruck, G.; Nobisbosch, R.; Wahn, V., Inhibition of Adhesion of S-Fimbriated Escherichia-Coli to Buccal Epithelial-Cells by Human-Milk Fat Globule-Membrane Components - a Novel Aspect of the Protective Function of Mucins in the Nonimmunoglobulin Fraction. *Infect Immun* **1992,** *60* (7), 2893-2899.

54.	(a) Mysore, J. V.; Wigginton, T.; Simon, P. M.; Zopf, D.; Heman-Ackah, L. M.; Dubois, A., Treatment of Helicobacter pylori infection in rhesus monkeys using a novel antiadhesion compound. *Gastroenterology* **1999,** *117* (6), 1316-1325; (b) Noach, L. A.; Rolf, T. M.; Tytgat, G. N. J., Electron-

Microscopic Study of Association between Helicobacter-Pylori and Gastric and Duodenal Mucosa. *J Clin Pathol* **1994,** *47* (8), 699-704; (c) Chmiela, M.; Paziakdomanska, B.; Rudnicka, W.; Wadstrom, T., The Role of Heparan Sulfate-Binding Activity of Helicobacter-Pylori Bacteria in Their Adhesion to Murine Macrophages. *Apmis* **1995,** *103* (6), 469-474; (d) Chmiela, M.; Lawnik, M.; Wadstrom, T.; Rudnicka, W., Lewis(x) determinants in the H-pylori-granulocyte interaction. *Gut* **1997,** *41*, A32-A32; (e) Boren, T.; Falk, P.; Roth, K. A.; Larson, G.; Normark, S., Attachment of Helicobacter-Pylori to Human Gastric Epithelium Mediated by Blood-Group Antigens. *Science* **1993,** *262* (5141), 1892-1895; (f) Angstrom, J.; Teneberg, S.; Milh, M. A.; Larsson, T.; Leonardsson, I.; Olsson, B. M.; Halvarsson, M. O.; Danielsson, D.; Naslund, I.; Ljungh, A.; Wadstrom, T.; Karlsson, K. A., The lactosylceramide binding specificity of Helicobacter pylori. *Glycobiology* **1998,** *8* (4), 297-309.

55. (a) Weinstein, D. L.; O'Neill, B. L.; Hone, D. M.; Metcalf, E. S., Differential early interactions between Salmonella enterica serovar typhi and two other pathogenic Salmonella serovars with intestinal epithelial cells. *Infect Immun* **1998,** *66* (5), 2310-2318; (b) Miyake, M.; Zhao, L. C.; Ezaki, T.; Hirose, K.; Khan, A. Q.; Kawamura, Y.; Shima, R.; Kamijo, M.; Masuzawa, T.; Yanagihara, Y., Vi-deficient and nonfimbriated mutants of Salmonella typhi agglutinate human blood type antigens and are hyperinvasive. *Fems Microbiol Lett* **1998,** *161* (1), 75-82; (c) Jafari, A.; Bouzari, S.; Farhoudimoghaddam, A. A.; Parsi, M.; Shokouhi, F., In-Vitro Adhesion and Invasion of Salmonella-Enterica Serovar Havana. *Microb Pathogenesis* **1994,** *16* (1), 65-70; (d) Altmeyer, R. M.; Mcnern, J. K.; Bossio, J. C.; Rosenshine, I.; Finlay, B. B.; Galan, J. E., Cloning and Molecular Characterization of a Gene Involved in Salmonella Adherence and Invasion of Cultured Epithelial-Cells. *Molecular Microbiology* **1993,** *7* (1), 89-98.

56. (a) Utsunomiya, A.; Nakamura, M.; Hamamoto, A., Expression of fimbriae and hemagglutination activity in Shigella boydii. *Microbiol Immunol* **2000,** *44* (6), 529-531; (b) Haque, M. A.; Qadri, F.; Ohki, K.; Kohashi, O., Surface Components of Shigellae Involved in Adhesion and Hemagglutination. *J Appl Bacteriol* **1995,** *79* (2), 186-194; (c) Guhathakurta, B.; Sasmal, D.; Ghosh, A. N.; Pal, C. R.; Datta, A., Purification of a cell-associated hemagglutinin from Shigella dysenteriae type 1. *Fems Immunol Med Mic* **1996,** *14* (2-3), 63-66.

57. Newburg, D. S.; Ashkenazi, S.; Cleary, T. G., Human-Milk Contains the Shiga Toxin and Shiga-Like Toxin Receptor Glycolipid Gb3. *J Infect Dis* **1992,** *166* (4), 832-836.

58. Newburg, D. S.; Pickering, L. K.; Mccluer, R. H.; Cleary, T. G., Fucosylated Oligosaccharides of Human-Milk Protect Suckling Mice from Heat-Stabile Enterotoxin of Escherichia-Coli. *J Infect Dis* **1990,** *162* (5), 1075-1080.

59. Chatterjee, S.; Khullar, M.; Shi, W. Y., Digalactosylceramide Is the Receptor for Staphylococcal-Enterotoxin-B in Human Kidney Proximal Tubular Cells. *Glycobiology* **1995,** *5* (3), 327-333.

60. (a) Finkelstein, R. A.; Boesmanfinkelstein, M.; Chang, Y.; Hase, C. C., Vibrio-Cholerae Hemagglutinin Protease, Colonial Variation, Virulence, and Detachment. *Infect Immun* **1992,** *60* (2), 472-478; (b) Benitez, J. A.; Spelbrink, R. G.; Silva, A.; Phillips, T. E.; Stanley, C. M.; BoesmanFinkelstein, M.; Finkelstein, R. A., Adherence of Vibrio cholerae to cultured differentiated human intestinal cells: An in vitro colonization model. *Infect Immun* **1997,** *65* (8), 3474-3477; (c) Attridge, S. R.; Manning, P. A.; Holmgren, J.; Jonson, G., Relative significance of mannose-sensitive hemagglutinin and toxin-coregulated pill in colonization of infant mice by Vibrio cholerae El Tor. *Infect Immun* **1996,** *64* (8), 3369-3373; (d) Alam, M.; Miyoshi, S. I.; Tomochika, K. I.; Shinoda, S., Vibrio mimicus attaches to the intestinal mucosa by outer membrane hemagglutinins specific to polypeptide moieties of glycoproteins. *Infect Immun* **1997,** *65* (9), 3662-3665.

61. Merritt, E. A.; Sarfaty, S.; Vandenakker, F.; Lhoir, C.; Martial, J. A.; Hol, W. G. J., Crystal-Structure of Cholera-Toxin B-Pentamer Bound to Receptor G(M1) Pentasaccharide. *Protein Sci* **1994,** *3* (2), 166-175.

62.   Mantle, M.; Husar, S. D., Binding of Yersinia-Enterocolitica to Purified, Native Small-Intestinal Mucins from Rabbits and Humans Involves Interactions with the Mucin Carbohydrate Moiety. *Infect Immun* **1994,** *62* (4), 1219-1227.

63.   (a) Payne, D.; Tatham, D.; Williamson, E. D.; Titball, R. W., The pH 6 antigen of Yersinia pestis binds to beta 1-linked galactosyl residues in glycosphingolipids. *Infect Immun* **1998,** *66* (9), 4545-4548; (b) Cowan, C.; Jones, H. A.; Kaya, Y. H.; Perry, R. D.; Straley, S. C., Invasion of epithelial cells by Yersinia pestis: Evidence for a Y pestis-specific invasin. *Infect Immun* **2000,** *68* (8), 4523-4530.

64.   Newburg, D. S., Bioactive components of human milk: evolution, efficiency, and protection. *Short and Long Term Effects of Breast Feeding on Child Health* **2001,** *501*, 3-10.

65.   Grulee, C. G.; Sanford, H. N.; Herron, P. H., Breast and artificial feeding - Influence on morbidity and mortality of twenty thousand infants. *J Amer Med Assoc* **1934,** *103*, 0735-0739.

66.   Morrow, A. L.; Ruiz-Palacios, G. M.; Altaye, M.; Jiang, X.; Guerrero, M. L.; Meinzen-Derr, J. K.; Farkas, T.; Chaturvedi, P.; Pickering, L. K.; Newburg, D. S., Human milk oligosaccharide blood group epitopes and innate immune protection against campylobacter and calicivirus diarrhea in breastfed infants. *Adv Exp Med Biol* **2004,** *554*, 443-446.

67.   (a) Macfarlane, G. T.; Macfarlane, S., Human colonic microbiota: Ecology, physiology and metabolic potential of intestinal bacteria. *Scand J Gastroentero* **1997,** *32*, 3-9; (b) Orrhage, K.; Nord, C. E., Factors controlling the bacterial colonization of the intestine in breastfed infants. *Acta Paediatr* **1999,** *88*, 47-57.

68.   (a) Newburg, D. S.; Ruiz-Palacios, G. M.; Altaye, M.; Chaturvedi, P.; Meinzen-Derr, J.; Guerrero, M. D.; Morrow, A. L., Innate protection conferred by fucosylated oligosaccharides of human milk against diarrhea in breastfed infants (vol 14, pg 253, 2004). *Glycobiology* **2004,** *14* (5), 13g-13g; (b) Morrow, A. L.; Ruiz-Palacios, G. M.; Altaye, M.; Jiang, X.; Guerrero, M. L.; Meinzen-Derr, J. K.; Farkas, T.; Chaturvedi, P.; Pickering, L. K.; Newburg, D. S., Human milk oligosaccharide homologs of Lewis blood group epitopes and protection against diarrhea in breastfed infants. *Glycobiology* **2002,** *12* (10), 648-648.

69.   Newburg, D. S.; Warren, C. D.; Chaturvedi, P.; Ruiz-Palacios, G., Human milk oligosaccharides and blood group type. *Pediatric Research* **1999,** *45* (5), 745-745.

70.   (a) Zopf, D.; Roth, S., Oligosaccharide anti-infective agents. *Lancet* **1996,** *347* (9007), 1017-1021; (b) Kelly, C. G.; Younson, J. S., Anti-adhesive strategies in the prevention of infectious disease at mucosal surfaces. *Expert Opin Inv Drug* **2000,** *9* (8), 1711-1721; (c) Ofek, I.; Hasy, D. L.; Sharon, N., Anti-adhesion therapy of bacterial diseases: prospects and problems. *Fems Immunol Med Mic* **2003,** *38* (3), 181-191.

71.   (a) Kotter, S.; Krallmann-Wenzel, U.; Ehlers, S.; Lindhorst, T. K., Multivalent ligands for the mannose-specific lectin on type 1 fimbriae of Escherichia coli: syntheses and testing of trivalent alpha-D-mannoside clusters. *J Chem Soc Perk T 1* **1998,** (14), 2193-2200; (b) Lindhorst, T. K.; Kieburg, C.; Krallmann-Wenzel, U., Inhibition of the type 1 fimbriae-mediated adhesion of Escherichia coli to erythrocytes by multiantennary alpha-mannosyl clusters: The effect of multivalency. *Glycoconjugate J.* **1998,** *15* (6), 605-613.

72.   Paulson, J. C.; Blixt, O.; Collins, B. E., Sweet spots in functional glycomics. *Nature Chemical Biology* **2006,** *2* (5), 238-248.

73.   Kiessling, L. L.; Gestwicki, J. E.; Strong, L. E., Synthetic multivalent ligands as probes of signal transduction. *Angewandte Chemie-International Edition* **2006,** *45* (15), 2348-2368.

74.   Horlacher, T.; Seeberger, P. H., Carbohydrate arrays as tools for research and diagnostics. *Chem. Soc. Rev.* **2008,** *37* (7), 1414-1422.

75.   Schena, M.; Shalon, D.; Davis, R. W.; Brown, P. O., Quantitative Monitoring of Gene-Expression Patterns with a Complementary-DNA Microarray. *Science* **1995,** *270* (5235), 467-470.

76.   MacBeath, G.; Schreiber, S. L., Printing proteins as microarrays for high-throughput function determination. *Science* **2000,** *289* (5485), 1760-1763.

77.	(a) Houseman, B. T.; Mrksich, M., Carbohydrate arrays for the evaluation of protein binding and enzymatic modification. *Chem Biol* **2002,** *9* (4), 443-454; (b) Wang, D. N.; Liu, S. Y.; Trummer, B. J.; Deng, C.; Wang, A. L., Carbohydrate microarrays for the recognition of cross-reactive molecular markers of microbes and host cells. *Nature Biotechnology* **2002,** *20* (3), 275-281; (c) Ratner, D. M.; Adams, E. W.; Su, J.; O'Keefe, B. R.; Mrksich, M.; Seeberger, P. H., Probing protein-carbohydrate interactions with microarrays of synthetic oligosaccharides. *Chembiochem* **2004,** *5* (3), 379-382.

78.	(a) Liu, Y.; Palma, A. S.; Feizi, T., Carbohydrate microarrays: key developments in glycobiology. *Biol. Chem.* **2009,** *390* (7), 647-656; (b) Feizi, T.; Fazio, F.; Chai, W. C.; Wong, C. H., Carbohydrate microarrays - a new set of technologies at the frontiers of glycomics. *Curr Opin Struc Biol* **2003,** *13* (5), 637-645; (c) Kiessling, L. L.; Cairo, C. W., Hitting the sweet spot. *Nature Biotechnology* **2002,** *20* (3), 234-235.

79.	Disney, M. D.; Seeberger, P. H., The use of carbohydrate microarrays to study carbohydrate-cell interactions and to detect pathogens. *Chem Biol* **2004,** *11* (12), 1701-1707.

80.	Polanski, M.; Anderson, N. L., A list of candidate cancer biomarkers for targeted proteomics. *Biomark Insights* **2007,** *1*, 1-48.

81.	Sun, Y. S.; Landry, J. P.; Fei, Y. Y.; Zhu, X. D., Effect of Fluorescently Labeling Protein Probes on Kinetics of Protein-Ligand Reactions. *Langmuir* **2008,** *24* (23), 13399-13405.

82.	Kodadek, T., Protein microarrays: prospects and problems. *Chem Biol* **2001,** *8* (2), 105-115.

83.	(a) Hood, L.; Heath, J. R.; Phelps, M. E.; Lin, B. Y., Systems biology and new technologies enable predictive and preventative medicine. *Science* **2004,** *306* (5296), 640-643; (b) Soper, S. A.; Brown, K.; Ellington, A.; Frazier, B.; Garcia-Manero, G.; Gau, V.; Gutman, S. I.; Hayes, D. F.; Korte, B.; Landers, J. L.; Larson, D.; Ligler, F.; Majumdar, A.; Mascini, M.; Nolte, D.; Rosenzweig, Z.; Wang, J.; Wilson, D., Point-of-care biosensor systems for cancer diagnostics/prognostics. *Biosensors & Bioelectronics* **2006,** *21* (10), 1932-1942; (c) Sidransky, D., Emerging molecular markers of cancer. *Nat Rev Cancer* **2002,** *2* (3), 210-219; (d) Wulfkuhle, J. D.; Liotta, L. A.; Petricoin, E. F., Proteomic applications for the early detection of cancer. *Nat Rev Cancer* **2003,** *3* (4), 267-275.

84.	Hernandez, J.; Thompson, I. M., Prostate-specific antigen: A review of the validation of the most commonly used cancer biomarker. *Cancer* **2004,** *101* (5), 894-904.

85.	(a) Nagahori, N.; Lee, R. T.; Nishimura, S.; Page, D.; Roy, R.; Lee, Y. C., Inhibition of adhesion of type 1 fimbriated Escherichia coli to highly mannosylated ligands. *Chembiochem* **2002,** *3* (9), 836-844; (b) Autar, R.; Khan, A. S.; Schad, M.; Hacker, J.; Liskamp, R. M. J.; Pieters, R. J., Adhesion inhibition of F1C-fimbriated Escherichia coli and Pseudomonas aeruginosa PAK and PAO by multivalent carbohydrate ligands. *Chembiochem* **2003,** *4* (12), 1317-1325; (c) Disney, M. D.; Zheng, J.; Swager, T. M.; Seeberger, P. H., Detection of bacteria with carbohydrate-functionalized fluorescent polymers. *J. Am. Chem. Soc.* **2004,** *126* (41), 13343-13346; (d) Smith, A. E.; Helenius, A., How viruses enter animal cells. *Science* **2004,** *304* (5668), 237-242.

86.	(a) Eisen, M. B.; Brown, P. O., DNA arrays for analysis of gene expression. In *Cdna Preparation and Characterization*, 1999; Vol. 303, pp 179-205; (b) Heller, M. J., DNA microarray technology: Devices, systems, and applications. *Annual Review of Biomedical Engineering* **2002,** *4*, 129-153.

87.	(a) Templin, M. F.; Stoll, D.; Schrenk, M.; Traub, P. C.; Vohringer, C. F.; Joos, T. O., Protein microarray technology. *Trends in Biotechnology* **2002,** *20* (4), 160-166; (b) Zhu, H.; Snyder, M., Protein chip technology. *Current Opinion in Chemical Biology* **2003,** *7* (1), 55-63.

88.	Blixt, O.; Head, S.; Mondala, T.; Scanlan, C.; Huflejt, M. E.; Alvarez, R.; Bryan, M. C.; Fazio, F.; Calarese, D.; Stevens, J.; Razi, N.; Stevens, D. J.; Skehel, J. J.; van Die, I.; Burton, D. R.; Wilson, I. A.; Cummings, R.; Bovin, N.; Wong, C. H.; Paulson, J. C., Printed covalent glycan array for ligand profiling of diverse glycan binding proteins. *P Natl Acad Sci USA* **2004,** *101* (49), 17033-17038.

89.	(a) Bally, M.; Halter, M.; Voros, J.; Grandin, H. M., Optical microarray biosensing techniques. *Surface and Interface Analysis* **2006,** *38* (11), 1442-1458; (b) Campbell, C. T.; Kim, G., SPR microscopy and

its applications to high-throughput analyses of biomolecular binding events and their kinetics. *Biomaterials* **2007,** *28* (15), 2380-2392.

90.   Newman, J. D.; Turner, A. P. F., Home blood glucose biosensors: a commercial perspective. *Biosensors & Bioelectronics* **2005,** *20* (12), 2435-2453.

91.   Pejcic, B.; De Marco, R., Impedance spectroscopy: Over 35 years of electrochemical sensor optimization. *Electrochimica Acta* **2006,** *51* (28), 6217-6229.

92.   Daniels, J. S.; Pourmand, N., Label-free impedance biosensors: Opportunities and challenges. *Electroanalysis* **2007,** *19* (12), 1239-1257.

93.   (a) Patolsky, F.; Zheng, G. F.; Lieber, C. M., Nanowire-based biosensors. *Analytical Chemistry* **2006,** *78* (13), 4260-4269; (b) Sadik, O. A.; Aluoch, A. O.; Zhou, A. L., Status of biomolecular recognition using electrochemical techniques. *Biosensors & Bioelectronics* **2009,** *24* (9), 2749-2765; (c) Bellan, L. M.; Wu, D.; Langer, R. S., Current trends in nanobiosensor technology. *Wiley Interdiscip Rev Nanomed Nanobiotechnol* **2011**.

94.   (a) Yu, X. B.; Lv, R.; Ma, Z. Q.; Liu, Z. H.; Hao, Y. H.; Li, Q. Z.; Xu, D. K., An impedance array biosensor for detection of multiple antibody-antigen interactions. *Analyst* **2006,** *131* (6), 745-750; (b) Lodes, M. J.; Suciu, D.; Elliott, M.; Stover, A. G.; Ross, M.; Caraballo, M.; Dix, K.; Crye, J.; Webby, R. J.; Lyon, W. J.; Danley, D. L.; McShea, A., Use of semiconductor-based oligonucleotide microarrays for influenza A virus subtype identification and sequencing. *J Clin Microbiol* **2006,** *44* (4), 1209-1218.

95.   Maurer, K.; McShea, A.; Strathmann, M.; Dill, K., The removal of the t-BOC group by electrochemically generated acid and use of an addressable electrode array for peptide synthesis. *J Comb Chem* **2005,** *7* (5), 637-640.

96.   (a) Maurer, K.; Yazvenko, N.; Wilmoth, J.; Cooper, J.; Lyon, W.; Danley, D., Use of a Multiplexed CMOS Microarray to Optimize and Compare Oligonucleotide Binding to DNA Probes Synthesized or Immobilized on Individual Electrodes. *Sensors* **2010,** *10* (8), 7371-7385; (b) Cooper, J.; Yazvenko, N.; Peyvan, K.; Maurer, K.; Taitt, C. R.; Lyon, W.; Danley, D. L., Targeted Deposition of Antibodies on a Multiplex CMOS Microarray and Optimization of a Sensitive Immunoassay Using Electrochemical Detection. *PLoS One* **2010,** *5* (3).

97.   (a) Patolsky, F.; Zheng, G. F.; Hayden, O.; Lakadamyali, M.; Zhuang, X. W.; Lieber, C. M., Electrical detection of single viruses. *P Natl Acad Sci USA* **2004,** *101* (39), 14017-14022; (b) Li, C.; Curreli, M.; Lin, H.; Lei, B.; Ishikawa, F. N.; Datar, R.; Cote, R. J.; Thompson, M. E.; Zhou, C. W., Complementary detection of prostate-specific antigen using ln(2)O(3) nanowires and carbon nanotubes. *J. Am. Chem. Soc.* **2005,** *127* (36), 12484-12485; (c) Cui, Y.; Wei, Q. Q.; Park, H. K.; Lieber, C. M., Nanowire nanosensors for highly sensitive and selective detection of biological and chemical species. *Science* **2001,** *293* (5533), 1289-1292; (d) Hahm, J.; Lieber, C. M., Direct ultrasensitive electrical detection of DNA and DNA sequence variations using nanowire nanosensors. *Nano Lett.* **2004,** *4* (1), 51-54; (e) Zhang, G. J.; Chua, J. H.; Chee, R. E.; Agarwal, A.; Wong, S. M.; Buddharaju, K. D.; Balasubramanian, N., Highly sensitive measurements of PNA-DNA hybridization using oxide-etched silicon nanowire biosensors. *Biosensors & Bioelectronics* **2008,** *23* (11), 1701-1707.

98.   Malhotra, B. D.; Chaubey, A.; Singh, S. P., Prospects of conducting polymers in biosensors. *Anal Chim Acta* **2006,** *578* (1), 59-74.

99.   (a) Hu, P.; Fasoli, A.; Park, J.; Choi, Y.; Estrela, P.; Maeng, S. L.; Milne, W. I.; Ferrari, A. C., Self-assembled nanotube field-effect transistors for label-free protein biosensors. *J. Appl. Phys.* **2008,** *104* (7), -; (b) Star, A.; Tu, E.; Niemann, J.; Gabriel, J. C. P.; Joiner, C. S.; Valcke, C., Label-free detection of DNA hybridization using carbon nanotube network field-effect transistors. *P Natl Acad Sci USA* **2006,** *103* (4), 921-926.

100.   Zheng, G. F.; Patolsky, F.; Cui, Y.; Wang, W. U.; Lieber, C. M., Multiplexed electrical detection of cancer markers with nanowire sensor arrays. *Nature Biotechnology* **2005,** *23* (10), 1294-1301.

101. Stern, E.; Klemic, J. F.; Routenberg, D. A.; Wyrembak, P. N.; Turner-Evans, D. B.; Hamilton, A. D.; LaVan, D. A.; Fahmy, T. M.; Reed, M. A., Label-free immunodetection with CMOS-compatible semiconducting nanowires. *Nature* **2007,** *445* (7127), 519-522.

102. Yang, Y. T.; Callegari, C.; Feng, X. L.; Ekinci, K. L.; Roukes, M. L., Zeptogram-scale nanomechanical mass sensing. *Nano Lett.* **2006,** *6* (4), 583-586.

103. (a) Marx, K. A., Quartz crystal microbalance: A useful tool for studying thin polymer films and complex biomolecular systems at the solution-surface interface. *Biomacromolecules* **2003,** *4* (5), 1099-1120; (b) Cooper, M. A.; Singleton, V. T., A survey of the 2001 to 2005 quartz crystal microbalance biosensor literature: applications of acoustic physics to the analysis of biomolecular interactions. *Journal of Molecular Recognition* **2007,** *20* (3), 154-184; (c) Seker, S.; Arslan, Y. E.; Elcin, Y. M., Electrospun Nanofibrous PLGA/Fullerene-C60 Coated Quartz Crystal Microbalance for Real-Time Gluconic Acid Monitoring. *Ieee Sens J* **2010,** *10* (8), 1342-1348.

104. Erickson, D.; Mandal, S.; Yang, A. H. J.; Cordovez, B., Nanobiosensors: optofluidic, electrical and mechanical approaches to biomolecular detection at the nanoscale. *Microfluidics and Nanofluidics* **2008,** *4* (1-2), 33-52.

105. Hianik, T.; Ostatna, V.; Zajacova, Z.; Stoikova, E.; Evtugyn, G., Detection of aptamer-protein interactions using QCM and electrochemical indicator methods. *Bioorg Med Chem Lett* **2005,** *15* (2), 291-295.

106. (a) Hook, F.; Ray, A.; Norden, B.; Kasemo, B., Characterization of PNA and DNA immobilization and subsequent hybridization with DNA using acoustic-shear-wave attenuation measurements. *Langmuir* **2001,** *17* (26), 8305-8312; (b) Su, X. D.; Robelek, R.; Wu, Y. J.; Wang, G. Y.; Knoll, W., Detection of point mutation and insertion mutations in DNA using a quartz crystal microbalance and MutS, a mismatch binding protein. *Analytical Chemistry* **2004,** *76* (2), 489-494.

107. (a) Liebau, M.; Hildebrand, A.; Neubert, R. H. H., Bioadhesion of supramolecular structures at supported planar bilayers as studied by the quartz crystal microbalance. *European Biophysics Journal with Biophysics Letters* **2001,** *30* (1), 42-52; (b) Shen, Z. H.; Huang, M. C.; Xiao, C. D.; Zhang, Y.; Zeng, X. Q.; Wang, P. G., Nonlabeled quartz crystal microbalance biosensor for bacterial detection using carbohydrate and lectin recognitions. *Analytical Chemistry* **2007,** *79* (6), 2312-2319; (c) Mahon, E.; Aastrup, T.; Barboiu, M., Dynamic glycovesicle systems for amplified QCM detection of carbohydrate-lectin multivalent biorecognition. *Chem Commun* **2010,** *46* (14), 2441-2443.

108. (a) Briand, E.; Zach, M.; Svedhem, S.; Kasemo, B.; Petronis, S., Combined QCM-D and EIS study of supported lipid bilayer formation and interaction with pore-forming peptides. *Analyst* **2010,** *135* (2), 343-350; (b) Linden, M. V.; Meinander, K.; Hellel, A.; Yohannes, G.; Riekkola, M. L.; Butcher, S. J.; Viitala, T.; Wiedmerl, S. K., Characterization of phosphatidylcholine/polyethylene glycol-lipid aggregates and their use as coatings and carriers in capillary electrophoresis. *Electrophoresis* **2008,** *29* (4), 852-862.

109. (a) Cooper, M. A.; Dultsev, F. N.; Minson, T.; Ostanin, V. P.; Abell, C.; Klenerman, D., Direct and sensitive detection of a human virus by rupture event scanning. *Nature Biotechnology* **2001,** *19* (9), 833-837; (b) Dickert, F. L.; Hayden, O.; Bindeus, R.; Mann, K. J.; Blaas, D.; Waigmann, E., Bioimprinted QCM sensors for virus detection - screening of plant sap. *Analytical and Bioanalytical Chemistry* **2004,** *378* (8), 1929-1934.

110. (a) Su, X. L.; Li, Y. B., A self-assembled monolayer-based piezoelectric immunosensor for rapid detection of Escherichia coli O157 : H7. *Biosensors & Bioelectronics* **2004,** *19* (6), 563-574; (b) Su, X. L.; Li, Y. B., A QCM immunosensor for Salmonella detection with simultaneous measurements of resonant frequency and motional resistance. *Biosensors & Bioelectronics* **2005,** *21* (6), 840-848.

111. Ma, Z. W.; Mao, Z. W.; Gao, C. Y., Surface modification and property analysis of biomedical polymers used for tissue engineering. *Colloids and Surfaces B-Biointerfaces* **2007,** *60* (2), 137-157.

112. Fawcett, N. C.; Craven, R. D.; Zhang, P.; Evans, J. A., QCM response to solvated, tethered macromolecules. *Analytical Chemistry* **1998,** *70* (14), 2876-2880.

113.   Rabe, J.; Buttgenbach, S.; Schroder, J.; Hauptmann, P., Monolithic miniaturized quartz microbalance array and its application to chemical sensor systems for liquids. *Ieee Sens J* **2003,** *3* (4), 361-368.

114.   Fritz, J.; Baller, M. K.; Lang, H. P.; Rothuizen, H.; Vettiger, P.; Meyer, E.; Guntherodt, H. J.; Gerber, C.; Gimzewski, J. K., Translating biomolecular recognition into nanomechanics. *Science* **2000,** *288* (5464), 316-318.

115.   Backmann, N.; Zahnd, C.; Huber, F.; Bietsch, A.; Pluckthun, A.; Lang, H. P.; Guntherodt, H. J.; Hegner, M.; Gerber, C., A label-free immunosensor array using single-chain antibody fragments. *P Natl Acad Sci USA* **2005,** *102* (41), 14587-14592.

116.   Wu, G. H.; Datar, R. H.; Hansen, K. M.; Thundat, T.; Cote, R. J.; Majumdar, A., Bioassay of prostate-specific antigen (PSA) using microcantilevers. *Nature Biotechnology* **2001,** *19* (9), 856-860.

117.   (a) Ilic, B.; Yang, Y.; Craighead, H. G., Virus detection using nanoelectromechanical devices. *Applied Physics Letters* **2004,** *85* (13), 2604-2606; (b) Gupta, A.; Akin, D.; Bashir, R., Single virus particle mass detection using microresonators with nanoscale thickness. *Applied Physics Letters* **2004,** *84* (11), 1976-1978; (c) Johnson, L.; Gupta, A. T. K.; Ghafoor, A.; Akin, D.; Bashir, R., Characterization of vaccinia virus particles using microscale silicon cantilever resonators and atomic force microscopy. *Sensor Actuat B-Chem* **2006,** *115* (1), 189-197.

118.   (a) Ilic, B.; Czaplewski, D.; Zalalutdinov, M.; Craighead, H. G.; Neuzil, P.; Campagnolo, C.; Batt, C., Single cell detection with micromechanical oscillators. *J. Vac. Sci. Technol. B* **2001,** *19* (6), 2825-2828; (b) Park, K.; Jang, J.; Irimia, D.; Sturgis, J.; Lee, J.; Robinson, J. P.; Toner, M.; Bashir, R., 'Living cantilever arrays' for characterization of mass of single live cells in fluids. *Lab Chip* **2008,** *8* (7), 1034-1041.

119.   Ilic, B.; Yang, Y.; Aubin, K.; Reichenbach, R.; Krylov, S.; Craighead, H. G., Enumeration of DNA molecules bound to a nanomechanical oscillator. *Nano Lett.* **2005,** *5* (5), 925-929.

120.   Lee, J. H.; Hwang, K. S.; Park, J.; Yoon, K. H.; Yoon, D. S.; Kim, T. S., Immunoassay of prostate-specific antigen (PSA) using resonant frequency shift of piezoelectric nanomechanical microcantilever. *Biosensors & Bioelectronics* **2005,** *20* (10), 2157-2162.

121.   (a) Burg, T. P.; Godin, M.; Knudsen, S. M.; Shen, W.; Carlson, G.; Foster, J. S.; Babcock, K.; Manalis, S. R., Weighing of biomolecules, single cells and single nanoparticles in fluid. *Nature* **2007,** *446* (7139), 1066-1069; (b) Barton, R. A.; Ilic, B.; Verbridge, S. S.; Cipriany, B. R.; Parpia, J. M.; Craighead, H. G., Fabrication of a Nanomechanical Mass Sensor Containing a Nanofluidic Channel. *Nano Lett.* **2010,** *10* (6), 2058-2063.

122.   (a) Godin, M.; Delgado, F. F.; Son, S. M.; Grover, W. H.; Bryan, A. K.; Tzur, A.; Jorgensen, P.; Payer, K.; Grossman, A. D.; Kirschner, M. W.; Manalis, S. R., Using buoyant mass to measure the growth of single cells. *Nat. Methods* **2010,** *7* (5), 387-U70; (b) Bryan, A. K.; Goranov, A.; Amon, A.; Manalis, S. R., Measurement of mass, density, and volume during the cell cycle of yeast. *P Natl Acad Sci USA* **2010,** *107* (3), 999-1004.

123.   von Muhlen, M. G.; Brault, N. D.; Knudsen, S. M.; Jiang, S. Y.; Manalis, S. R., Label-Free Biomarker Sensing in Undiluted Serum with Suspended Microchannel Resonators. *Analytical Chemistry* **2010,** *82* (5), 1905-1910.

124.   Rich, R. L.; Myszka, D. G., Grading the commercial optical biosensor literature-Class of 2008: 'The Mighty Binders'. *Journal of Molecular Recognition* **2010,** *23* (1), 1-64.

125.   Fan, X. D.; White, I. M.; Shopoua, S. I.; Zhu, H. Y.; Suter, J. D.; Sun, Y. Z., Sensitive optical biosensors for unlabeled targets: A review. *Anal. Chim. Acta* **2008,** *620* (1-2), 8-26.

126.   Liedberg, B.; Nylander, C.; Lundstrom, I., SURFACE-PLASMON RESONANCE FOR GAS-DETECTION AND BIOSENSING. *Sensors and Actuators* **1983,** *4* (2), 299-304.

127.   Homola, J., Surface plasmon resonance sensors for detection of chemical and biological species. *Chem. Rev.* **2008,** *108* (2), 462-493.

128.	Boozer, C.; Kim, G.; Cong, S. X.; Guan, H. W.; Londergan, T., Looking towards label-free biomolecular interaction analysis in a high-throughput format: a review of new surface plasmon resonance technologies. *Current Opinion in Biotechnology* **2006,** *17* (4), 400-405.

129.	Qavi, A. J.; Washburn, A. L.; Byeon, J. Y.; Bailey, R. C., Label-free technologies for quantitative multiparameter biological analysis. *Analytical and Bioanalytical Chemistry* **2009,** *394* (1), 121-135.

130.	Cooper, M. A., Optical biosensors in drug discovery. *Nat Rev Drug Discov* **2002,** *1* (7), 515-528.

131.	(a) Wassaf, D.; Kuang, G. N.; Kopacz, K.; Wu, Q. L.; Nguyen, Q.; Toews, M.; Cosic, J.; Jacques, J.; Wiltshire, S.; Lambert, J.; Pazmany, C. C.; Hogan, S.; Ladner, R. C.; Nixon, A. E.; Sexton, D. J., High-throughput affinity ranking of antibodies using surface plasmon resonance microarrays. *Anal. Biochem.* **2006,** *351* (2), 241-253; (b) Usui-Aoki, K.; Shimada, K.; Nagano, M.; Kawai, M.; Koga, H., A novel approach to protein expression profiling using antibody microarrays combined with surface plasmon resonance technology. *Proteomics* **2005,** *5* (9), 2396-2401.

132.	(a) Dhayal, M.; Ratner, D. A., XPS and SPR Analysis of Glycoarray Surface Density. *Langmuir* **2009,** *25* (4), 2181-2187; (b) Corn, R. M.; Chen, Y. L.; Nguyen, A.; Niu, L. F., Fabrication of DNA Microarrays with Poly(L-glutamic acid) Monolayers on Gold Substrates for SPR Imaging Measurements. *Langmuir* **2009,** *25* (9), 5054-5060.

133.	(a) Spangler, B. D.; Wilkinson, E. A.; Murphy, J. T.; Tyler, B. J., Comparison of the Spreeta (R) surface plasmon resonance sensor and a quartz crystal microbalance for detection of Escherichia coli heat-labile enterotoxin. *Anal. Chim. Acta* **2001,** *444* (1), 149-161; (b) Chinowsky, T. M.; Quinn, J. G.; Bartholomew, D. U.; Kaiser, R.; Elkind, J. L., Performance of the Spreeta 2000 integrated surface plasmon resonance affinity sensor. *Sensor Actuat B-Chem* **2003,** *91* (1-3), 266-274.

134.	(a) Codner, E. P. a. C., R.M. Portable Surface Plasmon Resonance Imaging Instrument. 2006; (b) Fu, E.; Chinowsky, T.; Nelson, K.; Johnston, K.; Edwards, T.; Helton, K.; Grow, M.; Miller, J. W.; Yager, P., SPR imaging-based salivary diagnostics system for the detection of small molecule analytes. *Ann Ny Acad Sci* **2007,** *1098*, 335-344; (c) Chinowsky, T. M.; Grow, M. S.; Johnston, K. S.; Nelson, K.; Edwards, T.; Fu, E.; Yager, P., Compact, high performance surface plasmon resonance imaging system. *Biosensors & Bioelectronics* **2007,** *22* (9-10), 2208-2215.

135.	Lee, C. Y.; Gong, P.; Harbers, G. M.; Grainger, D. W.; Castner, D. G.; Gamble, L. J., Surface coverage and structure of mixed DNA/alkylthiol monolayers on gold: Characterization by XPS, NEXAFS, and fluorescence intensity measurements. *Analytical Chemistry* **2006,** *78* (10), 3316-3325.

136.	(a) Laibinis, P. E.; Whitesides, G. M.; Allara, D. L.; Tao, Y. T.; Parikh, A. N.; Nuzzo, R. G., COMPARISON OF THE STRUCTURES AND WETTING PROPERTIES OF SELF-ASSEMBLED MONOLAYERS OF NORMAL-ALKANETHIOLS ON THE COINAGE METAL-SURFACES, CU, AG, AU. *J. Am. Chem. Soc.* **1991,** *113* (19), 7152-7167; (b) Ulman, A., Formation and structure of self-assembled monolayers. *Chem. Rev.* **1996,** *96* (4), 1533-1554.

137.	Kersey, A. D.; Davis, M. A.; Patrick, H. J.; LeBlanc, M.; Koo, K. P.; Askins, C. G.; Putnam, M. A.; Friebele, E. J., Fiber grating sensors. *J Lightwave Technol* **1997,** *15* (8), 1442-1463.

138.	Chryssis, A. N.; Saini, S. S.; Lee, S. M.; Yi, H. M.; Bentley, W. E.; Dagenais, M., Detecting hybridization of DNA by highly sensitive evanescent field etched core fiber bragg grating sensors. *Ieee J Sel Top Quant* **2005,** *11* (4), 864-872.

139.	DeLisa, M. P.; Zhang, Z.; Shiloach, M.; Pilevar, S.; Davis, C. C.; Sirkis, J. S.; Bentley, W. E., Evanescent wave long period fiber Bragg grating as an immobilized antibody biosensor. *Analytical Chemistry* **2000,** *72* (13), 2895-2900.

140.	Chen, X.; Zhou, K.; Zhang, L.; Bennion, I., Dual-peak long-period fiber gratings with enhanced refractive index sensitivity by finely tailored mode dispersion that uses the light cladding etching technique. *Appl Opt* **2007,** *46* (4), 451-5.

141.	Smith, K. H.; Ipson, B. L.; Lowder, T. L.; Hawkins, A. R.; Selfridge, R. H.; Schultz, S. M., Surface-relief fiber Bragg gratings for sensing applications. *Appl Optics* **2006,** *45* (8), 1669-1675.

142.   Washburn, A. L.; Bailey, R. C., Photonics-on-a-chip: recent advances in integrated waveguides as enabling detection elements for real-world, lab-on-a-chip biosensing applications. *Analyst* **2011,** *136* (2), 227-236.

143.   Szekacs, A.; Trummer, N.; Adanyi, N.; Varadi, M.; Szendro, I., Development of a non-labeled immunosensor for the herbicide trifluralin via optical waveguide lightmode spectroscopic detection. *Anal. Chim. Acta* **2003,** *487* (1), 31-42.

144.   Adanyi, N.; Levkovets, I. A.; Rodriguez-Gil, S.; Ronald, A.; Varadi, M.; Szendro, I., Development of immunosensor based on OWLS technique for determining Aflatoxin B1 and Ochratoxin A. *Biosensors & Bioelectronics* **2007,** *22* (6), 797-802.

145.   (a) Wittmer, C. R.; Van Tassel, P. R., Probing adsorbed fibronectin layer structure by kinetic analysis of monoclonal antibody binding. *Colloids and Surfaces B-Biointerfaces* **2005,** *41* (2-3), 103-109; (b) Blattler, T. M.; Pasche, S.; Textor, M.; Griesser, H. J., High salt stability and protein resistance of poly(L-lysine)-g-poly(ethylene glycol) copolymers covalently immobilized via aldehyde plasma polymer interlayers on inorganic and polymeric substrates. *Langmuir* **2006,** *22* (13), 5760-5769; (c) Horvath, R.; McColl, J.; Yakubov, G. E.; Ramsden, J. J., Structural hysteresis and hierarchy in adsorbed glycoproteins. *J Chem Phys* **2008,** *129* (7), -.

146.   Adrian, J.; Pasche, S.; Pinacho, D. G.; Font, H.; Diserens, J. M.; Sanchez-Baeza, F.; Granier, B.; Voirin, G.; Marco, M. P., Wavelength-interrogated optical biosensor for multi-analyte screening of sulfonamide, fluoroquinolone, beta-lactam and tetracycline antibiotics in milk. *Trac-Trend Anal Chem* **2009,** *28* (6), 769-777.

147.   Heideman, R. G.; Kooyman, R. P. H.; Greve, J., Performance of a Highly Sensitive Optical Wave-Guide Mach-Zehnder Interferometer Immunosensor. *Sensor Actuat B-Chem* **1993,** *10* (3), 209-217.

148.   Heideman, R. G.; Lambeck, P. V., Remote opto-chemical sensing with extreme sensitivity: design, fabrication and performance of a pigtailed integrated optical phase-modulated Mach-Zehnder interferometer system. *Sensor Actuat B-Chem* **1999,** *61* (1-3), 100-127.

149.   Shew, B. Y.; Cheng, Y. C.; Tsai, Y. H., Monolithic SU-8 micro-interferometer for biochemical detections. *Sensor Actuat a-Phys* **2008,** *141* (2), 299-306.

150.   Lechuga, J. S. d. R. L. G. C. F. J. B. M. M. J. B. A. C. C. D. L. M., Lab-on-a-chip platforms based on highly sensitive nanophotonic Si biosensors for single nucleotide DNA testing (Proceedings Paper). In *Silicon Photonics II* Reed, J. A. K. G. T., Ed. SPIE: San Jose, CA, USA, 2007; Vol. 64771B.

151.   Densmore, A.; Vachon, M.; Xu, D. X.; Janz, S.; Ma, R.; Li, Y. H.; Lopinski, G.; Delage, A.; Lapointe, J.; Luebbert, C. C.; Liu, Q. Y.; Cheben, P.; Schmid, J. H., Silicon photonic wire biosensor array for multiplexed real-time and label-free molecular detection. *Opt. Lett.* **2009,** *34* (23), 3598-3600.

152.   Brandenburg, A.; Henninger, R., Integrated Optical Young Interferometer. *Appl Optics* **1994,** *33* (25), 5941-5947.

153.   Brandenburg, A., Differential refractometry by an integrated-optical Young interferometer. *Sensor Actuat B-Chem* **1997,** *39* (1-3), 266-271.

154.   Ymeti, A.; Kanger, J. S.; Greve, J.; Lambeck, P. V.; Wijn, R.; Heideman, R. G., Realization of a multichannel integrated Young interferometer chemical sensor. *Appl Optics* **2003,** *42* (28), 5649-5660.

155.   Ymeti, A.; Subramaniam, V.; Beumer, T. A. M.; Kanger, J. S., An ultrasensitive Young interferometer handheld sensor for rapid virus detection. *Expert Rev Med Devic* **2007,** *4* (4), 447-454.

156.   Hoffmann, C.; Schmitt, K.; Schirmer, B.; Brandenburg, A.; Meyrueis, P., Interferometric biosensor based on planar optical waveguide sensor chips for label-free detection of surface bound bioreactions. *Biosensors & Bioelectronics* **2007,** *22* (11), 2591-2597.

157.   (a) Griffel, G.; Arnold, S.; Taskent, D.; Serpenguzel, A.; Connolly, J.; Morris, N., Morphology-dependent resonances of a microsphere-optical fiber system. *Opt. Lett.* **1996,** *21* (10), 695-697; (b) Vollmer, F.; Arnold, S.; Keng, D., Single virus detection from the reactive shift of a whispering-gallery mode. *P Natl Acad Sci USA* **2008,** *105* (52), 20701-20704.

158.	(a) Vollmer, F.; Braun, D.; Libchaber, A.; Khoshsima, M.; Teraoka, I.; Arnold, S., Protein detection by optical shift of a resonant microcavity. *Applied Physics Letters* **2002,** *80* (21), 4057-4059; (b) Hanumegowda, N. M.; Stica, C. J.; Patel, B. C.; White, I.; Fan, X. D., Refractometric sensors based on microsphere resonators. *Applied Physics Letters* **2005,** *87* (20).

159.	Hanumegowda, N. M.; White, I. M.; Oveys, H.; Fan, X. D., Label-free protease sensors based on optical microsphere resonators. *Sensor Letters* **2005,** *3* (4), 315-319.

160.	Jokerst, N.; Royal, M.; Palit, S.; Luan, L.; Dhar, S.; Tyler, T., Chip scale integrated microresonator sensing systems. *J Biophotonics* **2009,** *2* (4), 212-226.

161.	Armani, A. M.; Kulkarni, R. P.; Fraser, S. E.; Flagan, R. C.; Vahala, K. J., Label-free, single-molecule detection with optical microcavities. *Science* **2007,** *317* (5839), 783-7.

162.	Arnold, S.; Shopova, S. I.; Holler, S., Whispering gallery mode bio-sensor for label-free detection of single molecules: thermo-optic vs. reactive mechanism. *Optics Express* **2010,** *18* (1), 281-287.

163.	Squires, T. M.; Messinger, R. J.; Manalis, S. R., Making it stick: convection, reaction and diffusion in surface-based biosensors. *Nature Biotechnology* **2008,** *26* (4), 417-426.

164.	(a) Iqbal, M.; Gleeson, M. A.; Spaugh, B.; Tybor, F.; Gunn, W. G.; Hochberg, M.; Baehr-Jones, T.; Bailey, R. C.; Gunn, L. C., Label-Free Biosensor Arrays Based on Silicon Ring Resonators and High-Speed Optical Scanning Instrumentation. *Ieee J Sel Top Quant* **2010,** *16* (3), 654-661; (b) Carlborg, C. F.; Gylfason, K. B.; Kazmierczak, A.; Dortu, F.; Polo, M. J. B.; Catala, A. M.; Kresbach, G. M.; Sohlstrom, H.; Moh, T.; Vivien, L.; Popplewell, J.; Ronan, G.; Barrios, C. A.; Stemme, G.; van der Wijngaart, W., A packaged optical slot-waveguide ring resonator sensor array for multiplex label-free assays in labs-on-chips. *Lab Chip* **2010,** *10* (3), 281-290; (c) Chao, C. Y.; Fung, W.; Guo, L. J., Polymer microring resonators for biochemical sensing applications. *Ieee J Sel Top Quant* **2006,** *12* (1), 134-142.

165.	Huang, Y. Y.; Paloczi, G. T.; Yariv, A.; Zhang, C.; Dalton, L. R., Fabrication and replication of polymer integrated optical devices using electron-beam lithography and soft lithography. *J. Phys. Chem. B* **2004,** *108* (25), 8606-8613.

166.	(a) Yalcin, A.; Popat, K. C.; Aldridge, J. C.; Desai, T. A.; Hryniewicz, J.; Chbouki, N.; Little, B. E.; King, O.; Van, V.; Chu, S.; Gill, D.; Anthes-Washburn, M.; Unlu, M. S., Optical sensing of biomolecules using microring resonators. *Ieee J Sel Top Quant* **2006,** *12* (1), 148-155; (b) Ramachandran, A.; Wang, S.; Clarke, J.; Ja, S. J.; Goad, D.; Wald, L.; Flood, E. M.; Knobbe, E.; Hryniewicz, J. V.; Chu, S. T.; Gill, D.; Chen, W.; King, O.; Little, B. E., A universal biosensing platform based on optical micro-ring resonators. *Biosens Bioelectron* **2008,** *23* (7), 939-44.

167.	(a) Barrios, C. A.; Banuls, M. J.; Gonzalez-Pedro, V.; Gylfason, K. B.; Sanchez, B.; Griol, A.; Maquieira, A.; Sohlstrom, H.; Holgado, M.; Casquel, R., Label-free optical biosensing with slot-waveguides. *Opt. Lett.* **2008,** *33* (7), 708-710; (b) Hosseini, E. S.; Yegnanarayanan, S.; Atabaki, A. H.; Soltani, M.; Adibi, A., Systematic design and fabrication of high-Q single-mode pulley-coupled planar silicon nitride microdisk resonators at visible wavelengths. *Optics Express* **2010,** *18* (3), 2127-2136.

168.	(a) Xu, D. X.; Vachon, M.; Densmore, A.; Ma, R.; Delage, A.; Janz, S.; Lapointe, J.; Li, Y.; Lopinski, G.; Zhang, D.; Liu, Q. Y.; Cheben, P.; Schmid, J. H., Label-free biosensor array based on silicon-on-insulator ring resonators addressed using a WDM approach. *Opt. Lett.* **2010,** *35* (16), 2771-2773; (b) De Vos, K.; Girones, J.; Popelka, S.; Schacht, E.; Baets, R.; Bienstman, P., SOI optical microring resonator with poly(ethylene glycol) polymer brush for label-free biosensor applications. *Biosensors & Bioelectronics* **2009,** *24* (8), 2528-2533; (c) Washburn, A. L.; Gunn, L. C.; Bailey, R. C., Label-Free Quantitation of a Cancer Biomarker in Complex Media Using Silicon Photonic Microring Resonators. *Analytical Chemistry* **2009,** *81* (22), 9499-9506.

169.	Gylfason, K. B.; Carlborg, C. F.; Kazmierczak, A.; Dortu, F.; Sohlstrom, H.; Vivien, L.; Barrios, C. A.; van der Wijngaart, W.; Stemme, G., On-chip temperature compensation in an integrated slot-waveguide ring resonator refractive index sensor array. *Opt Express* **2010,** *18* (4), 3226-37.

170.   (a) Bailey, R. C., A robust silicon photonic platform for multiparameter biological analysis. In *Silicon Photonics IV*, Proc. SPIE 7220: 2009; Vol. 72200N; (b) Kirk, J. T.; Fridley, G. E.; Chamberlain, J. W.; Christensen, E. D.; Hochberg, M.; Ratner, D. M., Multiplexed inkjet functionalization of silicon photonic biosensors. *Lab Chip* **2011,** *11* (7), 1372-7.

171.   Washburn, A. L.; Luchansky, M. S.; Bowman, A. L.; Bailey, R. C., Quantitative, Label-Free Detection of Five Protein Biomarkers Using Multiplexed Arrays of Silicon Photonic Microring Resonators. *Analytical Chemistry* **2010,** *82* (1), 69-72.

172.   (a) Harris, J. M., *Poly(ethylene glycol) chemistry : biotechnical and biomedical applications*. Plenum Press: New York, 1992; p xxi, 385 p; (b) Harder, P.; Grunze, M.; Dahint, R.; Whitesides, G. M.; Laibinis, P. E., Molecular conformation in oligo(ethylene glycol)-terminated self-assembled monolayers on gold and silver surfaces determines their ability to resist protein adsorption. *J. Phys. Chem. B* **1998,** *102* (2), 426-436; (c) Zheng, J.; Li, L. Y.; Tsao, H. K.; Sheng, Y. J.; Chen, S. F.; Jiang, S. Y., Strong repulsive forces between protein and oligo (ethylene glycol) self-assembled monolayers: A molecular simulation study. *Biophysical Journal* **2005,** *89* (1), 158-166.

173.   (a) Jiang, S. Y.; Cao, Z. Q., Ultralow-Fouling, Functionalizable, and Hydrolyzable Zwitterionic Materials and Their Derivatives for Biological Applications. *Advanced Materials* **2010,** *22* (9), 920-932; (b) He, Y.; Hower, J.; Chen, S. F.; Bernards, M. T.; Chang, Y.; Jiang, S. Y., Molecular simulation studies of protein interactions with zwitterionic phosphorylcholine self-assembled monolayers in the presence of water. *Langmuir* **2008,** *24* (18), 10358-10364.

174.   Ko, K. S.; Jaipuri, F. A.; Pohl, N. L., Fluorous-based carbohydrate microarrays. *J. Am. Chem. Soc.* **2005,** *127* (38), 13162-13163.

175.   (a) Tessier, D.; Dao, L. H.; Zhang, Z.; King, M. W.; Guidoin, R., Polymerization and surface analysis of electrically-conductive polypyrrole on surface-activated polyester fabrics for biomedical applications. *J Biomater Sci Polym Ed* **2000,** *11* (1), 87-99; (b) Ramanaviciene, A.; Ramanavicius, A., Application of polypyrrole for the creation of immunosensors. *Crit Rev Anal Chem* **2002,** *32* (3), 245-252.

176.   (a) Feizi, T.; Chai, W. G., Oligosaccharide microarrays to decipher the glyco code. *Nat Rev Mol Cell Bio* **2004,** *5* (7), 582-588; (b) Fukui, S.; Feizi, T.; Galustian, C.; Lawson, A. M.; Chai, W. G., Oligosaccharide microarrays for high-throughput detection and specificity assignments of carbohydrate-protein interactions. *Nature Biotechnology* **2002,** *20* (10), 1011-1017.

177.   Vidal, J. C.; Garcia-Ruiz, E.; Espuelas, J.; Aramendia, T.; Castillo, J. R., Comparison of biosensors based on entrapment of cholesterol oxidase and cholesterol esterase in electropolymerized films of polypyrrole and diaminonaphthalene derivatives for amperometric determination of cholesterol. *Analytical and Bioanalytical Chemistry* **2003,** *377* (2), 273-280.

178.   Chamberlain, J. W.; Maurer, K.; Cooper, J.; Lyon, W. J.; Danley, D. L.; Ratner, D. M., Microelectrode array biosensor for studying carbohydrate-mediated interactions. *Biosens Bioelectron* **2012,** *34* (1), 253-60.

179.   Park, S. J.; Shin, I. J., Fabrication of carbohydrate chips for studying protein-carbohydrate interactions. *Angewandte Chemie-International Edition* **2002,** *41* (17), 3180-+.

180.   de Paz, J. L.; Horlacher, T.; Seeberger, P. H., Oligosaccharide microarrays to map interactions of carbohydrates in biological systems. *Glycobiology* **2006,** *415*, 269-292.

181.   Park, S.; Lee, M. R.; Shin, I., Fabrication of carbohydrate chips and their use to probe protein-carbohydrate interactions. *Nat. Protoc.* **2007,** *2* (11), 2747-2758.

182.   Sun, X. L.; Stabler, C. L.; Cazalis, C. S.; Chaikof, E. L., Carbohydrate and protein immobilization onto solid surfaces by sequential Diels-Alder and azide-alkyne cycloadditions. *Bioconjugate Chemistry* **2006,** *17* (1), 52-57.

183.   Pei, Z. C.; Yu, H.; Theurer, M.; Walden, A.; Nilsson, P.; Yan, M. D.; Ramstrom, O., Photogenerated carbohydrate microarrays. *Chembiochem* **2007,** *8* (2), 166-168.

184.   (a) Rich, R. L.; Myszka, D. G., Survey of the year 2006 commercial optical biosensor literature. *Journal of Molecular Recognition* **2007,** *20* (5), 300-366; (b) Rich, R. L.; Myszka, D. G., Survey of the year 2007 commercial optical biosensor literature. *Journal of Molecular Recognition* **2008,** *21* (6), 355-400.

185.   (a) Myers, F. B.; Lee, L. P., Innovations in optical microfluidic technologies for point-of-care diagnostics. *Lab Chip* **2008,** *8* (12), 2015-31; (b) Monat, C.; Domachuk, P.; Eggleton, B. J., Integrated optofluidics: A new river of light. *Nat Photonics* **2007,** *1* (2), 106-114; (c) Momeni, B.; Yegnanarayanan, S.; Soltani, M.; Eftekhar, A. A.; Hosseini, E. S.; Adibi, A., Silicon nanophotonic devices for integrated sensing. *J. Nanophotonics* **2009,** *3*; (d) Balslev, S.; Jorgensen, A. M.; Bilenberg, B.; Mogensen, K. B.; Snakenborg, D.; Geschke, O.; Kutter, J. P.; Kristensen, A., Lab-on-a-chip with integrated optical transducers. *Lab Chip* **2006,** *6* (2), 213-7.

186.   Seo, S. W.; Cho, S. Y.; Jokerst, N. M., A thin-film laser, polymer waveguide, and thin-film photodetector cointegrated onto a silicon substrate. *Ieee Photonic Tech L* **2005,** *17* (10), 2197-2199.

187.   Seo, S. W.; Cho, S. Y.; Huang, S.; Shin, J. J.; Jokerst, N. M.; Brown, A. S.; Brooke, M. A., High-speed large-area inverted InGaAs thin-film metal-semiconductor-metal photodetectors. *Ieee J Sel Top Quant* **2004,** *10* (4), 686-693.

188.   (a) Cho, S. Y.; Jokerst, N. M., Integrated thin film photodetectors with vertically coupled microring resonators for chip scale spectral analysis. *Applied Physics Letters* **2007,** *90* (10); (b) Cho, S. Y.; Jokerst, N. M., A polymer microdisk photonic sensor integrated onto silicon. *Ieee Photonic Tech L* **2006,** *18* (17-20), 2096-2098.

189.   Seo, S. W.; Cho, S. Y.; Jokerst, N. M., Integrated thin film InGaAsP laser and I X 4 polymer multimode interference splitter on silicon. *Opt. Lett.* **2007,** *32* (5), 548-550.

190.   Seo, J.; Lee, L. P., Disposable integrated microfluidics with self-aligned planar microlenses. *Sensor Actuat B-Chem* **2004,** *99* (2-3), 615-622.

191.   Llobera, A.; Demming, S.; Wilke, R.; Buttgenbach, S., Multiple internal reflection poly(dimethylsiloxane) systems for optical sensing. *Lab Chip* **2007,** *7* (11), 1560-1566.

192.   (a) Chediak, J. A.; Luo, Z. S.; Seo, J. G.; Cheung, N.; Lee, L. P.; Sands, T. D., Heterogeneous integration of CdS filters with GaN LEDs for fluorescence detection microsystems. *Sensor Actuat a-Phys* **2004,** *111* (1), 1-7; (b) Llobera, A.; Demming, S.; Joensson, H. N.; Vila-Planas, J.; Andersson-Svahn, H.; Buttgenbach, S., Monolithic PDMS passband filters for fluorescence detection. *Lab Chip* **2010,** *10* (15), 1987-1992.

193.   Ligler, F. S., Perspective on Optical Biosensors and Integrated Sensor Systems. *Analytical Chemistry* **2009,** *81* (2), 519-526.

194.   (a) Zhang, C. S.; Xing, D.; Li, Y. Y., Micropumps, microvalves, and micromixers within PCR microfluidic chips: Advances and trends. *Biotechnology Advances* **2007,** *25* (5), 483-514; (b) Oh, K. W.; Ahn, C. H., A review of microvalves. *J Micromech Microeng* **2006,** *16* (5), R13-R39.

195.   (a) Beebe, D. J.; Mensing, G. A.; Walker, G. M., Physics and applications of microfluidics in biology. *Annual Review of Biomedical Engineering* **2002,** *4*, 261-286; (b) Iverson, B. D.; Garimella, S. V., Recent advances in microscale pumping technologies: a review and evaluation. *Microfluidics and Nanofluidics* **2008,** *5* (2), 145-174; (c) Wang, X. Y.; Cheng, C.; Wang, S. L.; Liu, S. R., Electroosmotic pumps and their applications in microfluidic systems. *Microfluidics and Nanofluidics* **2009,** *6* (2), 145-162.

196.   (a) Mansur, E. A.; Ye, M. X.; Wang, Y. D.; Dai, Y. Y., A state-of-the-art review of mixing in microfluidic mixers. *Chin. J. Chem. Eng.* **2008,** *16* (4), 503-516; (b) Chang, C. C.; Yang, R. J., Electrokinetic mixing in microfluidic systems. *Microfluidics and Nanofluidics* **2007,** *3* (5), 501-525.

197.   (a) Wang, Y. C.; Han, J. Y., Pre-binding dynamic range and sensitivity enhancement for immuno-sensors using nanofluidic preconcentrator. *Lab Chip* **2008,** *8* (3), 392-394; (b) Yu, H.; Lu, Y.; Zhou, Y. G.; Wang, F. B.; He, F. Y.; Xia, X. H., A simple, disposable microfluidic device for rapid protein concentration and purification via direct-printing. *Lab Chip* **2008,** *8* (9), 1496-1501.

198.   (a) Weigl, B. H.; Yager, P., Microfluidics - Microfluidic diffusion-based separation and detection. *Science* **1999,** *283* (5400), 346-347; (b) Gossett, D. R.; Weaver, W. M.; Mach, A. J.; Hur, S. C.; Tse, H. T. K.; Lee, W.; Amini, H.; Di Carlo, D., Label-free cell separation and sorting in microfluidic systems. *Analytical and Bioanalytical Chemistry* **2010,** *397* (8), 3249-3267; (c) Di Carlo, D.; Irimia, D.; Tompkins, R. G.; Toner, M., Continuous inertial focusing, ordering, and separation of particles in microchannels. *Proc Natl Acad Sci U S A* **2007,** *104* (48), 18892-7.

199.   Reed, G. T.; Knights, A. P., *Silicon Photonics - An Introduction*. John Wiley & Sons Ltd.: West Sussex, England, 2004.

200.   (a) Intel Silicon Photonics Research. http://techresearch.intel.com/ResearchAreaDetails.aspx?Id=26 (accessed 4/8/2011); (b) Washington, U. o. OpSIS (Optoelectronic Systems Integration in Silicon). http://depts.washington.edu/uwopsis/ (accessed 4/8/2011).

201.   Hewitt, P. D.; Reed, G. T., Improving the response of optical phase modulators in SOI by computer simulation. *J Lightwave Technol* **2000,** *18* (3), 443-450.

202.   Luxtera http://www.luxtera.com/ (accessed 4/8/2011).

203.   (a) Mannoor, M. S.; Zhang, S. Y.; Link, A. J.; McAlpine, M. C., Electrical detection of pathogenic bacteria via immobilized antimicrobial peptides. *P Natl Acad Sci USA* **2010,** *107* (45), 19207-19212; (b) Jones, I. L.; Livi, P.; Lewandowska, M. K.; Fiscella, M.; Roscic, B.; Hierlemann, A., The potential of microelectrode arrays and microelectronics for biomedical research and diagnostics. *Analytical and Bioanalytical Chemistry* **2011,** *399* (7), 2313-2329.

204.   Suehiro, J.; Ohtsubo, A.; Hatano, T.; Hara, M., Selective detection of bacteria by a dielectrophoretic impedance measurement method using an antibody-immobilized electrode chip. *Sensor Actuat B-Chem* **2006,** *119* (1), 319-326.

205.   (a) Barghouthi, S.; Guerdoud, L. M.; Speert, D. P., Inhibition by dextran of Pseudomonas aeruginosa adherence to epithelial cells. *Am J Resp Crit Care* **1996,** *154* (6), 1788-1793; (b) Bouckaert, J.; Berglund, J.; Schembri, M.; De Genst, E.; Cools, L.; Wuhrer, M.; Hung, C. S.; Pinkner, J.; Slattegard, R.; Zavialov, A.; Choudhury, D.; Langermann, S.; Hultgren, S. J.; Wyns, L.; Klemm, P.; Oscarson, S.; Knight, S. D.; De Greve, H., Receptor binding studies disclose a novel class of high-affinity inhibitors of the Escherichia coli FimH adhesin. *Molecular Microbiology* **2005,** *55* (2), 441-455.

206.   (a) Aronson, M.; Medalia, O.; Schori, L.; Mirelman, D.; Sharon, N.; Ofek, I., Prevention of Colonization of the Urinary-Tract of Mice with Escherichia-Coli by Blocking of Bacterial Adherence with Methyl Alpha-D-Mannopyranoside. *J Infect Dis* **1979,** *139* (3), 329-332; (b) IdanpaanHeikkila, I.; Simon, P. M.; Zopf, D.; Vullo, T.; Cahill, P.; Sokol, K.; Tuomanen, E., Oligosaccharides interfere with the establishment and progression of experimental pneumococcal pneumonia. *J Infect Dis* **1997,** *176* (3), 704-712.

207.   (a) Ghindilis, A. L.; Smith, M. W.; Schwarzkopf, K. R.; Roth, K. M.; Peyvan, K.; Munro, S. B.; Lodes, M. J.; Stover, A. G.; Bernards, K.; Dill, K.; McShea, A., CombiMatrix oligonucleotide arrays: Genotyping and gene expression assays employing electrochemical detection. *Biosensors & Bioelectronics* **2007,** *22* (9-10), 1853-1860; (b) Roth, K. M.; Peyvan, K.; Schwarzkopf, K. R.; Ghindilis, A., Electrochemical detection of short DNA oligomer hybridization using the CombiMatrix ElectraSense Microarray reader. *Electroanalysis* **2006,** *18* (19-20), 1982-1988.

208.   Maurer, K.; Cooper, J.; Caraballo, M.; Crye, J.; Suciu, D.; Ghindilis, A.; Leonetti, J. A.; Wang, W.; Rossi, F. M.; Stover, A. G.; Larson, C.; Gao, H.; Dill, K.; McShea, A., Electrochemically Generated Acid and Its Containment to 100 Micron Reaction Areas for the Production of DNA Microarrays. *PLoS One* **2006,** *1* (1), -.

209.   (a) Bi, B.; Maurer, K.; Moeller, K. D., Building Addressable Libraries: Site-Selective Lewis Acid (Scandium(III)) Catalyzed Reactions. *ANGEWANDTE CHEMIE-INTERNATIONAL EDITION* **2009,** *48* (32), 5872-5874; (b) Hu, L. B.; Maurer, K.; Moeller, K. D., Building Addressable Libraries: Site-Selective Suzuki

Reactions on Microelectrode Arrays. *Org Lett* **2009,** *11* (6), 1273-1276; (c) Kesselring, D.; Maurer, K.; Moeller, K. D., Building addressable libraries: Site-selective formation of an N-acyliminium ion intermediate. *Org Lett* **2008,** *10* (12), 2501-2504; (d) Stuart, M.; Maurer, K.; Moeller, K. D., Moving known libraries to an addressable array: A site-selective hetero-Michael reaction. *Bioconjugate Chemistry* **2008,** *19* (8), 1514-1517.

210.   Dill, K.; Montgomery, D. D.; Ghindilis, A. L.; Schwarzkopf, K. R.; Ragsdale, S. R.; Oleinikov, A. V., Immunoassays based on electrochemical detection using microelectrode arrays. *Biosensors & Bioelectronics* **2004,** *20* (4), 736-742.

211.   Lodes, M. J.; Caraballo, M.; Suciu, D.; Munro, S.; Kumar, A.; Anderson, B., Detection of Cancer with Serum miRNAs on an Oligonucleotide Microarray. *PLoS One* **2009,** *4* (7).

212.   Bolotin, S.; Lombos, E.; Yeung, R.; Eshaghi, A.; Blair, J.; Drews, S. J., Verification of the Combimatrix influenza detection assay for the detection of influenza A subtype during the 2007-2008 influenza season in Toronto, Canada. *Virol J* **2009,** *6*, -.

213.   Oleinikov, A. V.; Gray, M. D.; Zhao, J.; Montgomery, D. D.; Ghindills, A. L.; Dill, K., Self-assembling protein arrays using electronic semiconductor microchips and in vitro translation. *J Proteome Res* **2003,** *2* (3), 313-319.

214.   Eddings, M. A.; Miles, A. R.; Eckman, J. W.; Kim, J.; Rich, R. L.; Gale, B. K.; Myszka, D. G., Improved continuous-flow print head for micro-array deposition. *Anal. Biochem.* **2008,** *382* (1), 55-59.

215.   Sokurenko, E. V.; Schembri, M. A.; Trintchina, E.; Kjaergaard, K.; Hasty, D. L.; Klemm, P., Valency conversion in the type 1 fimbrial adhesin of Escherichia coli. *Molecular Microbiology* **2001,** *41* (3), 675-686.

216.   Tchesnokova, V.; Aprikian, P.; Yakovenko, O.; Larock, C.; Kidd, B.; Vogel, V.; Thomas, W.; Sokurenko, E., Integrin-like allosteric properties of the catch bond-forming FimH adhesin of Escherichia coli. *J. Biol. Chem.* **2008,** *283* (12), 7823-33.

217.   Boddicker, J. D.; Ledeboer, N. A.; Jagnow, J.; Jones, B. D.; Clegg, S., Differential binding to and biofilm formation on, HEp-2 cells by Salmonella enterica Serovar Typhimurium is dependent upon allelic variation in the fimH gene of the fim gene cluster. *Molecular Microbiology* **2002,** *45* (5), 1255-1265.

218.   Stine, R.; Cole, C. L.; Ainslie, K. M.; Mulvaney, S. P.; Whitman, L. J., Formation of primary amines on silicon nitride surfaces: A direct, plasma-based pathway to functionalization. *Langmuir* **2007,** *23* (8), 4400-4404.

219.   Ahuja, T.; Mir, I. A.; Kumar, D.; Rajesh, Biomolecular immobilization on conducting polymers for biosensing applications. *Biomaterials* **2007,** *28* (5), 791-805.

220.   (a) Bertozzi, C. R.; Kiessling, L. L., Chemical glycobiology. *Science* **2001,** *291* (5512), 2357-2364; (b) Lee, Y. C.; Lee, R. T., Carbohydrate-Protein Interactions - Basis of Glycobiology. *Accounts Chem. Res.* **1995,** *28* (8), 321-327.

221.   (a) Ofek, I.; Mirelman, D.; Sharon, N., ADHERENCE OF ESCHERICHIA-COLI TO HUMAN MUCOSAL CELLS MEDIATED BY MANNOSE RECEPTORS. *Nature* **1977,** *265* (5595), 623-625; (b) Ofek, I.; Doyle, R. J., *Bacterial adhesion to cells and tissues*. Chapman & Hall: New York, 1994; p ix, 578 p; (c) Sokurenko, E. V.; Courtney, H. S.; Maslow, J.; Siitonen, A.; Hasty, D. L., Quantitative Differences in Adhesiveness of Type-1 Fimbriated Escherichia-Coli Due to Structural Differences in Fimh Genes. *J Bacteriol* **1995,** *177* (13), 3680-3686.

222.   (a) Krogfelt, K. A.; Bergmans, H.; Klemm, P., DIRECT EVIDENCE THAT THE FIMH PROTEIN IS THE MANNOSE-SPECIFIC ADHESIN OF ESCHERICHIA-COLI TYPE-1 FIMBRIAE. *Infect Immun* **1990,** *58* (6), 1995-1998; (b) Choudhury, D.; Thompson, A.; Stojanoff, V.; Langermann, S.; Pinkner, J.; Hultgren, S. J.; Knight, S. D., X-ray structure of the FimC-FimH chaperone-adhesin complex from uropathogenic Escherichia coli. *Science* **1999,** *285* (5430), 1061-6.

223.   (a) Sumetsky, M.; Windeler, R. S.; Dulashko, Y.; Fan, X., Optical liquid ring resonator sensor. *Optics Express* **2007,** *15* (22), 14376-14381; (b) White, I. M.; Oveys, H.; Fan, X. D., Liquid-core optical

ring-resonator sensors. *Opt. Lett.* **2006,** *31* (9), 1319-1321; (c) Zhu, H. Y.; White, I. M.; Suter, J. D.; Zourob, M.; Fan, X. D., Opto-fluidic micro-ring resonator for sensitive label-free viral detection. *Analyst* **2008,** *133* (3), 356-360.

224.   Luchansky, M. S.; Bailey, R. C., Silicon Photonic Microring Resonators for Quantitative Cytokine Detection and T-Cell Secretion Analysis. *Analytical Chemistry* **2010,** *82* (5), 1975-1981.

225.   Qavi, A. J.; Bailey, R. C., Multiplexed Detection and Label-Free Quantitation of MicroRNAs Using Arrays of Silicon Photonic Microring Resonators. *ANGEWANDTE CHEMIE-INTERNATIONAL EDITION* **2010,** *49* (27), 4608-4611.

226.   Luchansky, M. S.; Washburn, A. L.; Martin, T. A.; Iqbal, M.; Gunn, L. C.; Bailey, R. C., Characterization of the evanescent field profile and bound mass sensitivity of a label-free silicon photonic microring resonator biosensing platform. *Biosensors & Bioelectronics* **2010,** *26* (4), 1283-1291.

227.   Hatch, A.; Kamholz, A. E.; Hawkins, K. R.; Munson, M. S.; Schilling, E. A.; Weigl, B. H.; Yager, P., A rapid diffusion immunoassay in a T-sensor. *Nature Biotechnology* **2001,** *19* (5), 461-465.

228.   (a) Mori, T.; O'Keefe, B. R.; Sowder, R. C.; Bringans, S.; Gardella, R.; Berg, S.; Cochran, P.; Turpin, J. A.; Buckheit, R. W.; McMahon, J. B.; Boyd, M. R., Isolation and characterization of griffithsin, a novel HIV-inactivating protein, from the red alga Griffithsia sp. *J. Biol. Chem.* **2005,** *280* (10), 9345-9353; (b) Ziolkowska, N. E.; O'Keefe, B. R.; Mori, T.; Zhu, C.; Giomarelli, B.; Vojdani, F.; Palmer, K. E.; McMahon, J. B.; Wlodawer, A., Domain-swapped structure of the potent antiviral protein griffithsin and its mode of carbohydrate binding. *Structure* **2006,** *14* (7), 1127-1135.

229.   Olsnes, S.; Pihl, A., Different Biological Properties of 2 Constituent Peptide Chains of Ricin, a Toxic Protein Inhibiting Protein-Synthesis. *Biochemistry* **1973,** *12* (16), 3121-3126.

230.   Nagatsuka, T.; Uzawa, H.; Ohsawa, I.; Seto, Y.; Nishida, Y., Use of Lactose against the Deadly Biological Toxin Ricin. *Acs Appl Mater Inter* **2010,** *2* (4), 1081-1085.

231.   Li, J. Y.; Busscher, H. J.; Norde, W.; Sjollema, J., Analysis of the contribution of sedimentation to bacterial mass transport in a parallel plate flow chamber. *Colloids and Surfaces B-Biointerfaces* **2011,** *84* (1), 76-81.

232.   (a) [Anon] CombiMatrix Corporation Announces Strategic and Operational Restructuring. http://investor.combimatrix.com/releasedetail.cfm?ReleaseID=461153; (b) Timmerman, L. CombiMatrix Cuts Mukilteo Facility, CEO Resigns, Shifts to Diagnostic Strategy. http://www.xconomy.com/seattle/2010/04/19/combimatrix-cuts-mukilteo-facility-ceo-resigns-shifts-to-diagnostic-strategy/.

233.   (a) Zupancic, M. L.; Frieman, M.; Smith, D.; Alvarez, R. A.; Cummings, R. D.; Cormack, B. P., Glycan microarray analysis of Candida glabrata adhesin ligand specificity. *Molecular Microbiology* **2008,** *68* (3), 547-559; (b) Walz, A.; Odenbreit, S.; Mahdavi, J.; Boren, T.; Ruhl, S., Identification and characterization of binding properties of Helicobacter pylori by glycoconjugate arrays. *Glycobiology* **2005,** *15* (7), 700-708; (c) Day, C. J.; Tiralongo, J.; Hartnell, R. D.; Logue, C. A.; Wilson, J. C.; von Itzstein, M.; Korolik, V., Differential carbohydrate recognition by Campylobacter jejuni strain 11168: influences of temperature and growth conditions. *PLoS One* **2009,** *4* (3), e4927.

234.   Haensch, C.; Hoeppener, S.; Schubert, U. S., Chemical modification of self-assembled silane based monolayers by surface reactions. *Chem. Soc. Rev.* **2010,** *39* (6), 2323-2334.

235.   Park, S.; Lee, M. R.; Shin, I., Carbohydrate microarrays as powerful tools in studies of carbohydrate-mediated biological processes. *Chem Commun* **2008,** (37), 4389-4399.

236.   (a) Faverolle, F.; Attias, A. J.; Bloch, B.; Audebert, P.; Andrieux, C. P., Highly conducting and strongly adhering polypyrrole coating layers deposited on glass substrates by a chemical process. *Chem. Mat.* **1998,** *10* (3), 740-752; (b) Perruchot, C.; Chehimi, M. M.; Delamar, M.; Cabet-Deliry, E.; Miksa, B.; Slomkowski, S.; Khan, M. A.; Armes, S. P., Chemical deposition and characterization of thin polypyrrole films on glass plates: role of organosilane treatment. *Colloid Polym Sci* **2000,** *278* (12), 1139-1154.

237.   (a) Kim, Y. W.; Yoo, J. Y., Transport of solid particles in microfluidic channels. *Opt Laser Eng* **2012,** *50* (1), 87-98; (b) Segre, G.; Silberberg, A., Radial Particle Displacements in Poiseuille Flow of Suspensions. *Nature* **1961,** *189* (476), 209-&.

238.   (a) Hogt, A. H.; Dankert, J.; Feijen, J., Adhesion of Coagulase-Negative Staphylococci to Methacrylate Polymers and Copolymers. *J. Biomed. Mater. Res.* **1986,** *20* (4), 533-545; (b) Korber, D. R.; Lawrence, J. R.; Zhang, L.; Caldwell, D. E., Effect of gravity on bacterial deposition and orientation in laminar flow environments. *Biofouling* **1990,** *2* (4), 335-350.

239.   Li, J. Y.; Busscher, H. J.; van der Mei, H. C.; Norde, W.; Krom, B. P.; Sjollema, J., Analysis of the contribution of sedimentation to bacterial mass transport in a parallel plate flow chamber Part II: Use of fluorescence imaging. *Colloids and Surfaces B-Biointerfaces* **2011,** *87* (2), 427-432.

240.   Zhang, S. P.; Sun, Y., Further studies on the contribution of electrostatic and hydrophobic interactions to protein adsorption on dye-ligand adsorbents. *Biotechnol. Bioeng.* **2001,** *75* (6), 710-717.

241.   (a) Frydendahl, K.; Jensen, T. K.; Andersen, J. S.; Fredholm, M.; Evans, G., Association between the porcine Escherichia coli F18 receptor genotype and phenotype and susceptibility to colonisation and postweaning diarrhoea caused by E-coli O138 : F18. *Vet Microbiol* **2003,** *93* (1), 39-51; (b) Meijerink, E.; Neuenschwander, S.; Fries, R.; Dinter, A.; Bertschinger, H. U.; Stranzinger, G.; Vogeli, P., A DNA polymorphism influencing alpha(1,2)fucosyltransferase activity of the pig FUT1 enzyme determines susceptibility of small intestinal epithelium to Escherichia coli F18 adhesion. *Immunogenetics* **2000,** *52* (1-2), 129-136.

242.   Snoeck, V.; Verdonck, F.; Cox, E.; Goddeeris, B. M., Inhibition of adhesion of F18(+) Escherichia coli to piglet intestinal villous enterocytes by monoclonal antibody against blood group H-2 antigen. *Vet Microbiol* **2004,** *100* (3-4), 241-246.

243.   Gildersleeve, J. C.; Oyelaran, O.; Simpson, J. T.; Allred, B., Improved procedure for direct coupling of carbohydrates to proteins via reductive amination. *Bioconjugate Chemistry* **2008,** *19* (7), 1485-1490.

244.   Coddens, A.; Diswall, M.; Angstrom, J.; Breimer, M. E.; Goddeeris, B.; Cox, E.; Teneberg, S., Recognition of Blood Group ABH Type 1 Determinants by the FedF Adhesin of F18-fimbriated Escherichia coli. *J. Biol. Chem.* **2009,** *284* (15), 9713-9726.

245.   Gaynor, E. C.; Cawthraw, S.; Manning, G.; MacKichan, J. K.; Falkow, S.; Newell, D. G., The genome-sequenced variant of Campylobacter jejuni NCTC 11168 and the original clonal clinical isolate differ markedly in colonization, gene expression, and virulence-associated phenotypes (vol 186, pg 503, 2004). *J Bacteriol* **2004,** *186* (23), 8159-8159.

Curriculum Vitae

EDUCATION

University of Washington   Seattle, WA
Doctor of Philosophy, Bioengineering, August, 2012

Vanderbilt University   Nashville, TN
Bachelor of Engineering, Summa Cum-Laude, May 2007
- Biomedical Engineering Major with Honors, Engineering Management Minor

HONORS AND AWARDS

- National Science Foundation Graduate Research Fellowship (2008-2011)
- Thomas Francis Jr. Global Health Fellowship (2009)
  - Traveled to Mexico City in November 2009 to conduct research related to my Ph.D
- Thomas G. Arnold Prize for research in Biomedical Engineering" (2007)
  - Received for senior Honors Thesis research, report, and poster
- Honors in Biomedical Engineering (May 2007)
- Tau Beta Pi Engineering Honor Society – Inducted 2006 - Vice President (Spring 2006 - Spring 2007)
- Dean's List with High Honors - All semesters at Vanderbilt: Fall 2003 - Spring 2007

RESEARCH EXPERIENCE

University of Washington   Seattle, WA

Department of Bioengineering
Advisor: Dan Ratner
Graduate Student and Researcher, January 2008 – Present
- I am developing biosensing tools to study bacterial adhesion to biomolecules. These tools use sensing modalities such as Surface Plasmon Resonance (SPR), microelectrode microarrays, and silicon photonic ring resonators. By understanding the mechanism of bacterial binding, which is the first step in pathogenesis, we hope that we can aid in the development of novel prophylactics and therapeutics.
- Investigating various microarray functionalization, testing, and analysis approaches.
- Design and fabrication of microfluidic systems for interfacing with biosensors.
- Computer modeling of fluid flow to better understand the conditions of bacterial adhesion.
- Investigating and comparing bacterial binding inhibitors.

Vanderbilt University   Nashville, TN
Vanderbilt Institute for Integrative Biosystems Research and Education (VIIBRE)
Advisors: John Wikswo and Kevin Seale
Research Assistant, June 2005 – August 2008
Senior Design Team Leader, August 2006 – May 2007
- Performed research on T cells in microfluidic devices. Studied the frequency of T cell division in microfluidic devices under different culture conditions in order to gauge the appropriateness of this platform for long term studies.
- Led a senior design team in a project which optimized a microfluidic cell trapping device.

- Developed a semi-automated method for trapping cells for a novel 3D imaging technique.
- Learned techniques of photolithography and microfabrication in a cleanroom environment. Also learned the necessary process for device design.

LEADERSHIP POSITIONS, INVOLVEMENT, AND PROFESSIONAL AFFILIATIONS

University of Washington Science and Engineering Business Association (SEBA)
SEBA is a non-profit corporation which aims to support science and engineering students at the University of Washington in becoming successful in business through educational events, networking opportunities, and leadership experience. Our most important events include the Annual Science and Engineering Career Fair (the largest career fair on the UW campus), Entrepreneurship Week, and the Science and Technology Showcase. See www.uwseba.com
President Emeritus, April 2011 – Present
- In this role I serve on the advisory board for the organization where I have stayed closely involved with all SEBA activities. My primary involvement has included serving on the planning committee for Entrepreneurship Week, and aiding in revamping the marketing materials for the organization.
- Entrepreneurship Week is an annual event consisting of 10 events in five days all focused on various aspects of entrepreneurship – this is the fifth year the event has been held and I have been on the planning committee since the second year.

President, January 2010 – March 2011
- Oversee all of the operations of the organization; run meetings, manage relations with groups at the UW and in the Seattle business community, facilitate teamwork

Vice President of Membership, January 2009 – January 2010
- Organization and recruitment of SEBA membership

Officer of Membership, March 2008 – January 2009

Washington Biotechnology & Biomedical Association (WBBA)
Commercialization Committee, April 2011 – Present
- Responsible for providing a summary of all financings in the Seattle biotech and life sciences sector to the committee as well as taking minutes at the monthly meetings.

Board Member, August 2010 – Present
- Involved with the other members of the board to oversee WBBA operations, providing the student perspective for the organization. SEBA has an ex-officio spot on the WBBA board and I was eager to fill this position.

Life Sciences Innovation Northwest Planning Committee, Poster Session Chair; July 2010 – March 2011
- As chair of the poster session committee, I was responsible for organizing participants and running the poster sessions during the conference.
- Recruited 30 participants, more than doubling the size of the poster session from previous years.
- LSINW is an annual conference of life science companies, nonprofit research institutions, and global health organizations highlighting the strength of the Northwest's life science industry to state, national, and global leaders.

- SEBA has teamed up with the WBBA for the conference to put on a poster session for emerging and pre-emerging life science technologies since 2009.

Bioscience Careers Planning Committee
May 2008 – May 2009
Bioscience Careers is a student-run organization that organizes a monthly seminar series that brings in speakers who discuss non-academic career options for Ph.D. students. As a member of the committee, I assist with bringing in speakers and with general organizational requirements for the seminars.

Zeta Beta Tau Fraternity
President, January 2006 – January 2007
- *S*erved as the representative to the university and the manager of all house operations.
Treasurer, January 2005 – January 2006
- Responsible for managing a yearly budget of nearly $100,000.
- Established a record-keeping system, improved dues collection from 80% to 100%, eliminated wasteful spending.
National Budget Committee, September 2005 – September 2006
- Worked with the national office to develop a new budget for distributing fraternity funds.

Tau Beta Pi Engineering Honor Society
Inducted Spring 2006
Vice President of the Vanderbilt Chapter, May 2006 – May 2007
- Aid the president in the chapter operations including the induction ceremony and the regional annual assembly for delegates throughout the Southeast.

PUBLICATIONS AND PATENTS

Chamberlain, J.W., Maurer, K., Cooper, J., Lyon, W.J., Danley, D., Ratner, D.M., Microelectrode array biosensor for studying carbohydrate mediated interactions. *Biosensors and Bioelectronics*, 2012. DOI: http://dx.doi.org/10.1016/j.bios.2012.02.017

Chamberlain, J.W., Ratner, D.M., Label-Free Biosensors for Biomedical Applications: The Potential of Integrated Optical Biosensors and Silicon Photonics. Published in two books: (1) *Optical, Acoustic, Magnetic, and Mechanical Sensor Technologies*: Taylor and Francis, 2012. (2) *Biological and Medical Sensor Technologies*: Taylor and Francis, 2012.

Kirk, J. T.; Fridley, G. E.; **Chamberlain, J.W.**; Christensen, E. D.; Hochberg, M.; Ratner, D. M., Multiplexed inkjet functionalization of silicon photonic biosensors. *Lab Chip* **2011,** *11*(7), 1372-7.

Seale, K.T., Faley, S.L., **Chamberlain, J.W.**, Wikswo, J.P. "Macro to nano: A simple method for transporting culture cells from milliliter scale to nanoliter scale," *Experimental Biology and Medicine*: 235 (6), 777-783 (2010).

Patent: "Tip-based concentrator, sensor, and storage for biomaterials," UW Ref#8055. On the list of inventors. Submitted, pending.

Patent: "Photolithographed Micro-Mirror Well for 3D Tomogram Imaging of Individual Cells." Submitted May 20, 2011, Application No: 13/112,901. On list of inventors.

CONFERENCE PROCEEDINGS AND PRESENTATIONS

Chamberlain, J.W., Ranter, D.M. "Microelectrode Array Biosensor to Study Carbohydrate-Mediated Bacterial Adhesion," W.L. Gore & Assiciates Biomedical Engineering Partnership Meeting, 2010.

Chamberlain, J.W., Wikswo, J.P., Seale, K.T. "Long-Term Cytokinesis Studies of Human T Cell Populations in a Microfluidic Device," Biomedical Engineering Society Conference, 2007.

Seale, K.T., Reiserer, R.S., **Chamberlain, J.W.**, Janetopoulos, C., Wikswo, J.P. "Multiple Vantage Point Microscopy Using Mirrored Pyramidal Wells," BMES Annual Fall Meeting, Sept. 26-28, Platform presentation, 2007.